

Aus dem Institut für Schlaganfall- und Demenzforschung  
Institut der Ludwig-Maximilians-Universität München  
Direktor: Prof. Dr. med. Martin Dichgans

# **Brain-released alarmins as mediators of immunological comorbidities after stroke**

Dissertation

zum Erwerb des Doktorgrades der Medizin  
an der Medizinischen Fakultät der  
Ludwig-Maximilians-Universität zu München

vorgelegt von  
Jun Yang

aus Shanxi, China

2020

**Mit Genehmigung der Medizinischen  
Fakultät der Universität München**

Berichterstatter: Prof. Dr. med. Arthur Liesz

Mitberichterstatter: PD. Dr. med. Johann Szecsi  
PD. Dr. rer. nat. Florence Bayeyre

Mitbetreuung durch den  
promovierten Mitarbeiter: Dr. rer. nat. Stefan Roth

Dekan: Prof. Dr. med. dent. Reinhard Hickel

Tag der mündlichen Prüfung: 10.12.2020

# Eidesstattliche Versicherung

**Yang, Jun**

---

Name, Vorname

Ich erkläre hiermit an Eides statt,  
dass ich die vorliegende Dissertation mit dem Titel

**Brain-released alarmins as mediators of immunological comorbidities after stroke**

selbständig verfasst, mich außer der angegebenen keiner weiteren Hilfsmittel bedient und alle Erkenntnisse, die aus dem Schrifttum ganz oder annähernd übernommen sind, als solche kenntlich gemacht und nach ihrer Herkunft unter Bezeichnung der Fundstelle einzeln nachgewiesen habe.

Ich erkläre des Weiteren, dass die hier vorgelegte Dissertation nicht in gleicher oder in ähnlicher Form bei einer anderen Stelle zur Erlangung eines akademischen Grades eingereicht wurde.

München, 13.12.2020

---

Ort, Datum

Jun Yang

---

Unterschrift Doktorandin bzw. Doktorand

# Table of Contents

List of Figures .....	7
List of Tables .....	7
Abbreviations .....	8
Zusammenfassung .....	11
Summary .....	13
1 Introduction .....	15
1.1 Ischemic stroke .....	15
1.1.1 Pathogenesis of ischemic stroke .....	15
1.1.2 Pathophysiologic processes after ischemic stroke .....	18
1.2 Alarmins .....	21
1.2.1 HMGB1 released from necrotic brain lesions after stroke .....	22
1.2.2 Other key alarmins in tissue injury .....	23
1.2.3 Key receptors for alarmins .....	24
1.3 Immune system activation after stroke .....	27
1.3.1 Local brain inflammation after stroke .....	27
1.3.2 Peripheral immune system activation after stroke .....	29
1.3.3 Cytokine-induced sickness behavior (CISB) .....	32
1.4 Immunosuppression after stroke .....	34
1.4.1 Stress mediators .....	34
1.4.2 Soluble mediators .....	35
1.4.3 Pyroptosis in lymphopenia .....	36
2 The aims of this study .....	39
3 Materials and methods .....	40
3.1 Materials and research animals .....	40
3.1.1 Instruments .....	40
3.1.2 Reagents and materials .....	41
3.1.3 Antibodies .....	42

## Table of Contents

---

3.1.4	Research animals.....	42
3.2	Methods.....	43
3.2.1	Filamentous middle cerebral artery occlusion (fMCAo) .....	43
3.2.2	Mouse blood collection and preparation .....	44
3.2.3	Mouse organ sample collection and process .....	45
3.2.4	Behavior tests.....	45
3.2.5	Anti-cytokine treatment .....	50
3.2.6	Preparation of cells from lymphoid organs and blood .....	50
3.2.7	Flow Cytometry .....	50
3.2.8	Magnetic-activated cell sorting (MACS) .....	51
3.2.9	In-vitro assay.....	51
3.2.10	Reducing circulating alarmins .....	51
3.2.11	In vivo caspase-1 inhibition .....	52
3.2.12	Infarct volumetry.....	52
3.2.13	Statistical analysis.....	52
4	Results.....	54
4.1	Immune activation after experimental stroke: CISB.....	54
4.1.1	Motor and sensory deficits can be quantified by behavior tests after experimental stroke.....	56
4.1.2	Anxiety and depression can be detected after experimental stroke .....	61
4.1.3	The sensitivity and specificity of different behavior tests.....	65
4.1.4	Anti-cytokine treatment can improve sickness behavior after experimental stroke .....	66
4.2	Immunosuppression after experimental stroke .....	72
4.2.1	Large experimental stroke induces leukocyte reduction in mice .....	73
4.2.2	Soluble mediators released after ischemic stroke induce T cell death .....	76
4.2.3	Deletion of Myd88 reduces T cell death .....	79
4.2.4	The deletion or inhibition of caspase-1 reduces T cell death.....	80
5	Discussion .....	83
5.1	CISB after stroke.....	83
5.1.1	Optimal behavior tests for focal deficit assessment .....	83
5.1.2	The pitfalls of detecting anxiety, depression, memory, and learning deficits .....	85
5.1.3	Cytokines' effect on sickness behavior after stroke.....	87

## Table of Contents

---

5.1.4	Assessment of sickness behavior in other mouse strains and other stroke models .....	89
5.2	T cell reduction after stroke .....	91
5.2.1	Peripheral T cells die after large experimental stroke.....	91
5.2.2	Apoptosis and pyroptosis in ischemic stroke .....	92
5.2.3	HMGB1 in T cell death after stroke.....	95
5.2.4	Cell surface receptors in T cell death after stroke .....	96
5.2.5	Inflammasome complexes involved in caspase-1 activation .....	98
5.2.6	The non-canonical inflammasome pathway.....	99
5.3	Concluding remarks .....	100
References.....		102
Appendix.....		112
Acknowledgments.....		115

## List of Figures

Figure 1: Key receptors for alarmins. ....	26
Figure 2: Schematic diagram of immune system activation after stroke. ....	31
Figure 3: Representative scheme of the behavior test battery. ....	56
Figure 4: Characterization of filamentous middle cerebral artery occlusion and the general body condition after the surgical procedures. ....	57
Figure 5: Assessment of motor and sensory deficits up to 28 days after experimental stroke. ....	59
Figure 6: 56-point composite Neuroscore: general and focal deficits. ....	61
Figure 7: Assessment of anxiety, motivation, and depression-like behavior after stroke. ....	64
Figure 8: Physiological readouts after cytokine neutralization. ....	68
Figure 9: Impact of cytokine neutralization on sickness behavior in the acute and subacute phases after stroke. ....	72
Figure 10: Schematic diagram of the biphasic peripheral immunomodulation after stroke. ....	73
Figure 11: The kinetic alternation of the peripheral leukocyte number after ischemic stroke. ....	75
Figure 12: Soluble mediators released after ischemic stroke induce T cell death. ....	78
Figure 13: The effect of the deletion of RAGE or Myd88 in T cell death after stroke. ....	80
Figure 14: Deletion or inhibition of caspase-1 reduces T cell death. ....	81
Figure 15: Brain-released alarmins as mediators of immunological comorbidities after stroke. ....	101

## List of Tables

Table 1. ROC curve analysis of the behavior test battery. ....	66
--	----

**Abbreviations**

ADP	Adenosine diphosphate
AMPA	$\alpha$ -amino-3-hydroxy-5-methyl-4-propionate
ASC	Apoptosis-associated speck-like protein containing a CARD
ATP	Adenosine triphosphate
BBB	Blood-brain barrier
CCA	Common carotid artery
CCR1	C-C chemokine receptor type 1
CCR2	C-C chemokine receptor type 2
CCR7	C-C chemokine receptor type 7
CCR8	C-C chemokine receptor type 8
CISB	Cytokine-induced sickness behavior
CNS	Central nervous system
COX-2	Cyclooxygenase-2
DAMPs	Damage-associated molecular patterns
dMCAo	Distal middle cerebral artery occlusion
DNA	Deoxyribonucleic acid
ECA	External carotid artery
fMCAo	Filamentous middle cerebral artery occlusion
HMGB1	High-mobility group box-1



HPA	Hypothalamic-pituitary-adrenal axis
HSP	Heat shock proteins
ICA	Internal carotid artery
IFN- $\gamma$	Interferon-gamma
IL-1 $\beta$ / <i>IL1B</i>	Interleukin-1 beta
IL-6/ <i>IL6</i>	Interleukin-6
<i>IL8</i>	Interleukin-8
IP-10/ <i>IP10</i>	Interferon gamma-induced protein 10
iNOS	Inducible nitric oxide synthase
MACS	Magnetic-activated cell sorting
MCA	Middle cerebral artery
MCAO	Middle cerebral artery occlusion
<i>MCAP1</i>	Monocyte chemoattractant protein-1
MIP-2	Macrophage inflammatory protein-2
MyD88	Myeloid differentiation primary response 88
NF- $\kappa$ B	Nuclear factor kappa-light-chain-enhancer of activated B cells
NK cells	Natural killer cells
NLRP3	NOD-like receptor pyrin domain-containing-3
NMDA	N-methyl-d-aspartate
NO	Nitric oxide
PAMPs	Pathogen-associated molecular patterns

PRRs	Pattern recognition receptors
P2X7R	P2X7 receptor
RAGE	Receptor for advanced glycation end products
ROC	Receiver operating characteristic
ROS	Reactive oxygen species
SD	Standard deviation
SIRS	Systemic inflammatory response syndrome
SNS	Sympathetic nervous system
sRAGE	Soluble receptor for advanced glycation end products
TGF- $\beta$	Tumor growth factor-beta
TLR	Toll-like receptor
TNF- $\alpha$ / <i>TNFA</i>	Tumor necrosis factor-alpha
TOAST	Trial of Org 10172 in acute stroke treatment
TUNEL	Terminal UDP-nick end labeling
UTP	Uridine-5'-triphosphate

## **Zusammenfassung**

Ein ischämischer Schlaganfall wird durch einen lokalisierten Zelltod verursacht, der auf eine Unterbrechung der Blutversorgung und einen Mangel an Glukose und Sauerstoff zurückzuführen ist. Es verursacht eine hohe Mortalität, Morbidität und die zunehmende sozio-ökonomische Belastung. In den vergangenen Jahrzehnten wurde eine Wechselwirkung zwischen Immunität und Gehirn nach Schlaganfall etabliert. Nach einem ischämischen Schlaganfall beeinflusst das Immunsystem nicht nur das Gehirn, sondern auch der Schlaganfall trägt zur Modulation des peripheren Immunsystems bei. Alarmine, inflammatorische Moleküle, die nach einem Schlaganfall freigesetzt werden, können eine lokale Gehirnentzündung auslösen und auch die periphere Immunaktivierung vermitteln. Das Zytokin-induzierte Krankheitsverhalten wird als ein wichtiges pathophysiologische Element der Immunaktivierung nach einem ischämischen Schlaganfall angesehen. Daher charakterisieren wir verschiedene Verhaltensaspekte nach einem experimentellen Schlaganfall im Mausmodell mit einer breiten Palette verschiedener Verhaltenstests. Zusätzlich zeigten wir die Rolle von peripheren proinflammatorischen Zytokinen im Krankheitsverhalten nach Schlaganfall durch unsere ausgewählten Verhaltenstests. Andererseits ist es bekannt, dass nach einer tiefgreifenden frühen Aktivierung des peripheren Immunsystems eine schwere systemische Immunsuppression folgt. Die Immunsuppression nach Schlaganfall trägt vermutlich erheblich zu den häufigen Infektionen nach Schlaganfall bei, die häufig das klinische Outcome von Schlaganfallpatienten verschlechtern. Neben der Aktivierung des Immunsystems können

Alarmine auch eine Immunsuppression nach einem Schlaganfall auslösen. Um die Immunsuppression nach einem ischämischen Schlaganfall zu untersuchen, quantifizieren wir zunächst die Anzahl der peripheren Immunzellen und stellen fest, dass die Gesamtleukozyten und T-Zellen abnehmen. Danach zeigen wir, dass T-Zellen nach einem Schlaganfall absterben und dass dies mit der Stimulation von Alarminen zusammenhängt. Schließlich untersuchen wir die möglichen molekularen Wege, die am Tod von T-Zellen nach einem Schlaganfall beteiligt sind.

## Summary

Ischemic stroke is caused by localized cell death due to the interruption of the blood supply and depletion in glucose and oxygen. It causes high mortality, morbidity, and the increasing socio-economic burden. In recent decades, an interaction between immunity and the brain after stroke has been established. It is not only the case that the immune system influences the brain after ischemic stroke, but stroke also contributes to the modulation of the peripheral immune system. Alarmins, inflammatory molecules released after stroke, can trigger local brain inflammation and mediate peripheral immune activation. Cytokine-induced sickness behavior (CISB) is considered a key pathophysiological element of immune activation after ischemic stroke. Hence, we characterize different behavioral aspects after an experimental stroke in a mouse model with a broad battery of behavior tests. Additionally, we demonstrate the role of peripheral pro-inflammatory cytokines in sickness behavior after stroke through our selected behavior tests. It is known that, after a profound early activation of the peripheral immune system, severe systemic immunosuppression follows. The immunosuppression after stroke is believed to contribute significantly to frequent post-stroke infections, which often worsen stroke patients' clinical outcome. In addition to immune system activation, alarmins may also trigger post-stroke immunosuppression. To investigate immunosuppression after an ischemic stroke, we first quantify the number of peripheral immune cells and find a reduction in total leukocytes and T cells after stroke. After, we demonstrate that T cells die after stroke, which is related

to alarmins' stimulation. Finally, we investigate the possible molecular pathways involved in T cells' death after stroke.

# **1 Introduction**

## **1.1 Ischemic stroke**

The brain is critically dependent on the continued oxygen and glucose transport, and blood supply disruption can result in irreversible cerebrum damage.<sup>1</sup> Ischemic stroke is caused by localized cell death due to the restricted blood supply and depletion in glucose and oxygen.<sup>2</sup> In 2017, stroke was ranked as the fifth cause of death by the American Heart Association following heart disease, cancer, chronic lower respiratory disease, and unintentional injury.<sup>3</sup> Approximately 1.1 million Europeans suffer from a stroke each year, and ischemic stroke accounted for about 80% of these cases.<sup>4</sup> Furthermore, the stroke incidence in Europe is expected to increase by 1.5 million each year until 2025.<sup>4</sup> It is also a leading cause of severe long-term disability: approximately 3% of men and 2% of women struggle with disabilities caused by a stroke.<sup>3</sup> Although the understanding of strokes has developed in recent years, the therapy approaches are still limited, and the socio-economic burden continuously increases.

### **1.1.1 Pathogenesis of ischemic stroke**

The possible mechanisms of ischemic stroke include in situ thrombotic occlusion, arterio-arterial embolism, impaired clearance of emboli, branch occlusive disease, and hemodynamic insufficiency. Of these, arterio-arterial embolism, impaired clearance of emboli, and branch occlusive disease are more common, and arterio-arterial embolism frequently coexists with the impaired clearance of emboli.<sup>5</sup>

**In situ thrombotic occlusion.** In situ thrombotic occlusion begins with the atherosclerotic plaque cracking; the plaque instability is related to inflammation, autoimmunity, and genetic predisposition.<sup>6</sup> The tissue factors released after endothelial surface disruption promote clot formation next to the plaque, and local occlusion of the artery and secondary arterio-arterial embolism can finally result in brain infarction. In situ thrombotic occlusion usually induces a single, large subcortical infarct that sometimes only influences the border area but rarely produces infarction of the whole region.<sup>5</sup>

**Arterio-arterial embolism.** Debris is carried to distal branches when the blood flow breaks up the thrombus or plaque ulceration, after which arterio-arterial embolism takes place and leads to brain infarct.<sup>5</sup> Internal carotid artery (ICA) atherosclerotic disease is the most frequent cause of cerebral embolism.<sup>7</sup> The pattern of infarcts is multiple small cortical and subcortical lesions.<sup>5</sup>

**Impaired clearance of emboli.** Arterial luminal narrowing and decreased perfusion impair bloodstream's ability to clear or rinse emboli and microemboli, which could further block supply to the arteries and lead to ischemia.<sup>8</sup> The infarcts are multiple, small, and scattered and are along the border region.<sup>5</sup>

**Cardiac embolism.** In addition to embolism from the arteries, cardiac embolism is another cause of embolism. Atrial fibrillation, systolic heart failure, recent myocardial infarction, patent foramen ovale, aortic arch atheroma, prosthetic heart valves, and infective endocarditis are the main risk factors of cardioembolic stroke.<sup>9</sup>



**Branch occlusive disease.** Branch occlusive disease is usually caused by the occlusion of perforating a branch orifice or lumen by atherosclerotic plaques. Neuroimaging examinations can detect the small subcortical and lacuna-like infarcts due to this mechanism.<sup>10</sup> The pathological features of this type of branch occlusion include plaque hemorrhage microdissection and platelet and platelet-fibrin materials.<sup>11-14</sup>

**Hypoperfusion.** Along with atherosclerosis, plaque gradually increases and blood vessels become narrower, which eventually leads to the turbulence of the blood flow. Disturbed blood flow ultimately results in the hypoperfusion of distal branches. Hypoperfusion in a particular region of the brain plays an important role in the development of infarct. The collateral circulation may, meanwhile, influence the size of the lesion. Patients with insufficient collaterals will suffer from hemodynamic strokes or transient ischemic attacks (TIAs).<sup>5</sup>

These mechanisms are not isolated and in fact frequently co-exist. In addition to causing hypoperfusion, turbulence and fast flow velocity also increase the sheer stress on endothelium and can lead to plaque fissuring that could ultimately induce in situ thrombotic occlusion and arterio-arterial embolism.<sup>5</sup> The impaired clearance of emboli is also an important concept that intertwines with hypoperfusion and embolization.<sup>8</sup>

Because determining the cause of stroke is essential for choosing its management, an unambiguous, practical classification of ischemic stroke based on subtypes of pathogenesis is crucial in the clinic. The most widely used ischemic stroke classification system is based

on this pathogenesis and etiology, and it is the Trial of Org 10172 in acute stroke treatment (TOAST) classification.<sup>15</sup> The TOAST system consists of five major subtypes: large artery atherosclerosis (embolus/thrombosis), cardiac embolism (high-risk/medium-risk), small-vessel occlusion (lacuna), stroke of other determined etiology, and stroke of undetermined etiology (two or more causes identified, negative evaluation, incomplete evaluation).<sup>15</sup>

### **1.1.2 Pathophysiologic processes after ischemic stroke**

In ischemic stroke, a sequence of multistep pathophysiological events may be caused by reducing the blood flow in a brain region. These events occur like a cascade (ischemic cascade) and follow each other in a varying order with overlapping features.<sup>16-18</sup> The leading pathophysiologic events in ischemic cascade include energy failure, excitotoxicity, free radicals generation, blood-brain barrier (BBB) disruption, inflammation, and apoptosis.<sup>16</sup> Hence, I focus on these mechanisms to introduce the pathophysiologic processes after ischemic stroke.

**Energy failure.** Following the reduction of cerebral blood flow, glucose and oxygen that produce energy by undergoing oxidative phosphorylation are depleted in brain. This energy failure can cause an accumulation of lactate in the brain by anaerobic glycolysis. Lactate acidosis can induce many deleterious effects, such as free radical formation and loss of ionic homeostasis, and they can worsen ischemic brain injury.<sup>16,18-20</sup> In addition, this step is crucial in ischemic cascade, which triggers the subsequent downstream mechanisms.<sup>18</sup> Because of the failure of adenosine triphosphate (ATP)-dependent ion (sodium and calcium)

transport after ischemia, subsequent ion dyshomeostasis causes reversible cytotoxic edema and leads to an excess of intracellular  $\text{Ca}^{2+}$ .<sup>16,17</sup>

**Excitotoxicity.** Neurons and glia depolarize with energy failure, causing the release of excitatory neurotransmitters in the brain, especially glutamate.<sup>2,16</sup> Glutamate binds to glutamate receptors, such as the  $\alpha$ -amino-3-hydroxy-5-methyl-4-propionate (AMPA) receptor and the N-methyl-D-aspartate (NMDA) receptor, promoting a significant influx of calcium and increasing the intracellular  $\text{Na}^+$  and  $\text{Cl}^-$  levels.<sup>16,18</sup> Excitotoxicity thus aggravates cell edema and causes necrosis, and it can even initiate molecular events that lead to apoptosis.<sup>2,18</sup>

**Free radicals generation.** During the ischemic cascade, the excess of intracellular  $\text{Ca}^{2+}$ ,  $\text{Na}^+$ , and adenosine diphosphate (ADP) can stimulate excessive mitochondrial oxygen radicals generation.<sup>18</sup> These free radicals can directly damage lipids, protein, carbohydrates, and nucleic acid.<sup>21</sup> At the cellular level, free radicals can damage any cellular component, such as mutations of the genome, lipid peroxidation, dysregulation of cellular processes, and membrane damage.<sup>16</sup> At the vascular level, free radicals and their derivatives can cause vasodilation, increased BBB permeability, and the disruption of endothelial cell membranes.<sup>22</sup> Ultimately, this damage trigger inflammation and results in a complex mix of neuronal death, including apoptosis, necrosis, and autophagy.<sup>2,23</sup>

**BBB disruption.** In addition to free radicals, hypoxic and mechanical damage of endothelium, destruction of the basal lamina, and toxic damage of inflammatory molecules

are also potential causes of BBB disruption.<sup>16</sup> Following the disruption of BBB permeability, albumin and other high-molecular-weight compounds extravasate from brain capillaries, which results in increased extracellular fluid and causes irreversible vasogenic edema and increased intracranial pressure.<sup>17,24</sup> This may compress neurons, nerve tracts, and cerebral arteries, and it can also cause persistent ischemia and cerebral herniation.<sup>17</sup>

**Inflammation.** In ischemic cascade, pro-inflammatory genes, including interleukin-1 beta (*IL1B*), tumor necrosis factor-alpha (*TNFA*), and transcription factors, are up-regulated within minutes of occlusion.<sup>25-28</sup> Neutrophils followed by monocytes that interact with adhesion molecules at the vascular endothelium can transmigrate through the vascular wall from the blood into the brain parenchyma.<sup>29</sup> The inflammatory mechanism is a critical pathophysiological process after ischemic stroke and the foundation of our study; this, it is introduced in greater detail in the paragraphs titled “Immune system activation after stroke” and “Immunosuppression after stroke.”

**Apoptosis.** Unlike necrosis, which causes cell death in the ischemic core, apoptosis mainly occurs within the ischemic penumbra.<sup>17,30</sup> Apoptosis can be triggered by excitotoxicity, free radical formation, inflammation, mitochondrial and deoxyribonucleic acid (DNA) damage, and cytochrome c release from mitochondria.<sup>31-33</sup> It has been reported that caspases 1, 3, 8, and 9 are involved in ischemic stroke, and caspase activation can be triggered in response to many different pro-apoptotic signals following ischemia.<sup>16,32</sup> Apoptotic cell morphology is markedly different from necrotic cell morphology. Apoptotic cell's morphological characteristics are as follows: cytoplasm shrinkage, chromatin

condensation, membrane blebbing, and cell fragmentation by separating the bumps to form membrane-bound bodies that contain intact organelles and/or dense clumps (apoptotic bodies).<sup>32,34</sup>

## **1.2 Alarmins**

Damaged or dead/dying cells can release or secrete normal cell constituents as the generic markers for damage, which are alarmins, also known as damage-associated molecular patterns (DAMPs).<sup>35,36</sup> It has been found that pathogen-associated molecular patterns (PAMPs) can be recognized by pattern recognition receptors (PRRs) and lead to the synthesis and secretion of pro-inflammatory cytokines and chemokines.<sup>37</sup> Similar to PAMPs, innate immune cells can also respond to alarmins through peculiar receptors and relevant signaling pathways, and can directly or indirectly boost immune responses.<sup>35,36</sup> Alarmins are structurally diverse molecules, such as DNA, heparan sulfate, uric acid, hyaluronan fragments, ATP, uridine-5'-triphosphate (UTP), reactive oxygen species (ROS), high mobility group box 1 (HMGB1), heat shock proteins (HSP), peroxiredoxin family proteins, amyloid-beta, and many other molecular patterns.<sup>36,38-41</sup> In ischemic stroke, necrotic brain lesions are so-called “damaged tissue,” which can release alarmins to influence the immune system.<sup>40,42,43</sup> The key alarmins involved in ischemic stroke are introduced in more detail below.

### **1.2.1 HMGB1 released from necrotic brain lesions after stroke**

HMGB1 is one of the pro-inflammatory alarmins released after ischemic stroke.<sup>42</sup> It is a non-histone nuclear protein, and all cells can synthesize it.<sup>44</sup> HMGB1 binds to the minor groove of linear DNA.<sup>45</sup> In healthy and non-activated cells, it can also support the binding of several transcription factors to DNA.<sup>45</sup> However, HMGB1 is released with a pro-inflammatory cytokines function after necrotic cell death.<sup>46</sup> Innate immune cells may be further signaled by HMGB1 to respond to tissue injury.<sup>46</sup> In stroke patients, HMGB1 serum concentration is massively increased in the first several hours after symptom onset.<sup>42</sup> A similar increase has also been found at early time points after experimental stroke with large infarcts.<sup>42</sup> Moreover, previous study has reduced HMGB1 expression by injecting HMGB1-shRNA into intra-striatal, and has found a reduction of infarct size and also microglia activation.<sup>47</sup> These results suggest that after ischemic stroke, HMGB1 can be released from necrotic brain tissue into the peripheral blood circulation, and it can activate inflammation and aggravate brain damage. Nonetheless, no previous studies have demonstrated the cellular source of passively released HMGB1 in the acute phase after stroke.

In addition to passively released HMGB1 by necrotic brain tissue after stroke, activated immune cells in the brain and in the peripheral immune system may also actively secrete HMGB1 in response to tissue injury.<sup>46</sup> The active secretion of HMGB1 most likely originates from invasive monocytes in the brain and activated microglia and could further

explain the increased level of circulating HMGB1 over a prolonged time after ischemic brain injury.<sup>46-49</sup>

### **1.2.2 Other key alarmins in tissue injury**

In addition to HMGB1, ATP, UTP, HSP60, Peroxiredoxin family proteins, and amyloid-beta are also released as alarmins from injured tissue after ischemic stroke and cause the production of pro-inflammatory cytokines.<sup>38-41</sup>

ATP belongs to the purine family, and ubiquitous ecto-ATP/ADPases (CD39) in healthy tissues keep its extracellular concentration low.<sup>50</sup> Nevertheless, concentrations of extracellular ATP are increased during trauma, cell stress, or tissue injury. Extracellular ATP is involved in the recruitment and activation of macrophages, neutrophils, and dendritic cells, and it can serve as a chemotactic agent to facilitate the maturation of dendritic cells and to modulate the production of cytokines.<sup>51,52</sup> Moreover, both in vitro and in vivo studies have demonstrated that extracellular ATP is a potent activator of the NOD-like receptor pyrin domain-containing-3 (NLRP3)-dependent interleukin-1 beta (IL-1 $\beta$ ) release from macrophages.<sup>53-55</sup> In ischemic stroke, extracellular ATP increases due to stress and triggers microglia to develop several macrophage features, including ameboid morphology, migratory capacity, phagocytosis, and antigen presentation.<sup>56</sup>

Additionally, HSP60 and  $\beta$ -amyloid released from the intracellular compartment after neuron necrosis also induce the expression of pro-inflammatory molecules for antigen presentation in invading leukocytes and primary dendritic cells.<sup>56</sup>

Therefore, the alarmins released from stressed cells and necrotic cells can cause an inflammatory response in both resident brain cells and invading leukocytes.

### **1.2.3 Key receptors for alarmins**

**Toll-like receptors (TLRs)** consist of a extracellular domain, a transmembrane domain, and an intracellular domain, which is a receptor group for different microorganism-derived molecular patterns and recognizes alarmins.<sup>35,57</sup> The extracellular domain is associated with ligand recognition, and the intracellular domain is crucial for signal modulation through the adaptor protein myeloid differentiation primary response 88 (MyD88).<sup>58</sup> It has been demonstrated that, through stimulation of TLRs, the activation of the nuclear factor kappa-light-chain-enhancer of activated B cells (NF- $\kappa$ B) can regulate pro-inflammatory cytokines' production and the proliferation of different cells.<sup>59</sup> Furthermore, stimulation of TLRs has also been related to the development of ischemic strokes.<sup>60</sup> The main TLRs for HMGB1 are TLR2 and TLR4 (Figure 1). Increased expression of TLR2 and TLR4 on monocytes is linked to higher serum levels of IL-1 $\beta$ , interleukin-6 (IL-6), and tumor necrosis factor-alpha (TNF- $\alpha$ ) in stroke patients.<sup>61</sup> The TLR2 and TLR4 knockout mice had less damage to the brain and neuronal deficits in experimental stroke.<sup>62,63</sup> Similarly, knockout MyD88, the downstream effector molecule in TLR signaling, also resulted in smaller stroke lesions in experimental stroke.<sup>64</sup> These findings support the theory of an inflammatory worsening of stroke lesion via TLR signaling.



**The receptor for advanced glycation end products (RAGE)** is a cell surface multi-ligand receptor of the immunoglobulin superfamily, and it contains one “V”-type and two “C”-type domains. It is capable of modulating cellular responses to tissue injury by interacting with several alarmin ligands, including HMGB1<sup>46</sup> (Figure 1). Like TLR2 and TLR4, HMGB1-RAGE signaling also promotes the activation of NF- $\kappa$ B in an MyD88-dependent manner and allows the transcription of pro-inflammatory genes, such as *TNFA*, interleukin-6 (*IL6*), and *IL1B*.<sup>65</sup> RAGE has been found to increase in human and murine brains after stroke<sup>66</sup> and in vascular cells after experimental stroke.<sup>67</sup> An earlier study has shown that ablation of RAGE in mice limited the infarction and abrogated activation of macrophages.<sup>43</sup> This finding further confirms the critical role of RAGE in stroke progress.<sup>43</sup> Moreover, peripheral immune cells, including lymphocyte, monocyte, dendritic cell, and macrophage, also express RAGE.<sup>68-70</sup> This leads to the notion that the HMGB1-RAGE pathway could be a link between stroke and the peripheral immune system, and it could induce a sterile immune reaction after tissue injury.

**Purinergic receptors** are a family of plasma membrane receptors involved in cytokine secretion, apoptosis, the proliferation of neural stem cells, and several cellular functions.<sup>71,72</sup> The P2X7 receptor (P2X7R) is a member of the purinergic receptors (Figure 1), and they can be detected in the hemopoietic lineage cells, including microglia, macrophages, and some lymphocytes.<sup>73</sup> The P2X7R also serves as a PRR for the extracellular ATP-mediated MyD88/NF- $\kappa$ B pathway, inflammasome activation, and apoptotic cell death.<sup>74-77</sup> ATP released by damaged neurons and glia cells within minutes

after ischemia can activate P2X7R on microglia to release pro-inflammatory cytokines.<sup>73,78-</sup>  
<sup>80</sup> The over-activation of P2X7R also produced excitotoxic neuronal death<sup>81</sup> and mediated ischemic damage to oligodendrocytes and myelin.<sup>82</sup> P2X7R-deficient mice have a pronounced attenuation of inflammatory responses, including chronic and neuropathic inflammatory pain.<sup>73</sup> Thus, purinergic receptors can be a vital connection between the nervous system and the immune system.

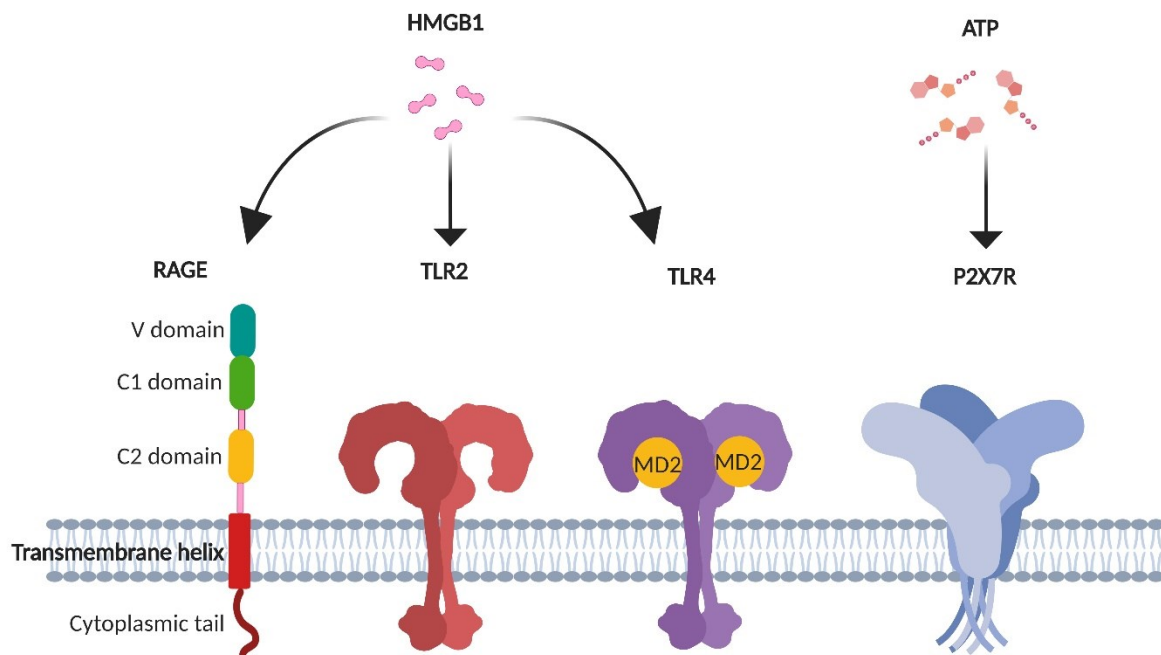


**Figure 1: Key receptors for alarmins.**

Cell surface receptors RAGE, TLR2, and TLR4 are the main receptors for HMGB1. P2X7R can bind to ATP and transduce the signals into cell plasma.

### **1.3 Immune system activation after stroke**

The cross-talk between immunity and stroke has been explored in depth, and it is known that stroke can engage both innate and adaptive immunity.<sup>56</sup> The immune system influences the brain after ischemic stroke, and stroke also contributes to the modulation of the peripheral immune system.

#### **1.3.1 Local brain inflammation after stroke**

Inflammation is a key pathophysiological process after ischemic stroke; it has been confirmed that local brain inflammatory processes after stroke can be induced by both clinical and experimental stroke.<sup>83,84</sup>

Microglial cells, as the resident macrophages of brain, are activated and increased in cell count up to 16 weeks after two-hour middle cerebral artery occlusion (MCAO) in rats.<sup>85</sup> The pro-inflammatory genes, including the cytokines genes *TNFA*, *IL1B* and *IL6*, and the chemokines genes interleukin-8 (*IL8*), interferon gamma-induced protein 10 (*IP10*) and monocyte chemoattractant protein-1 (*MCAP1*), are upregulated locally in brain tissue within hours after stroke.<sup>86-91</sup> There is solid evidence that, in response to ischemia, activated microglial cells and astrocytes are capable of releasing these pro-inflammatory cytokines and chemokines.<sup>92,93</sup> These pro-inflammatory molecules induce the primary neuroinflammation after stroke and exacerbate the initial brain lesion<sup>46</sup> (Figure 2).

The immune cells of the brain (microglia and dendritic cells) as well as neutrophils, macrophages, T cells, and other peripheral immune cells, which invade from the blood, can take part in tissue damage and secondary neuroinflammation.<sup>56</sup> Some of the sodium transporters are stimulated after ischemic stroke onset and result in edema and degradation of tight junction-constituent proteins and integrins, which may lead to increased paracellular leakage at the BBB.<sup>94</sup> Four to six hours after stroke onset, BBB breakdown becomes apparent. Afterward, inflammation contributes to continued barrier disruption.<sup>94</sup> Pro-inflammatory signaling expressed after stroke encourages vascular endothelial cells to express adhesion molecules, which generate blood monocytes, neutrophils, macrophages, and T cells that infiltrate the brain tissue with a consequent release of additional pro-inflammatory mediators and secondary brain injury.<sup>29,94-97</sup> Additionally, the accumulation of neutrophils and T cells in brain parenchyma can further enhance BBB permeability and worsen stroke outcomes.<sup>94</sup> Several experimental studies have demonstrated that the inhibition of leukocyte invasion into the ischemic brain can improve stroke outcomes.<sup>98-100</sup>

The way the local microglia, astrocyte, and peripheral immune cells are initially activated after stroke remains the key question in local brain inflammation. A bold hypothesis is that, when the initial inflammatory triggers are blocked after stroke, the inflammation after stroke is ablated. It has been reported that some of the alarmins, such as HMGB1, can be released after stroke.<sup>40,42,43</sup> Endogenous alarmins released from necrotic cerebral cells may be one of the primary triggers of local brain inflammation. Alarmins released from necrotic tissue can activate central immunocompetent cells and result in pro-inflammatory

cytokines and more alarmin secretion. These pro-inflammatory molecules can aggravate the brain lesion through primary neuroinflammation.<sup>46</sup> Moreover, alarmins and other pro-inflammatory molecules can pass into the peripheral circulation and cause the activation of peripheral immune cells. Secondary neuroinflammation is induced after the migration of these activated immune cells from the blood into the injured brain parenchyma<sup>46</sup> (Figure 2).

### **1.3.2 Peripheral immune system activation after stroke**

In addition to the inflammatory reaction in the brain, immunological alterations may exist in the bone marrow, spleen, blood, and other lymphoid organs. C- reactive protein, white blood cell counts, and the plasma concentration of pro-inflammatory cytokines (TNF- $\alpha$ , IL-6, and IL-1 $\beta$ ) have been detected at increased levels in patients with stroke and correlate with stroke outcome in most studies.<sup>101-103</sup> Six hours after experimental stroke, TNF- $\alpha$ , interferon-gamma (IFN- $\gamma$ ), IL-6, MCP-1, and IL-2 are secreted by activated splenic leukocytes.<sup>104</sup> Additionally, unstimulated splenocytes express increased chemokines and chemokine receptors, including macrophage inflammatory protein-2 (MIP-2), C-C chemokine receptor type 1 (CCR1), C-C chemokine receptor type 2 (CCR2), C-C chemokine receptor type 7 (CCR7), C-C chemokine receptor type 8 (CCR8), and interferon gamma-induced protein 10 (IP-10).<sup>104</sup>

While alarmins released after stroke can trigger local brain inflammation, these alarmins can also pass into the systemic blood circulation and mediate peripheral immune

activation<sup>46,65</sup> (Figure 2). When neutralizing antibodies block HMGB1, splenic expression and serum concentrations of pro-inflammatory cytokines were significantly attenuated.<sup>42</sup> Moreover, in vitro stimulation of splenocyte cultures with HMGB1 resulted in the increased expression of cytokine secretion.<sup>42</sup>

The majority of experimental and clinical studies have suggested that peripheral immune system activation has a deleterious role after stroke. Therefore, the antagonization of systemic pro-inflammatory molecules after stroke is a potential therapeutic approach to limiting cerebral tissue damage.<sup>103,105</sup>

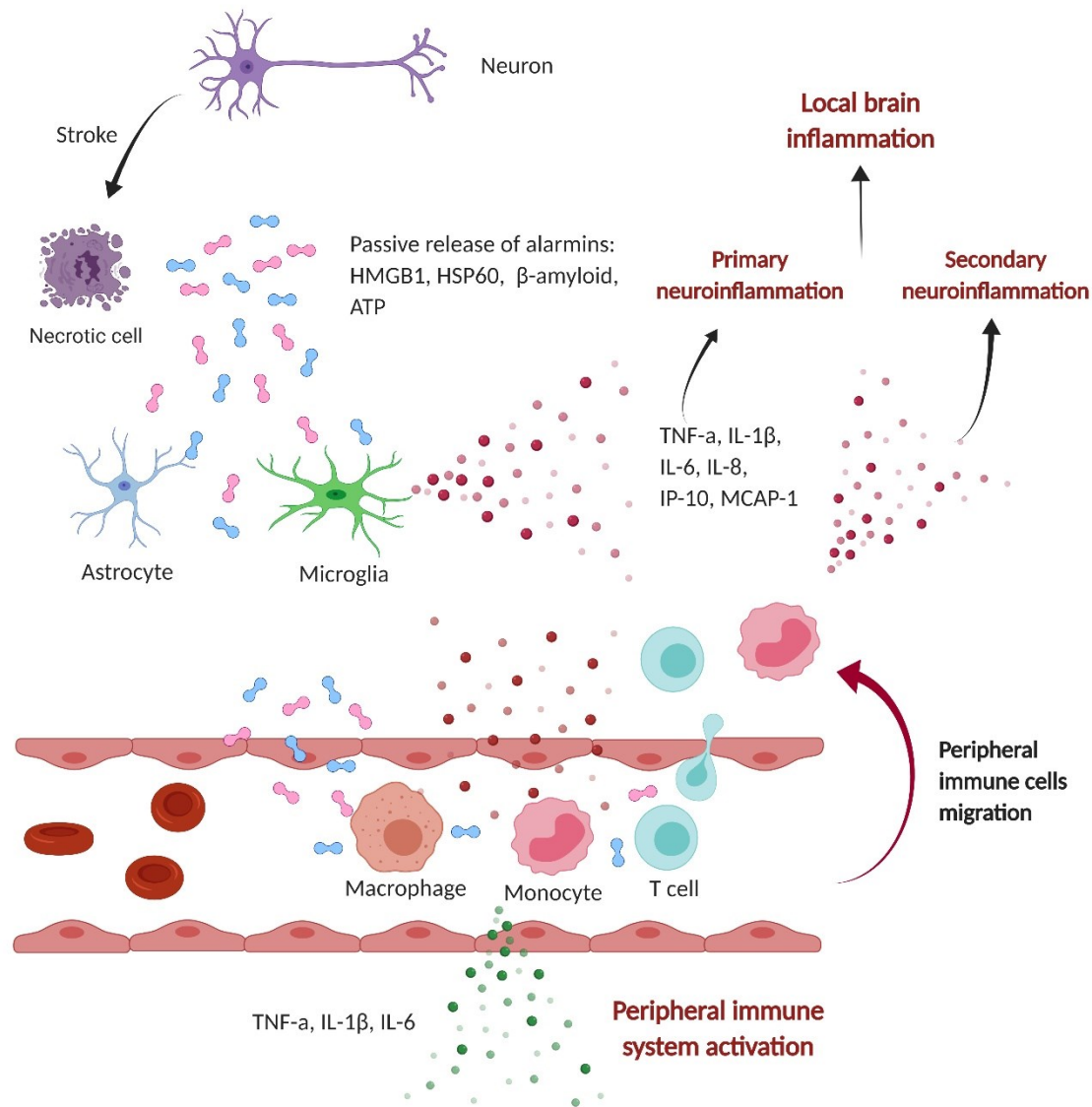


**Figure 2: Schematic diagram of immune system activation after stroke.**

Alarmins are passively released from necrotic cells after ischemic stroke onset and activate astrocytes and microglia in the surrounding tissue of the infarct core. Activated microglia and astrocytes release pro-inflammatory molecules and lead to primary neuroinflammation. Alarmins and pro-inflammatory cytokines pass into the peripheral circulation and induce peripheral immune cell activation. Some of the activated monocytes and lymphocytes from the peripheral immune system migrate into the brain parenchyma, release pro-inflammatory molecules, and lead to secondary neuroinflammation. The other activated peripheral immune cells secrete pro-inflammatory cytokines and induce peripheral immune system activation.

### 1.3.3 Cytokine-induced sickness behavior (CISB)

Cytokines are a group of small glycoproteins produced by a broad range of cells; they modulate the balance between humoral and cell-based immune responses, and they can be upregulated after stroke in the brain and the peripheral immune system. This release is a crucial feature of immune system activation after stroke. However, the hidden signaling of how these released cytokines impact the brain after stroke and the resulting pathophysiological implications remain unknown. TNF- $\alpha$ , IL-20, IL-1 $\beta$ , IL-10, IL-6, and tumor growth factor-beta (TGF- $\beta$ ) are the best-studied cytokines related to inflammation in ischemic stroke. Among these cytokines, IL-1 $\beta$  and TNF- $\alpha$  can exacerbate brain injury, while TGF- $\beta$  and IL-10 may be neuroprotective.<sup>106,107</sup>

In addition to brain damage, pro-inflammatory cytokines (IL-1 $\beta$ , IL-6, and TNF- $\alpha$ ) can also cause sickness behavior, which is a series of typical behavioral alterations including malaise, anxiety, lassitude, loss of appetite, depression, hyperalgesia, sleepiness, reduction in grooming, and failure to concentrate.<sup>108-110</sup> Sickness behavior was first reported in the context of infectious diseases, which have been investigated for decades.<sup>109</sup> PAMPs and peripheral cytokines induced by PAMPs can mediate behavioral changes, which has been confirmed in two main communication pathways. One is a neural pathway: peripheral cytokines activate afferent nerves, such as vagal nerves and trigeminal nerves, to project to the central nervous system (CNS).<sup>111-114</sup> The other is the humoral pathway: circulating PAMPs and cytokines induce the production and release of pro-inflammatory cytokines in



the circumventricular organs and choroid plexus, followed by the propagation of these immune signals into the brain parenchyma.<sup>115-119</sup>

In addition to infectious diseases, patients with stroke and other non-infectious diseases may also experience fatigue, sleep disorders, motivational inhibition, cognitive dysfunction, and depression.<sup>120,121</sup> In particular, post-stroke anxiety and depression can last from the acute stage until the chronic phase after stroke.<sup>122,123</sup> However, it remains unknown whether the pathways mentioned above induce sickness behavior after stroke. When the pro-inflammatory cytokines are antagonized, the sickness behaviors after stroke were significantly improved.<sup>42</sup> This has led to a scientific interest in whether sickness behavior after stroke is also induced by peripheral cytokines. The same is true of PAMPs; alarmins released after stroke can also induce cytokine secretion by stimulating innate immune cells.<sup>65</sup> Both HMGB1 neutralization and the elimination of its receptor RAGE attenuated the loss of body weight and hypothermia after stroke, which are the basal sickness markers in immune-mediated disease models.<sup>42</sup> These findings support the hypothesis that sickness behavior after stroke may share the same pathway as infectious diseases, and it suggests the need for further investigations of CISB beyond focal deficits after stroke. In order to delve into this topic, a sensitive, specific behavior test battery is needed to provide the opportunity to observe behavioral improvements over time and monitor pharmaceutical treatment effects. In the literature, dozens of behavior tests have been identified for assessing sickness behavior, but those available tests do not simplify the choice of tests for specific time points after stroke.<sup>124,125</sup> Thus, it is crucial to characterize different behavioral

aspects after stroke and to summarize a battery of behavioral acquisition approaches with the optimal choice of tests at specific time points after stroke.

## **1.4 Immunosuppression after stroke**

Immune activation in the acute phase after stroke is followed by dramatic immunosuppression, which is characterized by splenic atrophy, lymphopenia, the reduced functional activity of monocytes, anti-inflammatory cytokines upregulation, and apoptosis of lymphocytes.<sup>126-129</sup> This stroke-induced immunosuppression increases stroke patients' susceptibility to infection; moreover, it is the most frequent medical complication after stroke, and it is an major cause of death and secondary morbidity.<sup>130-133</sup> It has been noted that post-stroke immunosuppression could be a double-edged sword that increases the incidence of infections and limits the development of a pro-inflammatory response to the brain.<sup>56</sup> The mediation of systemic immunosuppression after stroke is still not fully understood. There is proof that sympathetic activation and the accompanying release of glucocorticoids and catecholamine are possibly involved.<sup>83,134</sup>

### **1.4.1 Stress mediators**

The sympathetic nervous system (SNS) innervates the spleen, bone marrow, the thymus, and lymph nodes.<sup>135,136</sup> It has been proposed that post-stroke immunosuppression is due to the over-activation of SNS or hypothalamic-pituitary-adrenal axis (HPA), which can induce leukocytes apoptosis in the peripheral immune system.<sup>133</sup> Catecholamines,

acetylcholine, and glucocorticoids can be released after SNS and HPA activation, and they all have immunosuppressive functions on different peripheral immune cells.<sup>137-141</sup> The over-activation of the SNS after stroke also primes liver resident invariant natural killer cells (NK cells) to secrete the anti-inflammatory cytokine IL-10, which can enhance immunosuppression.<sup>142</sup> Nonetheless, a clinical research has found intermediate increases of stress mediators after severe brain injuries, and none of the stress mediators was an independent predictor of post-stroke lymphocytopenia and bacterial infections.<sup>132</sup> A previous animal study has found that the glucocorticoid receptor blocker RU486 did not prevent post-stroke lymphocyte dysfunction (i.e., a decrease of IFN- $\gamma$  and an increase of IL-4 production) and bacterial infections.<sup>133</sup> Moreover, lymphocytopenia after experimental stroke was not prevented by the blockade of beta-adrenergic receptors in vivo and in vitro.<sup>143</sup> Nevertheless, recent results indicate that the soluble mediator HMGB1, which is released from the necrotic brain tissue, might be the initial event that triggers a multi-phasic systemic immune reaction after stroke.<sup>42</sup> Hence, pro-inflammatory indicators mediated by brain-released alarmins could bring a new connection for brain-immune interaction that also contributes to immunosuppression after stroke.<sup>46</sup>

#### **1.4.2 Soluble mediators**

HMGB1 passively released from necrotic brain tissue can behave as a cytokine, promoting inflammation and inducing inflammatory cytokine expression. Recombinant HMGB1 prompts the induction of TNF- $\alpha$ , IL-1 $\beta$ , cyclooxygenase-2 (COX-2), and inducible nitric oxide synthase (iNOS), and it also increases ischemic death of neurons in vitro.<sup>144</sup> The

microinjection of fully reduced recombinant HMGB1 into the parietal cortex of mice increases pro-inflammatory mediator transcript levels and sensitizes the tissue to ischemic damage.<sup>145</sup> The main receptors for HMGB1 are RAGE, TLR2, and TLR4. A recent study has shown that RAGE and the protein MyD88 deficiency can prevent splenic and circulating blood lymphocyte reduction after brain ischemia.<sup>42</sup> This finding suggests that HMGB1 partially mediates the immunosuppressive effect after ischemic stroke through the RAGE and TLR-MyD88 pathways. In addition, alarmins can stimulate TLR-MyD88 to mediate NF- $\kappa$ B pathway activation, which acts as the first signal (priming) that promotes the transcription of several genes that encode inflammatory mediators.<sup>74</sup> However, the complete molecular pathways underlying post-stroke immunosuppression are still largely unknown and require further investigation. Further, other soluble mediators induced by acute brain damage might be related to the peripheral immune alteration.

### **1.4.3 Pyroptosis in lymphopenia**

Lymphopenia is a key feature of immunosuppression after ischemic stroke, and previous studies have found that lymphopenia could be because of lymphocyte death after stroke.<sup>129,133</sup> Several cell death forms have been established, including apoptosis, necrosis, pyroptosis, entosis, autophagy, and cornification. Among these means of cell death, pyroptosis is a newly identified pro-inflammatory form. It was first discovered in infection in 1992,<sup>146</sup> but numerous studies have shown that it also occurs in sterile inflammation, including myocardial ischemia/reperfusion, renal ischemia/reperfusion, Alzheimer's disease, traumatic brain injury, diabetic atherosclerosis, and temporal lobe epilepsy.<sup>147-152</sup> The

progress of pyroptosis depends primarily on the activation of inflammatory caspases, including caspase-1 (canonical pathway) or caspase-4/5/11 (non-canonical pathway).<sup>153</sup> In adjacent cells, alarmins released from necrotic cells function on cell membranes or intracellular receptors (PRRs) to induce inflammasome formation and activation of caspase-1 or caspase-11. Afterward, pyroptosis arises, and IL-1 and IL-18 are released.<sup>154-</sup>

157

Previous research has demonstrated that pyroptosis can occur in microglia following ischemic stroke, which is resident macrophage that serves to provide the primary immune defense in the brain.<sup>158</sup> Nevertheless, there is still a lack of evidence demonstrating that peripheral lymphocytes develop pyroptosis after stroke. In the non-canonical pathway, LPS binds to precursor caspase-4/5/11 in the cytosol of bacteria-infected cells, which contributes to the activation of caspase-4/5/11. However, the sterile inflammatory substances (alarmins) mainly activate caspase-1 to lead to the canonical inflammasome pathway.<sup>154</sup> The immune reaction after stroke is also considered sterile inflammation, and a canonical pathway of pyroptosis in lymphocytes could be a potential mechanism of lymphopenia after stroke. The progression of pyroptosis depends primarily on the activation of inflammatory caspases,<sup>153</sup> and in a sterile environment (stroke), caspase-1 plays a critical role that is primarily activated to lead to the canonical inflammasome pathway.<sup>154</sup> Caspase-1 activation usually arises in the inflammasome (a multi-protein complex), which contains three components: sensor-PRRs in the cytoplasm; effectors, the caspase-1 precursor (pro-caspase-1); and an apoptosis-associated, speck-like protein

containing a CARD (ASC), which is an adaptor protein that connects PRRs and pro-caspase-1.<sup>154</sup> Inflammasome activation has been demonstrated in macrophages,<sup>159</sup> dendritic cells,<sup>160</sup> microglial,<sup>161</sup> epithelial cells,<sup>162</sup> neutrophils,<sup>163</sup> monocytes,<sup>164</sup> and T cells.<sup>165</sup> Some inflammasomes need two distinct steps: priming (signal 1) and inflammasome assembly (signal 2) to activate inflammasome. Priming involves the activation of MyD88 and the NF- $\kappa$ B pathway, which upregulate the expression of inflammasome components.<sup>166</sup> However, the mechanism and complete molecular pathways underlying lymphopenia after ischemic stroke are still not clear and require further investigation.

## **2 The aims of this study**

The aim of this study is as follows: (1) To characterize different behavioral aspects after large experimental stroke with a broad battery of behavioral acquisition approaches; (2) to optimize the choice of behavior tests at specific time points after stroke; (3) to investigate the role of the peripheral cytokines released in the acute phase after stroke in sickness behavior; (4) to explore the molecular pathways underlying post-stroke immunosuppression; and (5) to investigate the mechanism of peripheral immune cell death after stroke.

### 3 Materials and methods

#### 3.1 Materials and research animals

##### 3.1.1 Instruments

Equipment	Manufacturer
Centrifuge	Eppendorf
Laser Doppler Monitor and Probes	Perimed
DC Temperature Control System	FHC
Isoflurane Vaporizer	Harvard Apparatus UK
Surgery Instruments	F.S.T
Cylinder test	Evonik chemie
RotaRod	TSE systems
Von Frey filament	Bioseb
Elevated Plus Maze	Noldus
Open Field	Noldus
Porsolt Swim Test	Biobserve Viewer
Automated Cell Counter	BioRad
MagniSort® Magnet, 5ml	Invitrogen



### 3.1.2 Reagents and materials

General Reagents and Materials	Catalog Number	Manufacturer
Iso-Vet 1000 mg/g	AP/DRUGS/220/96	Piramal Healthcare UK Limited
Silicon-Coated Filament	701912PKRe	Docol
MagniSort® Mouse T cell Enrichment Kit	8804-6820	eBioscience
RPMI Media 1640	11875093	ThermoFischer
Fetal Bovine Serum	10270-106	ThermoFischer
Penicillin Streptomycin	15140-122	ThermoFischer
7-AAD Red Fluorescent Live/Dead Stain	6163	ImmunoChemistry Technologies
Propidium Iodide Stain	638	ImmunoChemistry Technologies
Caspase-1 Subfamily Inhibitor VX-765	inh-vx765-5	InvivoGen
Cresyl Violet acetate	C5042-10G	Sigma-Aldrich

### 3.1.3 Antibodies

Antibody	Clone	Manufacturer
Anti-CD3 FITC or APC	17A2	eBioscience
Anti-CD45 eF450	30-F11	eBioscience
Anti-IL-1 $\beta$	B122	Bio X Cell
Anti-TNF- $\alpha$	XT3.11	Bio X Cell
Anti-IL-6	MP5-20F3	Bio X Cell

### 3.1.4 Research animals

All experiments of animal were undertaken within the guidelines for the use of laboratory animals and were authorized by the Upper Bavaria Government Committee (Regierungspraesidium Oberbayern). Wild-type C57BL/6J (six- to eight-week-old male) mice were purchased from Charles River Laboratories (Sulzfeld, Germany). Caspase-1<sup>-/-</sup> Caspase11<sup>tg167</sup>, MyD88<sup>-/-168</sup>, and RAGE<sup>-/-169</sup> mice were bred in our Institute's in-house breeding facility under specified, pathogen-free conditions. Germ-free C57BL/6J mice were acquired from the Clean Mouse Facility of University of Bern (Bern, Switzerland). I excluded data from all mice that died during or after surgical procedures. Animals were randomized in the treatment groups, and data was analyzed by me and other investigators who were blinded to group allocation. Unblinding was completed once statistical analysis had been finished.

## 3.2 Methods

### 3.2.1 Filamentous middle cerebral artery occlusion (fMCAo)

fMCAo and sham surgeries were performed according to the previous protocols established by our lab.<sup>170,171</sup> Mice were anesthetized with isoflurane (Iso-Vet 1000 mg/g, catalog# AP/DRUGS/220/96, Piramal Healthcare UK Limited) delivered in a mixture of 1/3 O<sub>2</sub> and 2/3 N<sub>2</sub>O using a vaporizer (Harvard Apparatus UK). To reveal the temporal bone, I produced an incision between the ear and the eye. To measure blood flow during operation, a laser Doppler probe (Perimed) was attached to the skull above the left middle cerebral artery (MCA) territory. The mice were then positioned in the supine position, an incision of the midline neck was produced, and the common carotid artery (CCA) and the left external carotid artery (ECA) were isolated and ligated, and the third loose knot on the CCA was formed. The left ICA was isolated and clipped by a microvascular clip. Next, a 2mm silicon-coated filament (catalog #701912PKRe, Doccol) was inserted into the ICA through a small incision in the CCA, finally occluding the MCA after opening the clip on the ICA. The occlusion of MCA was indicated by a decrease in blood flow (decreased value of the laser Doppler flow signal <20% of baseline value). The third knot on the left ICA was closed to fix the filament in position. During the surgery, body temperature of each mouse was maintained at 36.5°C±0.5°C using the DC Temperature Control System. Mice were kept in a heated cage while recovering from anesthesia. The mice were re-anesthetized after 60 minutes of occlusion, and the filament was removed from CCA. The mice were held in their home cage after recovery, with enabled access to food and water.

The same surgical procedure was provided to sham-operated mice, except that the filament was immediately removed after insertion. Exclusion criteria were as follows: (1) insufficient occlusion of MCA (decrease in blood flow to  $> 20\%$  of baseline value); (2) death during the operation; and (3) lack of brain ischemia by histological examination. One hour after reperfusion, a stroke evaluation score was collected. A score from 0 (no stroke) to 5 (very severe stroke) based on general activity and body asymmetry ("modified Bederson Score") was performed to assess the deficits of mice after surgery.<sup>172</sup> The animals were checked daily after surgery for signs of discomfort.

### **3.2.2 Mouse blood collection and preparation**

Mice were deeply anesthetized with a mixture of ketamine (120 mg/kg) and xylazine (16 mg/kg). Blood was collected by intracardiac puncture and placed in tubes containing anticoagulant EDTA for FACS or plasma preparation, or collected in covered test tubes for serum preparation. When preparing serum, the blood (in covered test tubes) was placed at room temperature for 15 minutes to clot and subsequently centrifuged at  $2000 \times g$  for 10 minutes in a refrigerated centrifuge. The resulting supernatant was designated serum. For plasma preparation, the blood (in EDTA tubes) was centrifuged for 10 minutes at  $3000 \times g$ . The resulting supernatant was designated plasma.

### **3.2.3 Mouse organ sample collection and process**

Mice were deeply anesthetized with a mixture of ketamine (120 mg/kg) and xylazine (16 mg/kg). After blood collection, mice were then transcardially perfused with normal saline, and spleens were removed into the cold PBS. Brains were then removed carefully and frozen on dry ice and stored at -80°C for later use.

### **3.2.4 Behavior tests**

#### **3.2.4.1 Body weight and body temperature**

To evaluate the general condition of the mice, their body weight and body temperature were measured before and on relevant days after fMCAo or sham surgery. Body weight was measured using an electronic weight scale, and rectal temperature was measured by a mouse rectal thermometer.

#### **3.2.4.2 Neuroscore**

The Neuroscore was used to assess the general condition deficits and focal neurological deficits of mice after experimental stroke. It was performed before and on the relevant days after fMCAo and sham surgery, and it was performed as described.<sup>173</sup> The score ranged from 0 (no deficits) to 56 (poorest performance) and was calculated as the sum of the general and focal deficits (scoring sheets are in Appendix).

### **3.2.4.3 Cylinder test**

This test evaluates the use of the forepaws and body asymmetry by assessing behavioral imbalance and general activity at baseline and postoperative time points. Mice were positioned in a transparent acrylic glass cylinder (diameter 8 cm; height 25 cm), which was placed in front of a 90-degree mirror. The movement of mice in the cylinder was videotaped for five minutes. To assess independent forelimb use and body asymmetry, we calculated the contact to cylinder wall and ground by each forelimb during the mice's complete rearing and landing by watching the recorded videos frame by frame. All rearing movements were also recorded and used as an indicator of the overall activity of the mice.

### **3.2.4.4 RotaRod**

Mice were trained daily for three days before baseline acquisition and surgical procedures (fMCAo or sham). Baseline performance was acquired using the following strategy: the rod accelerated continuously from 8 to 40 rpm over 240 s. Per mouse and time point, three consecutive trials were acquired. The latency to fall off the rod was recorded. The post-operative performance was evaluated by dividing the post-operative values by the baseline performance of the individual mouse.

#### **3.2.4.5 Adhesive removal test**

This test was used for assessing sensory and motor deficits. A round adhesive sticker (4 mm-diameter) was applied on the forepaw's palmar side; the same pressure was put when sticking each adhesive sticker. Two days before baseline acquisition, mice were habituated to the test cage and the adhesive placement. Baseline and postsurgical time points were acquired as three consecutive trials per mouse. The latency to contact the adhesive and the latency to remove the adhesive were recorded. The latency to contact the adhesive on the impaired paw was recorded to evaluate sensory deficit, and the latency to remove the adhesive was influenced by both sensory and motor deficits.

#### **3.2.4.6 Von Frey filament test**

This test evaluates the sensory deficits of the forepaws after brain injury. Mechanosensitivity can be determined as a threshold of force required to provoke a behavioral response, such as removing the stimulated paw. In up-down test methods, a lack of response to a specific filament strength determines that the next higher strength filament is used in the subsequent stimulus, whereas a positive response determines the use of the next lower strength filament.

#### **3.2.4.7 Elevated plus maze**

The elevated plus maze test was performed according to the protocol established before.<sup>174</sup> The apparatus used for the elevated plus maze test was in the shape of a plus sign and

consisted of two open arms (25 x 5 cm) that were vertical to two closed arms (25 x 5 cm) with a center open square (5 x 5 cm). Each closed arm was enclosed by 16 cm high wall. The whole apparatus was 50 cm above the floor and was made of plastic. All the experimental mice were moved to the test room 30 min before the first trial to habituate to the environment of the test room.<sup>174</sup> A mouse was placed in one open arm with its head directed toward the central area. The elevated plus maze test was filmed using a video camera attached to a computer. In each trial, each mouse was allowed to move freely in the elevated plus maze for 5 min. We performed one trial at each time point. The application used for acquiring and automatically analyzing the behavioral data was EthoVision XT. The number of entries (an entry is defined as the center point of the mouse entering the arm) into each arm, and the time spent in the open arms and closed arms was recorded and analyzed.

#### **3.2.4.8 Open field**

The open field test was performed according to the protocol established before.<sup>175</sup> The apparatus consisted of four activity chambers. Each chamber (50 x 50 cm) was enclosed by 38 cm high wall and made of plastic. A series of 10x10 cm blocks were identified, and the central area consisted of nine blocks, while the peripheral area consisted of 16 blocks. A maximum of four individual mice could be recorded and tracked at the same time by using each chamber of the apparatus. All the experimental mice were moved to the test room 30 min before the first trial to habituate to the environment of the test room.<sup>175</sup> Mice were placed in the middle of the chamber to begin and were allowed to move freely in the



chamber for 5 min in each trail. Each mouse received three trials at each time point with at least 10 min intervals between the trails. The application used for acquiring and automatically analyzing the behavioral data was EthoVision XT. The time spent in the peripheral area and the central area was recorded and analyzed.

#### **3.2.4.9 Sucrose consumption test**

This test is used to evaluate the lack of interest in rewarding stimuli (i.e., anhedonia) of mice after brain injury. This test was performed with mice that were single-caged for 24 hours. Two drinking bottles were provided, one with plain water and the second one with 3% sucrose solution. To counteract any locational bias, the bottle position was changed after 12 h. After 24 h, fluid intake was calculated by the ratio of sucrose solution volume against the total volume of fluid intake.<sup>176</sup>

#### **3.2.4.10 Porsolt swim test**

This test is used to assess depression-like behavior. Mice were placed in an inescapable transparent tank filled with water ( $22\pm 2^{\circ}\text{C}$ ). The animals were videotaped for five minutes, and this test was only performed at postsurgical time points. The analysis was done frame-to-frame to define the periods in which mice either struggled to escape, swam to explore, or floated without active movements.<sup>177</sup>

### **3.2.5 Anti-cytokine treatment**

According to previous study,<sup>42</sup> the neutralization of circulating cytokines was accomplished by the intraperitoneal injection of 4mg/kg each of anti-IL-1  $\beta$ , anti-TNF-  $\alpha$ , and anti-IL-6 antibodies (all from Bio X Cell) in a total volume of 200  $\mu$ l PBS 60 minutes before stroke induction. Control mice received 300 g of isotype control antibody.

### **3.2.6 Preparation of cells from lymphoid organs and blood**

Mice were deeply anesthetized with a mixture of ketamine (120 mg/kg) and xylazine (16 mg/kg). Blood was collected by the intracardiac puncture and placed in tubes containing the anticoagulant EDTA. The mice were then transcardially perfused with normal saline, and spleens were removed into the cold PBS. The spleens were homogenized and filtered through 40  $\mu$ m cell strainers. The erythrocytes of both the blood and spleen samples were lysed with isotonic ammonium chloride buffer. Next, the samples were washed with PBS twice. The total count of cells per organ was calculated using an automated counter (BioRad). The total cell counts per  $\mu$ l blood were measured manually by a hemocytometer. The cell suspensions were then used for further experiments.

### **3.2.7 Flow Cytometry**

The cells were labeled with specific antibodies in compliance with the manufacturer's instructions and conducted with flow cytometry to quantify the different cell populations.

The following mouse antigen-specific antibodies were purchased from eBioscience: CD3 FITC or APC (17A2), CD45 eF450 (30-F11).

### **3.2.8 Magnetic-activated cell sorting (MACS)**

After preparing single-cell suspensions, cells were washed once in MACS buffer and then purified for CD3<sup>+</sup> T cells using commercially available MACS kits. We sorted T cells by negative selection (MagneSort® Mouse T cell Enrichment Kit, catalog #8804-6820, eBioscience) and manually separated cells with MagneSort® Magnet (Invitrogen) to avoid the touch of microbeads to targeted cells.

### **3.2.9 In-vitro assay**

T cells isolated from the spleens of wild-type naïve mice (by MACS) were cultured in 96-well plates with the medium (RPMI Media 1640+10%Fetal Bovine Serum+1%Penicillin Streptomycin). Each well contained 50,000 cells in 50µl volume. Serum from wild-type naïve, sham, and stroke mice was collected three hours after operations. Each well received 50ul serum from an individual animal. Eighteen hours later, dead cells were stained by 7-AAD (ImmunoChemistry Technologies, catalog #6163) or Propidium Iodide (PI; ImmunoChemistry Technologies, catalog #638) before analysis by flow cytometry.

### **3.2.10 Reducing circulating alarmins**

According to previous study,<sup>170</sup> mice were treated 30 min before surgery and four hours after surgery with an intraperitoneal bolus (4mg/kg) of soluble receptor for advanced

glycation end products (sRAGE) or a vehicle (saline) according to our previous study.<sup>170</sup> Mice were sacrificed 18 h post-reperfusion, and splenic and blood immune cells were analyzed by flow cytometry.

### **3.2.11 In vivo caspase-1 inhibition**

Mice were injected intraperitoneally with caspase-1 subfamily inhibitor VX765 (100 mg/kg in 15% Cremphor EL; catalog #inh-vx765-5, InvivoGen) or with vehicle 2 h before fMCAo or sham surgeries. Mice were sacrificed 18 h post-reperfusion, and splenic and blood immune cells were analyzed by flow cytometry.

### **3.2.12 Infarct volumetry**

According to the protocol we established before,<sup>171</sup> serial coronal cross-sections (20- $\mu$ m thick) were made in 400- $\mu$ m intervals after brain removal. The sections were stained under standard protocols with cresyl violet, and scanned at 600 dpi. In each section, the area of infarction was measured using ImageJ software (NIH). We performed an edema correction for infarct volume using the following formula: (Ischemic area) = (Direct lesion volume) - [(Ipsilateral hemisphere) - (Contralateral hemisphere)]. The total infarct volume was quantified by integrating the measured areas and intervals between the sections.

### **3.2.13 Statistical analysis**

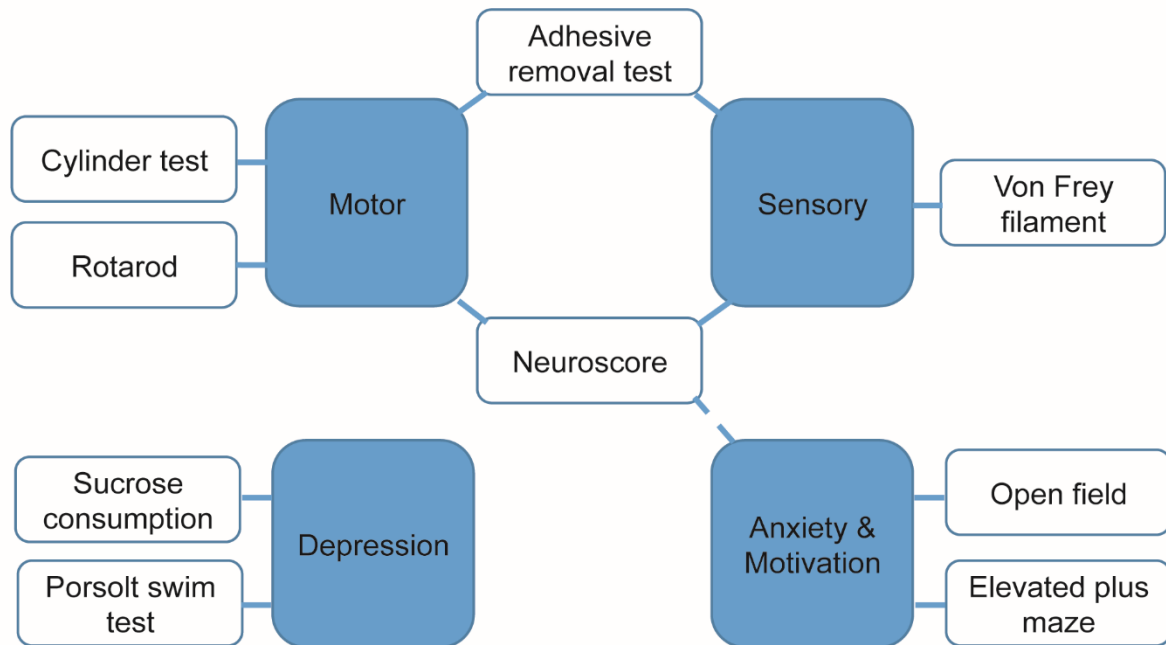
Data were analyzed using GraphPad Prism version 6.0, and all data sets were tested for normality. For unreplicated measured data, the groups with normally distributed data were

tested using a Student's t-test (for two groups) or ANOVA (for more than two groups); the groups without normally distributed data were analyzed using the Mann-Whitney U test (for two groups) or the Kruskal-Wallis test (for more than two groups). For repeated measured data, two-way ANOVA was used for analysis. Differences with a p-value  $<0.05$  were considered to be statistically significant.

## 4 Results

### 4.1 Immune activation after experimental stroke: CISB

Based on the published literature, we selected a battery of tests to assess different types of post-stroke behavior deficits up to 35 days after experimental stroke (Figure 3A). For focal deficits, we used the cylinder test, which was first developed by Schallert and has been proved efficient in detecting unilateral motor deficits of the forelimbs.<sup>178</sup> Rotarod, a motorized treadmill, was designed for the semi-automatic evaluation of motor coordination and balance functions.<sup>179</sup> The latency of rodents to fall off the rotating rod was recorded as a parameter of assessment.<sup>180</sup> An adhesive removal test can be used to assess motor and sensory deficits.<sup>181</sup> The time to sense and remove the adhesive was measured as an indicator of sensory and motor deficits. For a more detailed sensory deficit assessment, we used the von Frey filament test.<sup>182</sup> As the first indicator of sufficient neurological deficits, we used a 56-point Neuroscore to assess general and focal deficits after stroke;<sup>173</sup> it covered motor and sensory deficits and gave evidence of the lack of overall motivation after stroke. Anxiety and depression-like behavior after stroke were detected with elevated plus maze,<sup>183</sup> open field,<sup>184</sup> sucrose consumption test,<sup>185</sup> and the Porsolt swim test.<sup>186,187</sup> The time points to assess the above behavior tests and the general body condition (body weight and temperature) started seven days before the surgical procedures and lasted until 35 days after the surgical procedures (Figure 3B).

**A: Overview test battery****B: Time points for behavior assessment**

Timepoint	-7d	-3d	-1d		1d	2d	3d	4d	5d	7d	14d	21d	28d
Neuroscore			BL	<b>Stroke or Sham</b>	X		X	X	X	X	X	X	X
Cylinder test			BL		X		X			X	X	X	X
Rotarod			BL				X	X	X	X	X	X	X
ART			BL		X	X	X		X	X	X	X	X
Von Frey		BL								X	X	X	X
Open field		BL					X			X	X	X	X
EPM		BL					X			X	X	X	X
Sucrose cons.	BL									X	X	X	X
Porsolt swim										X			
Weight			BL		X	X	X	X	X	X	X	X	X
Temperature			BL		X	X	X	X	X	X	X	X	X

**Figure 3: Representative scheme of the behavior test battery.**

(A) Individual tests cover separate domains of typical post-stroke behavior deficits. To classify motor deficits, the cylinder test and Rotarod were used. The adhesive removal test also covered motor (adhesive removal) and sensory (sensing of adhesive) deficits after stroke. The von Frey filament test was the only test that exclusively covered sensory deficits. The 56-point composite Neuroscore included motor and sensory deficits. Moreover, it gave evidence of the lack of overall motivation after stroke. Elevated plus maze and open field included the anxiety and motivation domains. Depression was acquired using the Porsolt swim test, which shows behavior aspects in inescapable situations, and the sucrose consumption test, which was used to detect possible changes in anhedonia after stroke. (B) Time points to assess the behavior tests from the battery above and the general body condition (body weight and temperature). ART, adhesive removal test; EPM, elevated plus maze; BL, baseline.

#### **4.1.1 Motor and sensory deficits can be quantified by behavior tests after experimental stroke**

To characterize CISB and the progression of focal deficits up to 35 days after surgery, six- to eight-week-old male C57BL6/J mice received either a 60 minutes fMCAo or a sham operation (Figure 4A, B). Body weight loss and hypothermia, key indicators of CISB,<sup>108</sup> were monitored during the experimental period of 28 days (Figure 4C, D).



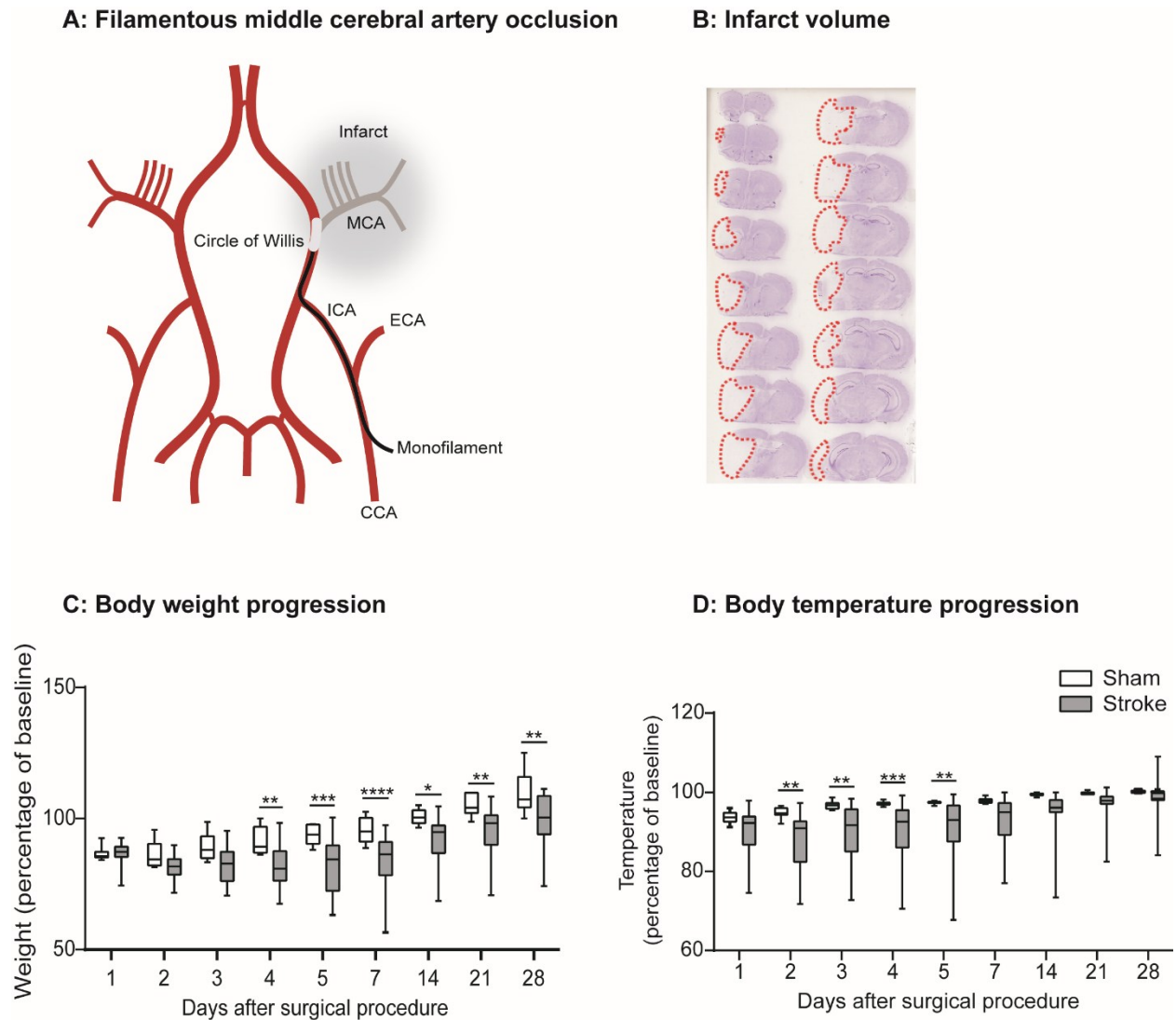


**Figure 4: Characterization of filamentous middle cerebral artery occlusion and the general body condition after the surgical procedures.**

(A) Schematic overview of the procedure of filamentous middle cerebral artery occlusion (fMCAo). A silicon-coated monofilament was introduced via the CCA and placed via the ICA at the bifurcation of the MCA for 60 minutes. (B) Representative cresyl violet brain sections of a transient MCA stroke; the imaginary red line surrounds the area of ischemic infarction. (C) Body weight progression within one month after stroke or sham surgery represented as a percentage of weight before the surgical procedure (two-way ANOVA,  $n=10-25$  per group). (D) Body temperature progression within one month after stroke or sham surgery represented as a percentage of initial temperature before the surgical procedure (two-way ANOVA,  $n=12-25$  per group). (C)-(D) data are shown as box plots with mean + min to max. \* $P<0.05$ , \*\* $P<0.01$ , \*\*\* $P<0.001$ .

Motor deficits could be detected after experimental stroke with the well-established test paradigms of the cylinder test and Rotarod in stroke mice compared to sham-operated mice. The cylinder test exhibited forelimb asymmetry during rearing movements up to 21 days after stroke compared to sham mice (Figure 5A). The latency to fall from the accelerating Rotarod decreased after stroke (Figure 5B). Differences in latency to fall could be detected up to 28 days after stroke compared to sham-operated mice. Both tests provided convincing information about motor deficits in mice with large ischemic stroke until the chronic phase of stroke outcome.

To evaluate both somatosensory and motor outcomes, the adhesive removal test was applied. An increase of latency to remove the adhesive from the impaired paw in the acute phase after stroke was detected within the first two days after stroke (Figure 5D). Moreover, the latency to contact the adhesive on the impaired paw was increased up to seven days after stroke (Figure 5C). For further analysis of sensory deficits, the von Frey filament test was conducted to evaluate the change of the impaired paw's sensory threshold after stroke. This was achieved by stimulating mouse paws with different sizes of monofilaments that provided different forces to a mouse paw. We found the threshold for paw retraction due to pain sensation was significantly higher in stroke-impaired paws seven days after surgery in comparison with stroke unimpaired paws and sham paws (Figure 5E).

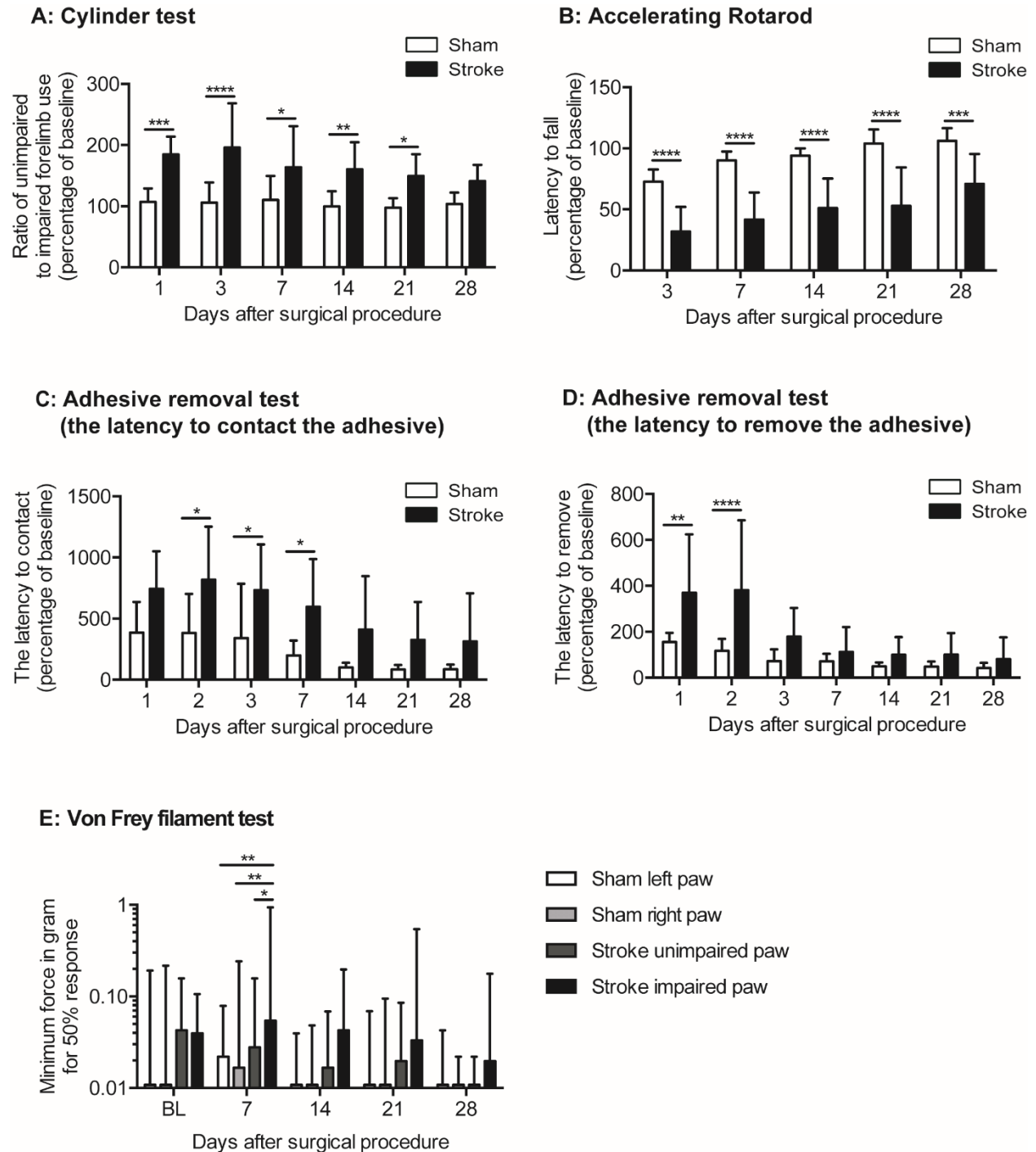


**Figure 5: Assessment of motor and sensory deficits up to 28 days after experimental stroke.**

(A) Quantification of cylinder test performance as forelimb use asymmetry up to 28 days after sham or stroke. The ratio of unimpaired to impaired forelimb use was calculated at each time point, and the values are shown as a percentage of the baseline (two-way ANOVA,  $n=10-11$  per group).

(B) Accelerating Rotarod for general motor deficit assessment up to 28 days after the surgical

procedure. Performance is shown as time spent on the rod (latency to fall) normalized to baseline performance (two-way ANOVA, n=10-12 per group). (C) Quantification of the adhesive removal test for the latency to contact the adhesive on stroke-impaired paws normalized to baseline performance (two-way ANOVA, n=10-11 per group). (D) Quantification of the adhesive removal test for the latency to remove the adhesive on stroke-impaired paws normalized to baseline performance (two-way ANOVA, n=10-11 per group). (E) Quantification of the von Frey filament test shown as the threshold for paw retraction due to pain sensation (the minimum force that was needed to obtain at least a 50% response throughout the attempts). Both front limbs of sham- and stroke-operated mice were compared up to 28 days after surgery (two-way ANOVA, n=10-11 per group). (A)-(D) data are shown as mean  $\pm$  standard deviation (SD); (E) data are shown as median  $\pm$  range. \*P<0.05, \*\*P<0.01, \*\*\*P<0.001, \*\*\*\*P<0.0001.

A 56-composite Neuroscore was performed to quantify the overall deficits after stroke. As with previous tests, the Neuroscore also detected noticeable focal deficits up to seven days after surgery (Figure 6A). Accompanied with focal deficits, general deficits after stroke (in the aspects of fur, ears, eyes, posture, spontaneous activity, and epileptic behavior) were also very prominent up to seven days in comparison with sham-operated mice (Figure 6B). These general deficits are not the specific characteristics of stroke but can reflect the basic sickness status. The sum of focal and general deficit scores can provide immediate information regarding whether the induction of experimental ischemia leads to sufficient neurological impairment (Figure 6C). Taken together, these analyses demonstrate and characterize severe focal and general deficits after large experimental stroke.

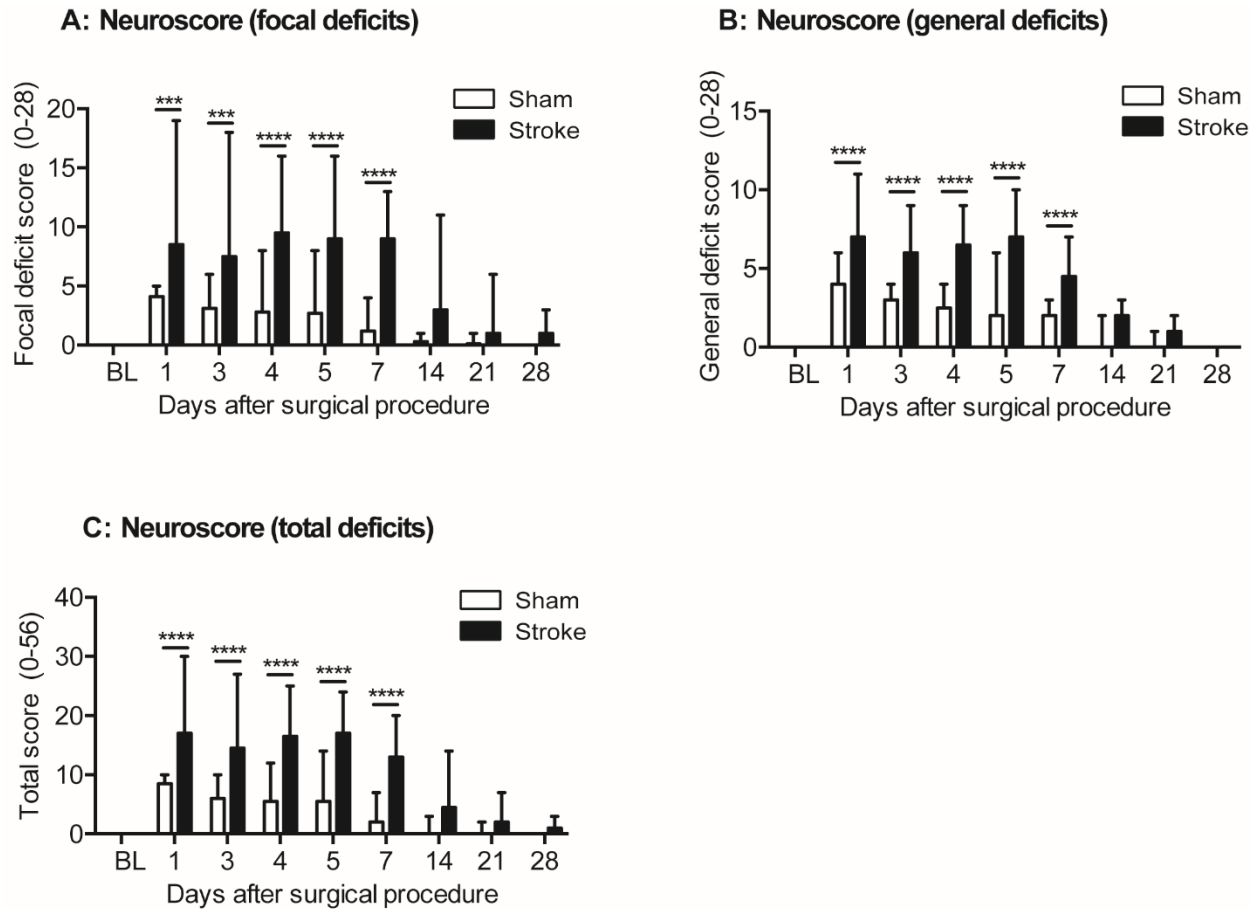


**Figure 6: 56-point composite Neuroscore: general and focal deficits.**

(A) Quantification of focal deficits acquired within the Neuroscore (two-way ANOVA,  $n=10-16$  per group). (B) Quantification of the general deficit section of sham- and stroke-operated mice (two-way ANOVA,  $n=10-16$  per group). (C) The total score represents the addition of general and focal deficits to achieve an overall score (two-way ANOVA,  $n=10-16$  per group). All graphs are shown as median  $\pm$  range. \* $P<0.05$ , \*\* $P<0.01$ , \*\*\* $P<0.001$ , \*\*\*\* $P<0.0001$ .

#### 4.1.2 Anxiety and depression can be detected after experimental stroke

As is mentioned above, sickness behavior includes a lack of motivation and a higher level of anxiety. In order to assess the level of anxiety after stroke, elevated plus maze and open field were conducted on both sham- and stroke-operated mice. These two tests are based

on the instinctive aversion of rodents to open spaces and a preference to stay in enclosed or bounded spaces.<sup>175,188</sup> An increase in the proportion of time spent in the open arms or central field can indicate anxiety reduction and increased exploratory activity. In the elevated plus maze, the ratio of time duration in the open arms to the closed arms steadily decreased within 14 days after stroke (Figure 7A, left panel). In addition, the frequency of entries into the open arms decreased in this period (Figure 7A, right panel). In the second setup for exploratory activity, open field, the ratio of time duration in the central to wall area in the open field was also reduced (Figure 7B left panel). Furthermore, the overall distance moved per trial continued to decrease over the whole experimental period of 28 days (Figure 7B right panel), which indicates reduced activity after stroke. Moreover, the Neuroscore also gave evidence of a lack of overall motivation after stroke (Figure 6B). These results revealed an anxiety-like behavior and reduced motivation after experimental stroke.

Rodents and other mammals have an innate preference for sweetened food or liquid.<sup>189</sup> The reduced ability to experience pleasure (including sweet consumption) was defined as anhedonia, which is one of the core features of depression.<sup>190</sup> Based on this rationale, the sucrose consumption test is often applied to evaluate depression-like behavior in different disease models. The previous research on depression-associated behavior in experimental epilepsy has shown that, when mice are offered both tap water and sweetened fluid, a healthy subject prefers the sweetened fluid, while an anhedonic animal consumes less of the sweet solution but an equal amount of tap water.<sup>176</sup> According to the usage of the

sucrose consumption test in previous studies, we conducted this test to investigate the depression-like behavior in experimental stroke. Our results showed that, after experimental stroke, mice consumed less sucrose liquid compared to sham-operated mice up to 14 days after stroke (Figure 7C).

Moreover, the Porsolt swim test was also performed to assess the mice's response to an inescapable situation. The Porsolt swim test was first developed by Porsolt and colleagues in 1977 to investigate the effect of antidepressant treatment on rodents.<sup>191,192</sup> It sets up a situation in which “behavioral despair” is induced, and the animal loses hope of escaping from the water tank. As with the sucrose consumption test, some studies have also performed it to measure post-stroke depression.<sup>186,187</sup> In our experiment, we found that, after stroke, mice showed a lower urge to escape the water tank. However, this effect could only be detected within the first 90 seconds after starting the experiment. (Figure 7D). This finding can be interpreted as “behavioral despair” and further confirms the presence of depressive disorders after stroke.<sup>191,192</sup>

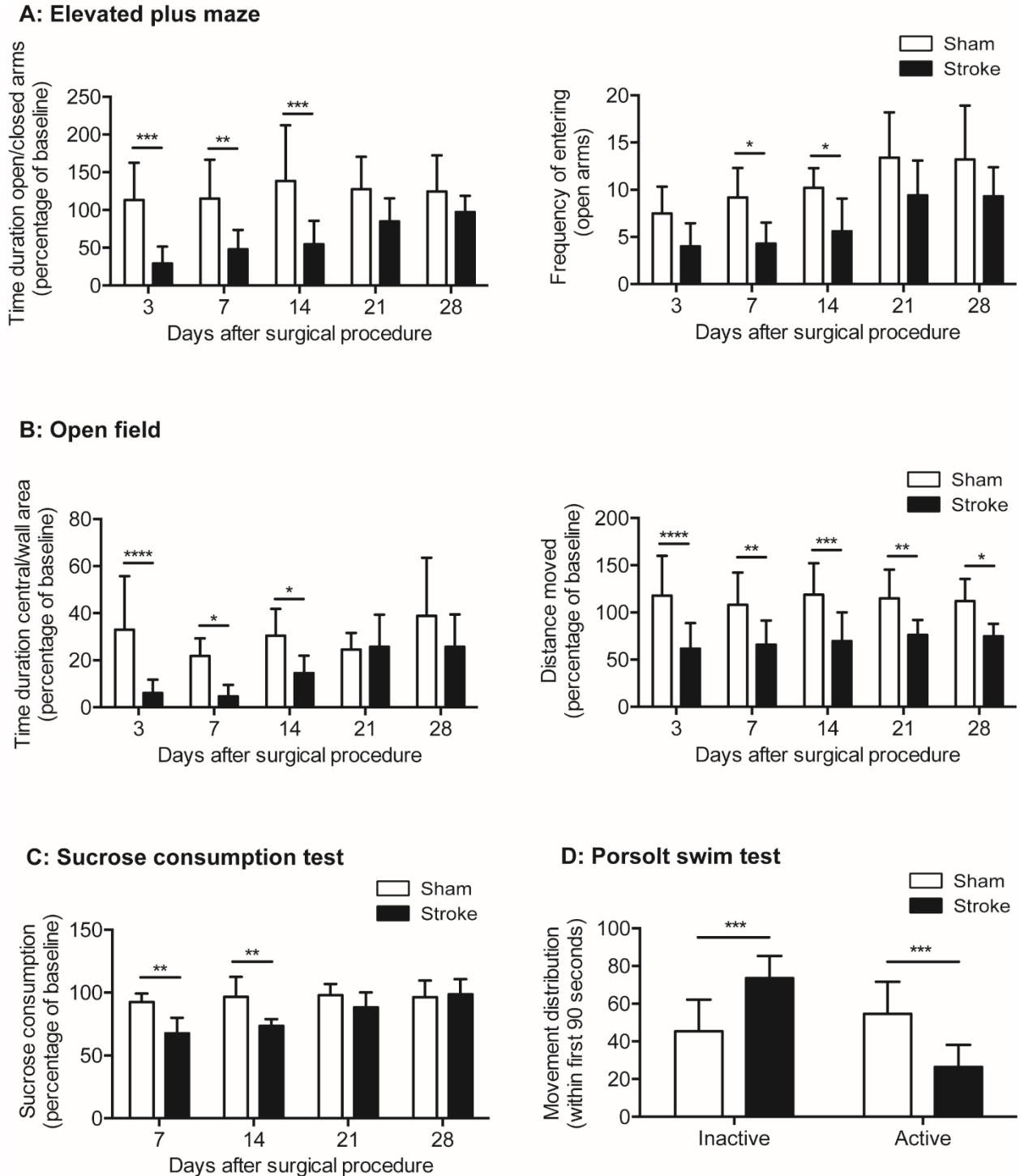


**Figure 7: Assessment of anxiety, motivation, and depression-like behavior after stroke.**

(A) Elevated plus maze was performed throughout 28 days after the operation. Exploration activity was quantified as a ratio of time spent in the open arms divided by time spent in the closed arms normalized to the baseline (left panel, two-way ANOVA,  $n=10$  per group). The quantification of



the frequency of entries into the open arms throughout the elevated plus maze trial (right panel, two-way ANOVA, n=10 per group). **(B)** Quantification of exploration activity acquired as time spent in the central area divided by time spent in the wall area normalized to the baseline (left panel, two-way ANOVA, n=11 per group). Quantification of the overall distance moved during open field trials normalized to the baseline (right panel, two-way ANOVA, n=10-12 per group). **(C)** Quantification of sucrose consumption; data is shown as a change in sucrose preference (ratio of sucrose solution volume to the total volume of fluid intake) after stroke or sham surgery compared to the baseline preference (two-way ANOVA, n=6 per group). **(D)** Quantification of the Porsolt swim test performance as the distribution of movement ability (active escape attempt versus inactivity) within the first 90 s of the trial (two-way ANOVA, n=8-10 per group). All graphs are shown as mean  $\pm$  SD. \*P<0.05, \*\*P<0.01, \*\*\*P<0.001, \*\*\*\*P<0.0001.

Together, these findings demonstrate that anxiety and depression-like behavior can be detected by behavior tests after experimental stroke.

#### **4.1.3 The sensitivity and specificity of different behavior tests**

To rate the behavior test panel at different time points after stroke, we ran the receiver operating characteristic (ROC) curve analysis for every test individually. This method is based on plotting the sensitivity of a test, which represents the probability of detection against the false positive rate, which is calculated as 1 – specificity. The area under the curve demonstrates the ability of the test to classify the stroke-induced deficits with the tests used correctly. We used all available time points and compared the area under the curve and p-value of the created ROC plots (Table1). Based on this analysis and the general advantages and disadvantages of the individual approach (stress for rodents, safety for animals, repetition, difficulty to perform, and time consumption), we developed a more accurate battery of behavior tests for each time point. The cylinder test, elevated plus maze, and sucrose consumption test were selected to assess motor deficits, anxiety, and depression-like behavior after experimental stroke. This battery could provide the ability

to classify a double-blind treatment approach against CISB within the first seven days after surgery against a control group.

**Table 1. ROC curve analysis of the behavior test battery**

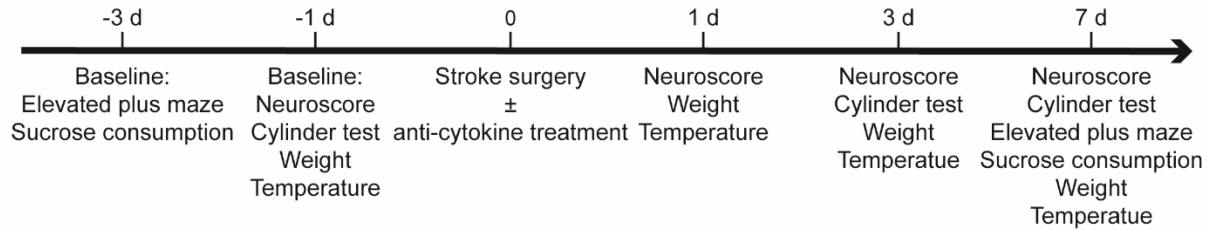
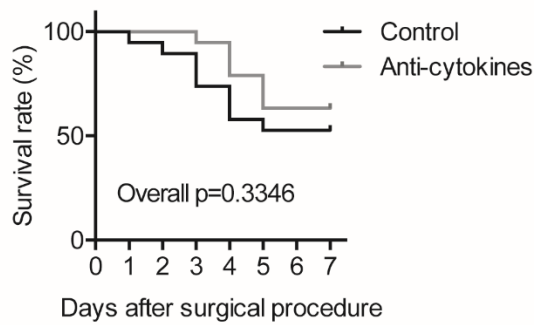
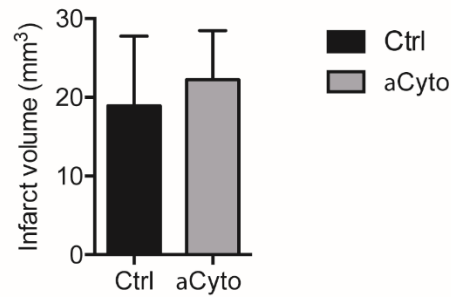
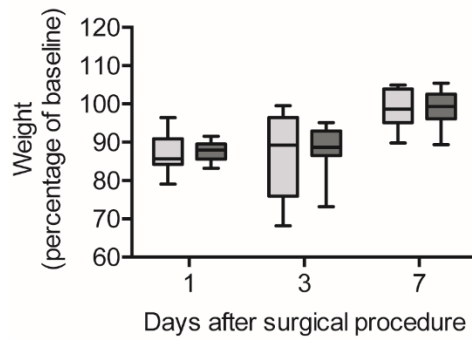
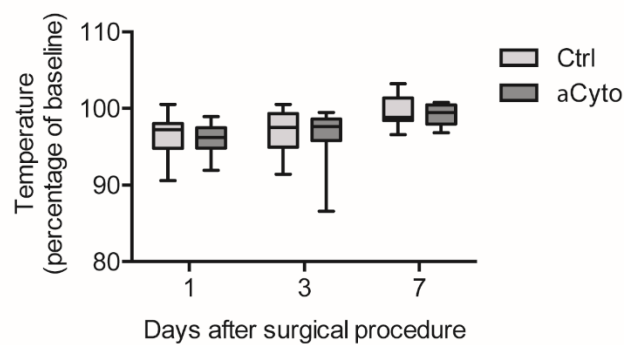
Time point	1 d	2 d	3 d	4d	5d	7 d	14 d	21 d	28 d
Cylinder test	1.0000	-	0.9182	-	-	0.8455	0.9364	0.9909	0.9273
Rotarod	-	-	0.9667	-	-	1.0000	0.98833	0.9500	0.9417
ART (the latency to remove)	0.8455	0.8364	0.7455	-	-	0.5909	0.7182	0.6182	0.5545
ART (the latency to contact)	0.8091	0.8364	0.9000	-	-	0.9364	0.9273	0.9636	0.6455
Von Frey	-	-	-	-	-	0.5350	0.5450	0.5150	0.5500
Neuroscore (total)	0.9156	-	0.9063	0.9250	0.9031	0.9063	0.8594	0.7875	0.7813
Neuroscore (focal)	0.8625	-	0.8531	0.8688	0.8563	0.8563	0.8188	0.7813	0.7813
Neuroscore (general)	0.8719	-	0.9313	0.9594	0.9531	0.9063	0.7906	0.6719	0.5000
Open field (open/closed)	-	-	0.9504	-	-	0.9669	0.9008	0.5041	0.6612
Open field (distance)	-	-	0.8750	-	-	0.8500	0.8750	0.8500	0.9417
EPM (open/closed)	-	-	0.9600	-	-	0.9200	0.9100	0.7900	0.7200
EPM (entry frequency)	-	-	0.8300	-	-	0.9150	0.8750	0.7600	0.7100
Sucrose Cons.	-	-	-	-	-	1.000	0.8611	0.8472	0.8472
Porsolt swim (90s)	-	-	-	-	-	0.9500	-	-	-

Quantification of testability to classify differences between surgical procedure groups by receiver operating characteristics curves. Values are shown as the area under the curve (AUC>0.9 is marked in red). ART, adhesive removal test; EPM, elevated plus maze.

#### 4.1.4 Anti-cytokine treatment can improve sickness behavior after experimental stroke

To investigate the role of the peripheral cytokines released in the acute phase after stroke in sickness behavior and confirm the usefulness of our optimized behavior test battery, three key pro-inflammatory cytokines, IL-1 $\beta$ , TNF- $\alpha$ , and IL-6, were antagonized before

operations, and key features of sickness behavior as selected above were analyzed (Figure 8A). The same mice as in the battery characterization were used (six- to eight-week-old male C57BL6/J) and divided into the treatment and control groups (IgG isotype vehicle). We selected the cylinder test, elevated plus maze, and sucrose consumption test to address motor deficits, anxiety, and depressive behavior. In addition, we assessed body weight, body temperature, and the composite Neuroscore.

**A: Schematic overview cytokine neutralization****B: Post-surgery survival rate****C: Infarct volume****D: Body weight progression****E: Body temperature progression****Figure 8: Physiological readouts after cytokine neutralization.**

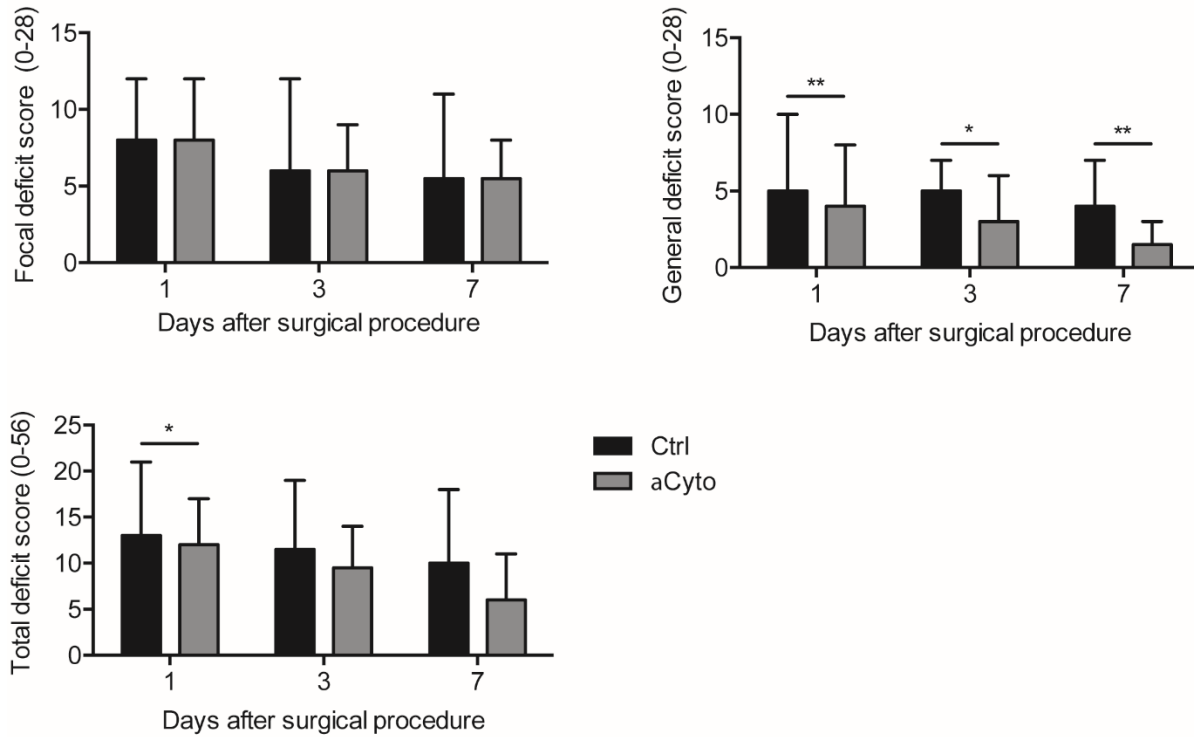
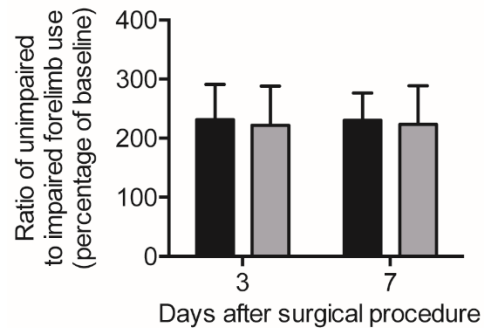
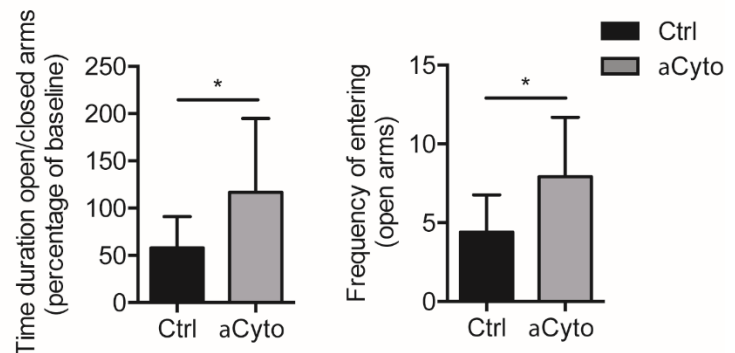
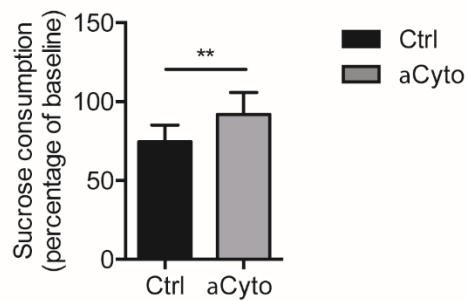
(A) Schematic overview of the experimental timeline for cytokine neutralization. (B) Kaplan-Meier curve of the overall survival rate after stroke surgery with anti-cytokines (63%) or control (52%) treatment. (C) Quantification of infarct volume seven days after stroke with anti-cytokines or control treatment (Student's t-test, n=10-12 per group). (D) Weight progression one, three, and seven days after stroke with anti-cytokines or control treatment represented as a percentage of weight before the surgical procedure (two-way ANOVA, n=10-12 per group). (E) Temperature progression one, three, and seven days after stroke with anti-cytokines or control treatment represented as a percentage of temperature before the surgical procedure (two-way ANOVA,

n=10-12 per group). (D)-(E) data are shown as box plots with mean + min to max. Ctrl, control; aCyto, anti-cytokines.

The general deficit score was reduced in the anti-cytokine treatment group after stroke in comparison to the control treatment group (Figure 9A, upper right panel). Combined in a total deficit score, general deficits were masked by the focal deficits (Figure 9A, lower left panel). Furthermore, the elevated plus maze was performed in order to assess anxiety behavior after stroke. Both the ratio of time duration in the open arms to the closed arms and the frequency of open arm-entering were higher in the anti-cytokine treatment group seven days after stroke (Figure 9C). To test for a possible lack of anhedonia, the sucrose consumption test was performed seven days after stroke. Both groups consumed less sucrose solution than in the baseline, but the anti-cytokine treatment group consumed more than control mice (Figure 9D).

On the other hand, the infarct volume and mortality seven days after the operation did not show a significant difference between anti-cytokine and control treatment groups (Figure 8B, C). Body weight and body temperature were also similar in the two groups (Figure 8D, E), but we anticipated that the body temperature would be different due to the role of IL-6 in body temperature mediation. The cylinder test was applied at three and seven days after stroke operation; the ratio of non-impaired to impaired forelimb use while rearing against the wall was not different between anti-cytokine and control treatment groups (Figure 9B). Moreover, the focal deficits score of the composite Neuroscore also showed no differences between the two groups (Figure 9A, upper left panel).

These findings indicate that the neutralization of these cytokines can alter some behavioral aspects indicative of CISB, but it cannot alter the stroke outcomes. Thus, we speculate that the peripheral pro-inflammation cytokines might induce the sickness behavior after large experimental stroke, but they do not influence focal deficits and infarct lesions. Through our optimized behavior tests battery, we were able to acquire differences in sickness behavior due to cytokine neutralization after stroke.

**A: Composite Neuroscore****B: Cylinder test****C: Elevated plus maze****D: Sucrose consumption**

**Figure 9: Impact of cytokine neutralization on sickness behavior in the acute and subacute phases after stroke.**

(A) Quantification of the 56-points Neuroscore, focal deficit (upper left), general deficit (upper right), and total Neuroscore (lower left) at one, three, and seven days after stroke surgery with anti-cytokine or control treatment (two-way ANOVA,  $n=10-12$  per group). (B) Quantification of forelimb asymmetry in the cylinder test three and seven days after stroke with anti-cytokines or control treatment represented as a percentage of the baseline (two-way ANOVA,  $n=10-12$  per group). (C) Quantification of the elevated plus maze seven days after stroke with anti-cytokines or control treatment. Exploration activity as time spent in open arms divided by time spent in closed arms normalized to the baseline (left panel, Mann-Whitney test,  $n=10-12$  per group) and time-independent analysis as the frequency of entering the open arms (right panel, Student's t-test,  $n=10-12$  per group). (D) Quantification of sucrose preference seven days after stroke with anti-cytokines or control treatment (Student's t-test,  $n=10-12$  per group). Graph (A) is shown as the median  $\pm$  range. Graphs (B)-(D) are shown as mean  $\pm$  SD. \* $P<0.05$ , \*\* $P<0.01$ . Ctrl, control; aCyto, anti-cytokines.

## 4.2 Immunosuppression after experimental stroke

It is known that, after a profound early activation on the peripheral immune system, severe systemic immunosuppression usually follows (Figure 10). Immunosuppression after stroke has been widely detected and is believed to make a significant contribution to widespread infections that often worsen the clinical outcome of patients with strokes.<sup>193</sup> Previous studies have demonstrated immunosuppression after experimental stroke from the reduction in the number of peripheral immune cells and a significant increase in apoptosis T cells, B cells, and NK cells.<sup>129,194</sup> However, the relationship between widespread immunosuppression and CNS pathology, as well as the concurrent systemic infection after stroke in animals and humans, are still not well understood. Thus, we further address the topic of immunosuppression after ischemic stroke.



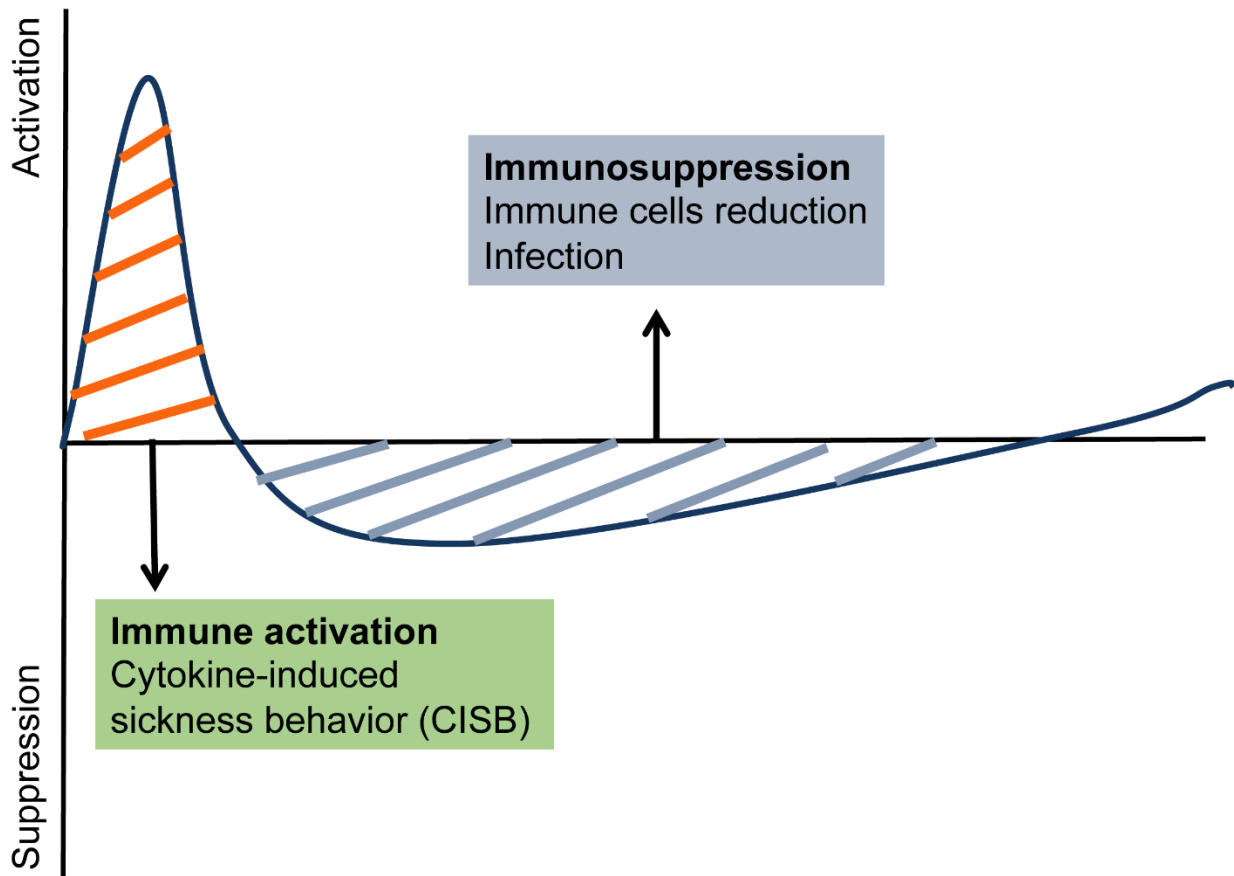


**Figure 10: Schematic diagram of the biphasic peripheral immunomodulation after stroke.**

An initial overactivation of the peripheral immune system changes in the later phase to an immunosuppressive phenotype. CISB, immune cell reduction, and infection are the key pathophysiological elements of the particular phases.

#### **4.2.1 Large experimental stroke induces leukocyte reduction in mice**

A previous study has detected a significant reduction of splenocytes in stroke mice 22 hours and 96 hours post-occlusion and spleen atrophy 96 hours after large experimental stroke.<sup>129</sup>

To further investigate the earliest time point of immunosuppression after stroke, we experimented to observe and quantify the leukocyte reduction at the time points of two, six, 12, and 18 hours after stroke. We found that, two hours after stroke, the total leukocyte

(CD45+ population) number in the spleen of stroke mice was more than the number of sham mice (Figure 11A). At six hours after stroke, the leukocyte number was slightly reduced in the spleen and significant until 18 hours after stroke (Figure 11A). Similar to the spleen, the number of circulating leukocytes in the blood was also increased two hours after stroke, but without significant effect. It was also decreased from six hours after stroke in the blood, but only until 18 hours after stroke, the effect was significant compared to sham mice (Figure 11B). The previous report has demonstrated that B cells that constitute the majority of splenocytes were decreased after stroke.<sup>129</sup> In our study, we focused more on T cell reduction after large experimental stroke. After FACS analysis, we found that the change of the T cell number was almost the same as the total leukocytes in both the spleen and blood. The T cell number was decreased 12 hours after stroke in comparison to sham mice in the spleen, and it was decreased 18 hours after stroke in both the spleen and blood (Figure 11C, D).

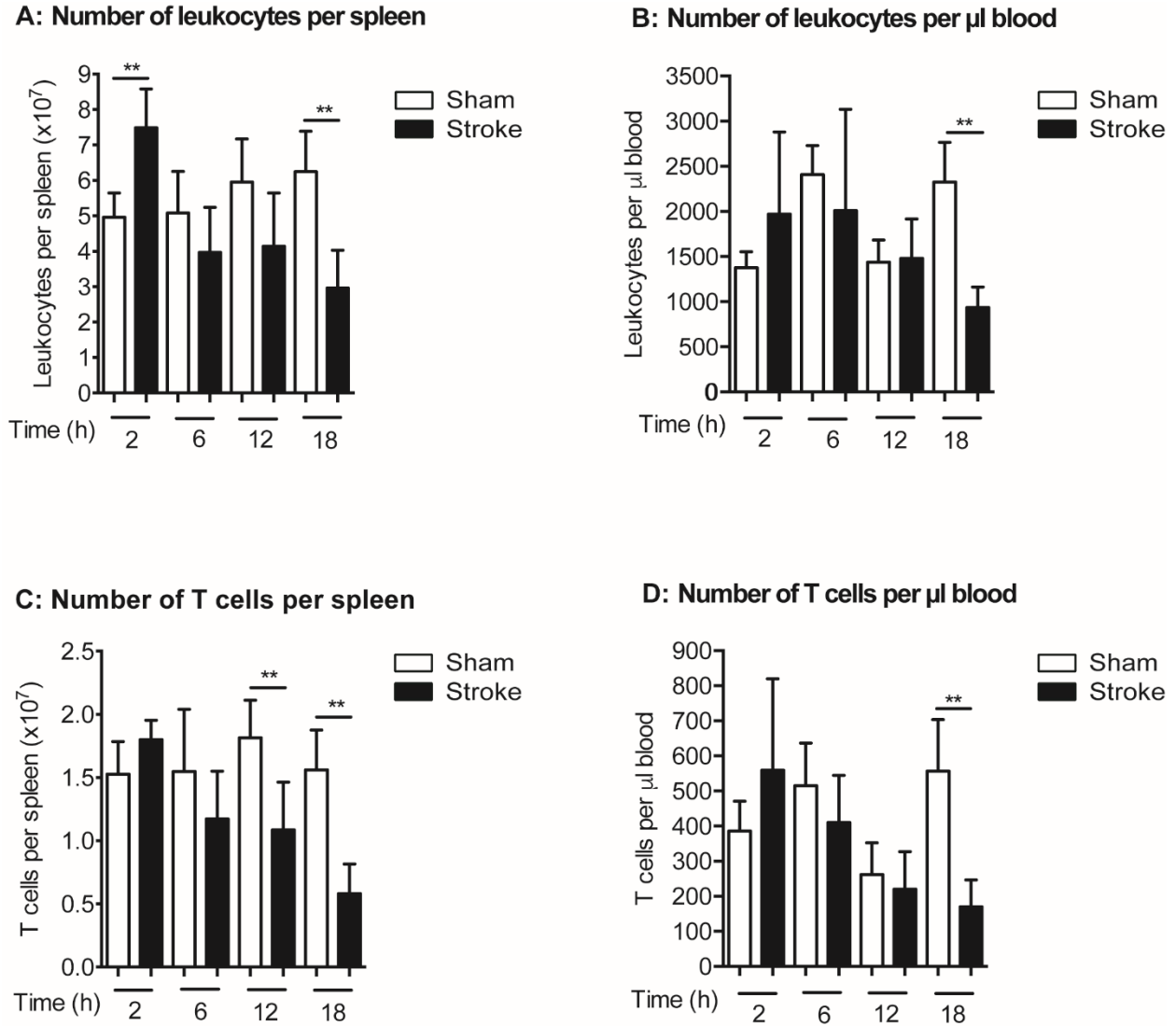


**Figure 11: The kinetic alternation of the peripheral leukocyte number after ischemic stroke.**

Number of leukocytes per spleen (**A**), number of leukocytes per µl blood (**B**), number of T cells per spleen (**C**), and number of T cells per µl blood (**D**) two, six, 12, and 18 hours after stroke or sham operations were analyzed by flow cytometry. All graphs are shown as mean  $\pm$  SD. Data are representative of two individual experiments per time point; n=5-6 mice per group; P values were calculated by the Mann-Whitney U test. \*\*P<0.01.

Taken together, we found that large experimental stroke can induce leukocytes to increase in the superacute phase after stroke and also lead to a subsequent leukocyte decrease in

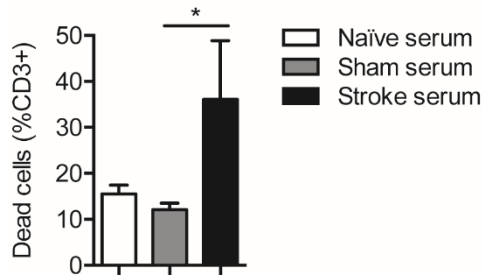
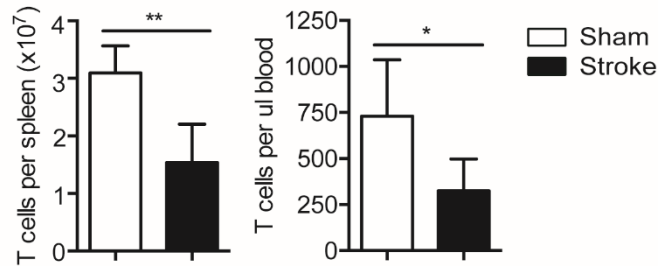
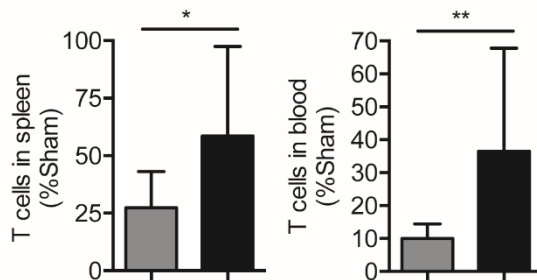
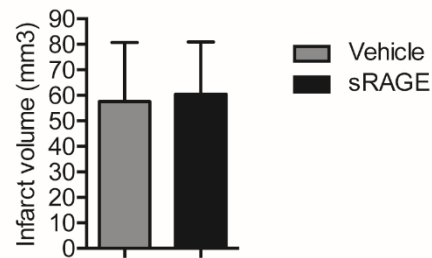
mice. The total leukocyte reduction can be detected as early as 18 hours after stroke in both the spleen and blood, in which T cells were detected as reduced 12 hours after stroke.

#### **4.2.2 Soluble mediators released after ischemic stroke induce T cell death**

As we mentioned above, soluble mediators like HMGB1 can trigger immunosuppression after stroke, but the complete molecular pathways are still unknown. We hypothesized that T cell reduction after stroke is also induced by soluble mediators released after ischemic stroke. In order to distinguish the effect of soluble mediators from other factors, we used an in vitro system in which T cells were only treated with serum and medium (Figure 12A). T cells were isolated by MACS from naïve mice spleens, cultured in 96-well plates, and challenged by the serum of naïve, sham, and stroke mice (three hours after operations). Eighteen hours later, cells were stained with anti-CD3 and 7-ADD or PI to quantify dead T cells. Our results showed that the percentage of dead CD3<sup>+</sup> cells with the stroke serum challenge was higher than with the sham serum challenge, although the effect was not prominent in comparison with naïve serum treatment (Figure 12A). This result indicates that serum from stroke mice must contain molecules that can trigger T cell death.

To exclude potential contamination with bacterial products, we used germ-free C57BL/6J mice and performed the surgeries in a relatively sterile environment to eliminate the effects from PAMPs. Similar to wild-type mice, we detected T cell reduction 18 hours after stroke in the spleen and blood (Figure 12B). This gave us the evidence that not bacterial, but sterile, host-derived mediators in the blood induce lymphocyte cell death after stroke.

Alarmins are host-derived mediators that can be released after ischemic stroke and lead to consequent immune alternations. We next reduced the circulating alarmins in vivo using sRAGE decoy receptors, and control mice received vehicle treatment. sRAGE is a soluble isoform of RAGE, and it acts as a decoy for RAGE ligands and prevents their interaction with the receptor.<sup>195</sup> After the treatment, mice were conducted with stroke or sham operations. We obtained more T cells in both the spleen and blood in the sRAGE treatment group 18 hours after stroke (Figure 12C left and right panel). The infarct volume between treatment groups did not differ (Figure 12D), which means that the T cell reduction was not influenced by infarct volume size. These results indicate that reducing the circulating alarmins can attenuate T cell death after experimental stroke.

**A: In vitro serum treatment****B: Germ-free mice****C: In vivo sRAGE treatment****D: Infarct volume of in vivo sRAGE treatment**

**Figure 12: Soluble mediators released after ischemic stroke induce T cell death.**

(A) T cells from naïve mice were challenged by naïve, sham, and stroke mice (three hours after operations) serum individually in vitro for 18 hours; dead cells were detected by 7-ADD or PI through flow cytometry analysis. Data are representative of two individual experiments,  $n=3-4$  mice (serum donor) per group. (B) T cell number per spleen (left panel) and T cell number per  $\mu$ l blood (right panel) 18 hours after stroke and sham operations were analyzed by flow cytometry in germ-free C57BL/6J mice. Data are representative of two individual experiments,  $n=5-7$  mice per group. (C) T cell number in spleen (left panel) or in the blood (right panel) 18 hours after stroke was normalized to relevant sham mice in sRAGE and vehicle treatment groups; data are shown as a percentage of the sham mice T cell number of each treatment group. (D) Infarct volume 18 hours after stroke of sRAGE and vehicle treatment groups were quantified. Data are representative of three to five individual experiments;  $n=5-9$  mice per group. All graphs are shown as mean  $\pm$  SD. Kruskal-Wallis test (A), P values were calculated by the Mann-Whitney U test (B and C middle panel) or Student's t-test (C left and right panel). \* $P<0.05$ , \*\* $P<0.01$ .

Together, these findings demonstrate that soluble mediators released after ischemic stroke, most likely some alarmins, can induce T cell death and, further, immunosuppression.

### **4.2.3 Deletion of Myd88 reduces T cell death**

According to the results above, peripheral T cells and other leukocytes may be induced by alarmins and die after ischemic stroke. Thus, we hypothesized that pyroptosis might be the possible death form of T cells after ischemic stroke, and a canonical pathway of pyroptosis may be involved.

In order to further investigate the mechanism of T cell death after stroke, we first tried to confirm the role of cell surface receptors (PRRs), which can recognize alarmins. TLRs are a class of receptors on the cell membrane and can recognize various alarmins and transduce signals into the cytoplasm via the adaptor protein MyD88.<sup>35,58</sup> We thus used MyD88 knockout (MyD88<sup>-/-</sup>) mice to investigate the role of TLRs in cell death after stroke. We found that the deletion of MyD88 can improve splenic leukocytes and T cell reduction after stroke in comparison with wild-type mice (Figure 13A, B). Afterward, we deleted RAGE, which has the potential to modulate the cellular response to tissue injury.<sup>46</sup> Surprisingly, RAGE knockout (RAGE<sup>-/-</sup>) mice did not present an improvement in splenic leukocytes and T cell reduction in comparison to wild-type mice (Figure 13A, B). There was no difference in infarct volume among wild-type, RAGE<sup>-/-</sup>, and MyD88<sup>-/-</sup> mice (Figure 13C).

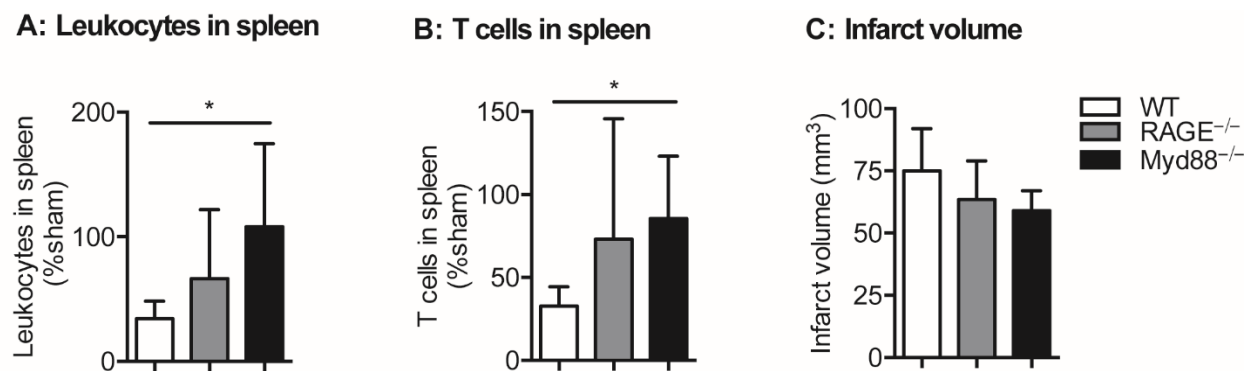


**Figure 13: The effect of the deletion of RAGE or Myd88 in T cell death after stroke.**

The number of leukocytes in the spleen (A) and the number of T cells in the spleen (B) of WT, RAGE<sup>-/-</sup>, and Myd88<sup>-/-</sup> mice 18 hours after stroke were normalized to relevant sham mice. Infarct volume (C) 18 hours after stroke of WT, RAGE<sup>-/-</sup>, and Myd88<sup>-/-</sup> mice were quantified. Data are representative of three to five individual experiments, n=7-10 mice per group. All graphs are shown as mean ± SD. P values were calculated by one-way ANOVA (A&C) or the Kruskal-Wallis test (B). \*P<0.05. WT, wild-type mice.

These findings suggest that MyD88 is involved in leukocyte death after ischemic stroke.

TLRs can interact with soluble alarmins released after stroke and transduce signals into the cytoplasm through MyD88, which may further induce pyroptosis.

#### 4.2.4 The deletion or inhibition of caspase-1 reduces T cell death

In order to confirm the role of caspase-1 in T cell death, we deleted caspase-1 using caspase-1 knockout (caspase-1<sup>-/-</sup> caspase-11<sup>tg</sup>) mice. We acquired more splenic leukocytes and T cells from the mice without caspase-1 expression after experimental stroke (Figure 14A, left and right panel). There was no difference in infarct volume between wild-type and caspase-1 knockout mice (Figure 14B). Additionally, we pharmacologically inhibited caspase-1 by VX-765. In comparison with vehicle treatment, caspase-1 inhibition



attenuated splenic leukocyte death and T cell death after stroke (Figure 14C, left and right panel). The infarct volume did not differ between the two treatment groups (Figure 14D).

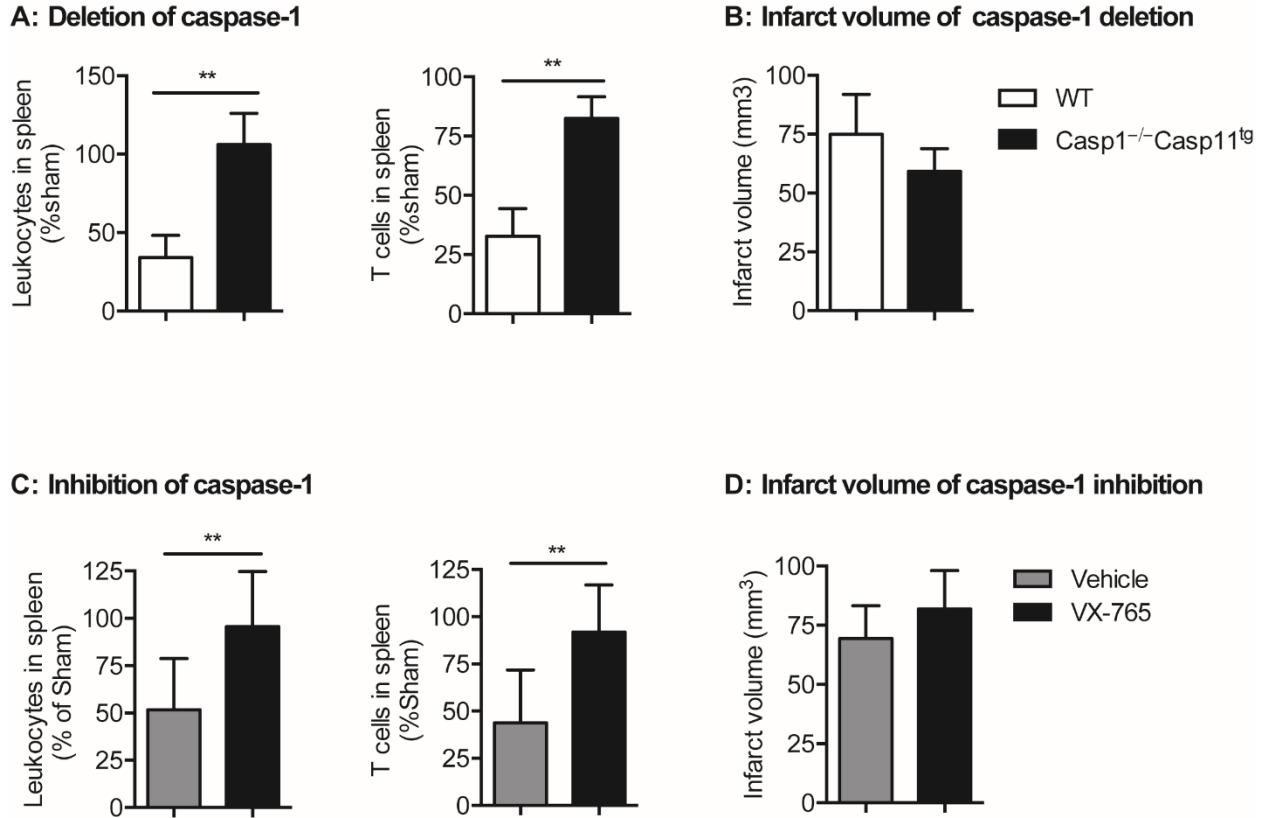


**Figure 14: Deletion or inhibition of caspase-1 reduces T cell death.**

(A) The leukocyte number in the spleen (left panel) and the T cell number in the spleen (right panel) of WT and caspase-1<sup>-/-</sup> caspase11<sup>tg</sup> mice 18 hours after stroke were normalized to relevant sham mice; data are shown as a percentage of the sham mice splenic leukocyte number and the T cell number of each strain. (B) The infarct volume 18 hours after stroke of WT and caspase-1<sup>-/-</sup> caspase11<sup>tg</sup> mice were quantified. Data are representative of two individual experiments; n=6-7 mice per group. (C) The leukocyte number in the spleen (left panel) and the T cell number in the spleen (right panel) of Vehicle and VX-765 treatment groups 18 hours after stroke were normalized to relevant sham mice; data are shown as a percentage of the sham mice splenic leukocyte number and T cell number of each treatment. (D) The infarct volume 18 hours after stroke of Vehicle and VX-765 treatment groups were quantified. Data are representative of three individual experiments; n=7 mice per group. All graphs are shown as mean  $\pm$  SD. P values were calculated by the Mann-Whitney U test (A-B). \*\*P<0.01. WT, wild-type mice.

Together, these results demonstrate the vital role of caspase-1 in peripheral immune cell death after ischemic stroke. Caspase-1 can induce leukocyte and T cell death, and it is crucial in the process of immunosuppression after stroke.

## **5 Discussion**

### **5.1 CISB after stroke**

CISB is a key feature of immune system activation after stroke, and the first part of this dissertation concerns characterizing different behavioral aspects after stroke and optimizing the choice of various behavior tests. In our study, we were able to acquire acute, sub-acute, and chronic deficits of focal as well as CISB deficits after large experimental stroke. We used a battery of the most common tests for behavioral performance assessment and classified them in categories: motor, sensory, anxiety and motivation, learning and memory, and depression. For post-hoc analysis, we ranked all behavioral approaches by their sensitivity and specificity using ROC curve analysis and established a more accurate battery of behavior tests for each time point after experimental stroke.

#### **5.1.1 Optimal behavior tests for focal deficit assessment**

In our study, we observed prominent focal deficits through the cylinder test, Rotarod, the adhesive removal test, and Neuroscore. These deficits can be explained by the infarct lesion generated by the transient stroke model, in which both the striatum and cortex were damaged.<sup>196</sup> Both the cylinder test and Rotarod detected motor deficits in the (sub)acute phase. The cylinder test enables us to detect motor deficits up to day 21 while still providing high sensitivity and specificity (AUC=0.9909). A sensitive Rotarod test (AUC=0.9417) was possible up to day 28 after stroke. This gave us the option to choose certain tests according to different phases after stroke. It was reported that motor learning can also

influence Rotarod test readout.<sup>124</sup> Animal performance gradually improves over time due to motor learning.<sup>124</sup> Therefore, it is crucial to distinguish motor learning from actual recovery after stroke. Moreover, motivation is also an important factor in Rotarod testing.<sup>124</sup> Mice with stroke often lack of motivation, which could result in falling off early. This would confuse our results on motor deficit assessment after stroke. However, accelerating the Rotarod always ends with mice falling from the apparatus; we considered that falling is harmful to a weak mouse with severe stroke and often aggravates mouse sickness condition. During the cylinder test, however, mice were simply placed in a transparent cylinder, which is safer to perform for a severe stroke model.

The adhesive removal test combined motor function (removal of adhesive) with a sensory readout (recognition of adhesive). The recognition impairments (the latency to contact the adhesive) after stroke were detectable up to seven days post-lesion. Differences in the latency to remove the adhesive were only observable up to day two due to the high capacity of mice to compensate for the motor deficit. This problem was also visible in the ROC curve analysis, which revealed a low overall sensitivity of the parameter of the latency to remove the adhesive throughout the acquisition time points. Since animals react quickly to adhesives, the latency to contact in the adhesive removal test is usually extremely short and causes inaccuracy in measuring. Nevertheless, it is difficult to separate sensory deficits from motor deficits using this test, as it was designed for assessing initial sensorimotor deficits.<sup>181</sup> Perception measurement in non-self-reporting subjects is always a challenge because perception is internal and individual.<sup>182</sup> Blix, von Frey, Weber, Fechner, and others

investigated this problem in the late nineteenth century.<sup>182</sup> Here, we performed the von Frey filament test and detected a large variability in the sensory threshold. Although the monofilaments provided a consistent force to a mouse paw, it is still difficult to distinguish the reaction due to a stimulus from spontaneous movements, as some mice are irritable after stroke.

In consideration of the time it consumes, safety, cost, and operative difficulty, the combined 56-point Neuroscore is simpler and more sensitive to quantifying focal deficits after stroke. To avoid inaccuracy from subjective factors, it is necessary to be blinded when evaluating the scores in this test. Similarly, in clinical research and neurology wards, neurologic scores, such as the modified Rankin Score and the National Institutes of Health Stroke Scale, are regularly used to assess functional outcomes after stroke. Thus, neurologic scores could play an important role in translational medicine and bridge the gap between clinical trials and animal studies. However, more sensitive tests to assess stroke deficits should be established, and tests that are sensitive enough to detect therapeutic drugs' effect in stroke rehabilitation at relatively late time points should be developed.<sup>124</sup>

### **5.1.2 The pitfalls of detecting anxiety, depression, memory, and learning deficits**

The elevated plus maze and open field in our study detected anxiety-like behavior. Compared to the open field, the elevated plus maze was slightly more prominent in evaluating the deficits up to 14 days after stroke. There was no detectable anxiety from 21

days after stroke in both tests. In clinical studies, post-stroke anxiety is correlated with post-stroke depression.<sup>197</sup> Our results also show that the depression-like behavior was accompanied by anxiety up to 14 days after stroke. The differences in the Porsolt swim test were only detectable in the first 90 seconds. We speculate that both sham- and stroke-operated mice were “desperate” and “exhausted” in the water tank after a long exposure to the apparatus, which resulted in a short struggling time overall in both groups. After the mice learned they would be rescued regardless after a five-minute trial, they may also have given up struggling after 90 seconds in both groups. The same problem also arose in the elevated plus maze and open field. When performing the tests frequently on the same set of mice, animals learn and remember the apparatus, and the tests lose their sensitivity to assessing deficits. Therefore, it is more important to choose certain time points to conduct these tests and avoid performing them frequently. However, anxiety-like behavior can also influence the assessment of depression in the Porsolt swim test since animals do not realize that they are in a hopeless situation and can become anxious due to the apparatus.<sup>176</sup> Thus, a sucrose consumption test that can be performed in the home cage could eliminate stress factors and reflect the absolute depression level, and it could also detect the deficits with higher accuracy. Aside from the assessment of anxiety and exploratory locomotion in rodents, the open field can also evaluate motor function and activity.<sup>198,199</sup> It is known that, after ischemic stroke, mice develop hypoactivity in the acute phase.<sup>124</sup> We also found this phenotype from the decreased distance moved after stroke. Interestingly, subsequent hyperactivity, which starts several days after stroke and may last up to months, has also been reported.<sup>200,201</sup> In the hyperactive phase, mice with motor deficits can still show high

locomotive activity with rotation preference in the open field.<sup>124</sup> In our study, we also observed some stroke mice with fast rotation behavior during the open field test, but the distance moved in the apparatus remained very short, and we could not conclude hyperactivity from this parameter. Therefore, other behavior tests or parameters that can assess rotation behavior after stroke should also be considered. Additionally, the lighting condition is also a factor that could affect anxiety behavior. Dark light is normally related to increased exploratory behavior and reduced anxiety, while bright light is often associated with increased anxiety and reduced exploration.<sup>124</sup> It is important to maintain the same lighting condition level between each trial of anxiety assessment. Thus, we always conducted the elevated plus maze and open field in the dark.

### **5.1.3 Cytokines' effect on sickness behavior after stroke**

Pro-inflammatory cytokines are rapidly and broadly expressed and secreted as early as six hours after experimental stroke.<sup>104</sup> Therefore, we designed our anti-cytokine experiment to investigate the acute effect of the pro-inflammatory cytokines (TNF- $\alpha$ , IL- $\beta$ , and IL-6) on sickness behavior after experimental stroke. The previous study showed that infarct volumes and focal sensorimotor deficits did not differ between control and anti-cytokine-treated mice, while home cage behavior analysis revealed that the cytokine neutralization improved the disturbances of circadian rhythm induced by stroke and overall motility.<sup>42</sup> We also did not detect differences in infarct volume and focal deficits between the two groups. This again demonstrated that the neutralization of peripheral cytokines had no acute effect on primary brain lesions. In contrast, the elevated plus maze and sucrose

consumption test revealed that anxiety-like and depression-like behavior was improved by anti-cytokine treatment. This supports the concept of “CISB after stroke.” Interestingly, body temperature did not change after cytokine neutralization, which differed from our hypothesis because IL-6 plays an important role in body temperature mediation. As we neutralized cytokines from the peripheral immune system but not from the central immune system, this raised the concern that peripheral IL-6 neutralization may not affect the central IL-6 level and the following temperature mediation. However, the previous study showed that the inhibition of peripheral TNF by etanercept, which does not cross the BBB, can block the sickness behavior associated with CNS lesions.<sup>202</sup> This result indirectly eliminated our concern. IL-6 is critical for inducing the febrile response during infection and for maintaining the core body temperature during cold exposure.<sup>203,204</sup> Both PAMPs and alarmins can induce IL-6 secretion and a subsequent fever response.<sup>205,206</sup> However, we did not observe a fever response in our study; on the contrary, the body temperature decreased after experimental stroke. Hypothermia can be observed after surgery and anesthesia, under systemic inflammatory response syndrome (SIRS), or due to other causes.<sup>207,208</sup> In our study, the body temperature decreased not only in the stroke group, but also in the sham group. Therefore, the reason for the temperature change is most likely due to surgery and anesthesia rather than IL-6 increasing. This could partially explain why the neutralization of IL-6 did not alter the body temperature. However, mice that died before seven days after stroke were excluded from data analysis; these dead mice had more severe stroke, as well as lower body weight and body temperature. The exclusion of the data



concerning the dead mice could be another reason we did not detect differences in body weight and body temperature between the control and anti-cytokine treatment groups.

#### **5.1.4 Assessment of sickness behavior in other mouse strains and other stroke models**

Our behavior tests were applied on C57BL6/J mice, and the optimal behavior test panel was selected based on the behavioral phenotype of this specific wild-type, inbred strain. Different mouse strains could behave differently,<sup>209,210</sup> and the specificity and sensitivity of these behavior tests may need to be re-evaluated before use in new strains. Types of aggressive behavior have been demonstrated individually in mice with the targeted deletion of specific genes in comparison with wild-type mice. Therefore, the tests to assess aggressive behavior may not be suitable for knockout mice with different aggressive behavior.<sup>211</sup> The previous study has also shown the lack of aggression, the development in non-aggressive exploration, and anxiolytic-like behavior in TNF receptor-deficient mice.<sup>212</sup> Meanwhile, these results also identify potent roles for TNF and TNF-receptor signaling in regulating aggression and anxiety-related behavior, and for modulating activity in brain domains that underlie these behaviors.<sup>212</sup> Therefore, when investigating the roles of knockout genes in sickness behavior, we should also consider the different behaviors of knockout mice in normal conditions (baseline). It is suggested that further baseline characterization is necessary to exclude basic differences in test performance, especially when knockout mice are used.<sup>124</sup> In fact, the differences can be significant, not only between wild-type and knockout mice, but also between individual mice. Therefore,

it may be necessary to subgroup the mice based on the primary variations of baseline performances.<sup>124</sup>

Moreover, the stroke model we used was a large, severe stroke model; for some smaller stroke models, such as distal middle cerebral artery occlusion (dMCAo) and the photothrombotic stroke model, more sensitive and precise behavior tests such as the skilled reaching test and Catwalk gait analysis might be necessary for better assessment.<sup>213,214</sup> More automated behavior analyses also need to be developed in the future to reduce time consumption and rater bias. The previous study has used a novel automated home cage analysis system to analyze individual mouse activity in group-housed animals over long periods of time,<sup>215</sup> while the conventional home cage test apparatus can only test a single mouse in each cage. Further, the novel home cage analysis system can provide unique insights into the relationship between individual and group behavior.<sup>215</sup> Recently, a support vector machine has been used to automatically analyze the behavior of freely moving rodents.<sup>216</sup> In comparison with conventional red-green-blue camera-based methods, the novel system operating on three-dimensional depth images enables stable performances regardless of the lighting condition and animal color contrast with the background; the lighting and the color contrast conditions are often the major problems in animal tracking for behavior tests.<sup>216</sup>

## **5.2 T cell reduction after stroke**

After the activation of the peripheral immune system in the acute phase post-stroke, severe systemic immunosuppression often follows. Therefore, the second part of this dissertation is focused on immunosuppression after stroke. Because of the critical role of T cells in the immune system and their dramatic reduction after stroke, we aim to investigate the reason for the T cell reduction and the possible mechanism behind it.

### **5.2.1 Peripheral T cells die after large experimental stroke**

Previous animal studies have found that the spleen shrinks over one to four days after stroke,<sup>129,217</sup> paired with a simultaneous increased release of lymphocytes and monocytes into the blood.<sup>218,219</sup> However, in clinical research, a study of 30 patients with suspected acute ischemic stroke found that the spleen volume tended to decrease by 24 hours after symptom onset and then increase, and the blood neutrophil count showed an inverse association with spleen volume over the period of observation, while the blood lymphocyte count and monocyte count were not associated with spleen volume.<sup>220</sup> Another study of 100 patients with ischemic stroke or intracerebral hemorrhage also observed a biphasic change in splenic volume that decreased over 48 hours and then slowly increased. However, the splenic size was significantly related to blood neutrophil count and inversely associated with blood lymphocyte count, and it had no relationship with blood monocyte count.<sup>221</sup> Both animal and patient studies have demonstrated that splenic volume is inversely related

to blood lymphocyte count, which indicates that lymphocytes can be released into the blood, while the spleen shrinks after acute ischemic stroke.

However, previous animal study has also reported that the leukocyte count in the blood was decreased, especially for B cells and CD3+ T cells.<sup>129</sup> In our study, we observed that splenic T cell count reduction was accompanied by blood T cell count reduction after ischemic stroke. Thus, in our case, T cell count reduction in the spleen cannot be explained by the release of T cells from the spleen into the blood after stroke. We then formed two hypotheses about the peripheral T cells' fate after stroke: one was that they migrated into other organs, and the other was they died after ischemic stroke. As we know, one of the key features of the neuroimmunological response to brain ischemia is that circulating leukocytes infiltrate into the brain. However, it was observed that fewer than 100,000 CD45+ cells and 15,000 CD3+ cells migrated into the brain parenchyma per hemisphere five days after fMCAO.<sup>222</sup> In our study, we found that more than 50% of splenic T cells (i.e., nearly 10 million) were reduced 18 hours after stroke. The T cells that had disappeared in the spleen far outnumber the T cells that infiltrate into the brain after stroke, and no previous studies have explained how and to which organ these massive numbers of T cells migrate. Thus, we hypothesized that peripheral T cells die after ischemic stroke.

### **5.2.2 Apoptosis and pyroptosis in ischemic stroke**

Since we posited that the reduction in peripheral leukocytes and T cells was due to cell death, we further explored the cell death forms of T cells. The three defined pathways to

cell death that have been investigated intensively in recent years are apoptosis, pyroptosis, and necroptosis.<sup>223</sup> Among these cell death forms, apoptosis was the first programmed cell death described.<sup>224</sup> Previous studies have evaluated splenocyte apoptosis using annexin V assay or Terminal UDP-nick end labeling (TUNEL) assay. With fluorescein-labeled Annexin V, the translocation of phosphatidylserine to the external cell surface during apoptosis is detected.<sup>225</sup> TUNEL is a another method established for detecting DNA fragmentation. During apoptosis, the 3'- hydroxyl termini in the double-strand DNA breaks can also be generated, which can be detected through TUNEL method.<sup>226</sup> The previous study found an increase in annexin V staining in CD4+ T cells 22 hours after stroke and a striking increase in TUNEL+ cells in the spleen 96 hours after stroke.<sup>129</sup> Another study has also detected a marked increase in apoptotic lymphocytes from the spleen and thymus 12 hours after experimental stroke. The increased apoptosis affected all lymphocyte subsets and all thymocyte subsets. In addition, they showed that the pharmacological inhibition of either SNS or HPA prevented the lymphocyte apoptosis and lymphopenia induced by stroke.<sup>133</sup> This finding revealed the role of stress mediators in post-stroke lymphocyte apoptosis and immunodepression. Our previous study found a significant suppressive feature of the expanding marrow-derived suppressor cells (CD11b+ Ly-6C+ population) on lymphocytes and a significant increase in the expression of Arg1 in the splenic monocyte population.<sup>42</sup> Marrow-derived suppressor cells were considered to provide a suppressive and toxic feature on lymphocytes through Arg1 upregulation, which may induce apoptosis in activated lymphocytes by restricting the essential concentration of L-arginine required for lymphocyte viability.<sup>227,228</sup> This novel finding of marrow-

derived suppressor cells' expansion and increased Arg1 expression could be another mechanism that explains the induction of lymphocytes' apoptosis after stroke.

In our study, we found that alarmins released after ischemic stroke can induce peripheral immune cell death. Many alarmins released from cellular stress and tissue injury are recognized by PRRs expressed on or in innate immune system cells to trigger the activation of the inflammasomes and subsequently induce pyroptosis.<sup>154-157</sup> Pyroptosis is a newly identified pro-inflammatory form of cell death that differs from apoptosis. It is a mode of lytic cell death, which allows potential immunostimulatory molecules to be released. Pyroptosis was first defined in 1992,<sup>146</sup> and the term itself was invented in 2001 after the finding that bacteria-infected macrophages underwent a dramatic lytic cell death depending on caspase-1 activity.<sup>229</sup> In our study, through caspase-1 knockout and caspase-1 inhibitor experiments, we found that the absence of caspase-1 attenuated splenic T cell death after stroke. This finding supports the role of caspase-1 in T cell death and proved our hypothesis that peripheral T cells may undergo pyroptosis after stroke. Although the traditionally defined form is caspase-1-mediated pyroptosis, studies have demonstrated that other caspases, such as caspase-11 (caspase-4 and -5 in humans),<sup>167,230</sup> and more recently, the apoptotic effector caspase, caspase-3, are capable of triggering pyroptosis.<sup>231,232</sup> Whether these caspases are also involved in T cell pyroptosis after ischemic stroke remains unknown, and future studies are needed.

In the literature, alarmins have mostly been described as promoting inflammatory pathways in the innate immune system. In our study, we considered that alarmins also played an

important role in adaptive immunity and lead T cell death after ischemic stroke. It has been reported that alarmins can also shape the adaptive immune responses through the activation of specialized antigen-presenting cells.<sup>233</sup> In addition,  $\gamma\delta$  T cells can be directly activated by alarmins via TLR1/2 and dectin receptors to sense tissue damage in stroke.<sup>234</sup> T cell pyroptosis has been investigated for many years in HIV infection.<sup>235</sup> Nevertheless, there is still an absence of evidence that T cells undergo pyroptosis in sterile inflammation. In our study, we did not confirm the direct role of alarmins and caspase-1 in T cell death; we only eliminated caspase-1 globally to observe the change in T cell reduction after experimental stroke. It is still not clear that T cell death after ischemic stroke is directly induced by alarmins or triggered by other activated immune cells from innate immunity. Experiments on specific caspase-1 knockout T cells should be performed to further investigate this pathway.

### **5.2.3 HMGB1 in T cell death after stroke**

Pyroptosis can be triggered by both PAMPs and alarmins following numerous pathological stimuli, such as infection, heart attack, cancer, or stroke.<sup>236</sup> In our study, we excluded the effect of PAMPs in T cell death after stroke with the germ-free C57BL/6J mice experiment and focused on danger signals released after sterile inflammation. We found that reducing the circulating alarmins, including HMGB1, can attenuate T cell death in the peripheral immune system. This finding showed an enhanced role of alarmins in T cell death after stroke.

Nonetheless, previous studies have not demonstrated the cellular source of passively released HMGB1 in the acute phase after stroke. Except for passive release of HMGB1 by cerebral necrotic tissue after stroke, activated cells in the brain and the peripheral immune system can also actively secrete HMGB1 in response to tissue injury.<sup>46</sup> Interestingly, it has also been reported that inflammasome-mediated pyroptosis can promote the release of HMGB1.<sup>237</sup> Cells undergoing unprimed pyroptosis (through a priming-free inflammasome activation system) appear to release a chemotactic isoform of HMGB1, while priming through surface TLRs during pyroptosis leads to the release of a TLR-agonist cysteine redox isoform of HMGB1.<sup>237</sup> This form of HMGB1 is called disulfide HMGB1; it can interact with TLR4 receptors and activates NF- $\kappa$ B signaling in microglia/macrophages.<sup>238</sup> The disulfide HMGB1 can also increase neuronal cell death induced by NMDA in vitro via its interaction with TLR-4 receptors.<sup>239</sup> Thus, the HMGB1 and some inflammasome components released after pyroptosis may also join the other extracellular alarmins to propagate inflammasome assembling and amplify pyroptosis. The interaction between HMGB1 and pyroptosis may explain the possible cellular sources of passively released HMGB1 after stroke. However, the more precise cellular sources of HMGB1 after ischemic stroke still require further investigation and research.

#### **5.2.4 Cell surface receptors in T cell death after stroke**

HMGB1's inflammatory roles are mediated through binding to the cell surface receptors, including RAGE, TLR-2, and TLR-4.<sup>240,241</sup> The cytoplasmic domain of TLRs is important for signal transduction through interaction with the adaptor protein MyD88.<sup>58</sup> It has been



proposed that MyD88's function as a downstream effector in TLR signaling is associated with post-stroke immunomodulation induced by HMGB1.<sup>46</sup> In our study, we only detected the change in MyD88<sup>-/-</sup> mice that reduced the splenic leukocytes and T cell death after stroke, but with no alternation in RAGE<sup>-/-</sup> mice. In contrast to our finding, a previous study has demonstrated a novel pathway of HMGB1-induced pyroptosis through RAGE on macrophages.<sup>242</sup> According to their results, an early detectable caspase-1 activation was NLRP3-dependent, and the late HMGB1-induced caspase-1 cleavage was independent of NLRP3 but involved the endocytosis of HMGB1, cathepsin B activation, and release from ruptured lysosomes.<sup>242</sup> Both TLRs and RAGE and IL-1 receptors that bind to HMGB1 can interact with MyD88.<sup>46,65</sup> Therefore, the role of MyD88 in immune cell death after stroke cannot be directly interpreted as the role of TLRs in cell death signaling. Further experiments should focus on TLR deletion in immune cell death after stroke. In addition, TLR-MyD88 can mediate the activation of the NF- $\kappa$ B pathway, which acts as the first signal promoting the transcription of many genes that encode inflammatory mediators, including pro-IL-1 $\beta$ , and inflammasome components such as NLRP3 and ASC.<sup>74</sup> Our result of MyD88 reveals its critical role in immune cell death after stroke and provides an indirect indication that the signal 1 priming may be necessary for pyroptosis in leukocytes after stroke. Moreover, we conducted the deletion of MyD88 and RAGE using global knockout mice. The cell-type specificity still needs to be further explored. Therefore, our future goal is verifying the receptors that induce leukocyte death after stroke in a specific cell type. Although we demonstrated that circulating alarmins play a role in peripheral leukocyte death after stroke, we could not confirm that HMGB1 is the main

alarmin involved in this pathway. Thus, other receptors that do not interact with HMGB1 but rather with other alarmins may also take part in peripheral leukocyte death after stroke.

### **5.2.5 Inflammasome complexes involved in caspase-1 activation**

Caspase-1 activation has long been regarded as the core of the process of pyroptosis, and it can be activated within different inflammasomes to against different infectious and immunological threats. In 2002, the inflammasome complex was proposed as a molecular platform for caspase-1 activation.<sup>243</sup> In the past decade, extensive studies have found several inflammasomes with the ability to identify specific microbial challenges and endogenous hazards. Among these inflammasomes, the most characterized ones are AIM2/ASC, NAIP/NLRC4, NLRP3/ASC, Pyrin/ASC, and NLRP1. Previous study has summarized that the NAIP/NLRC4, Pyrin/ASC, and NLRP1 inflammasomes can recognize PAMPs, while the AIM2/ASC and NLRP3/ASC inflammasomes can be activated by DAMPs.<sup>157</sup>

In our study, we did not investigate the inflammasome complexes that might be involved in caspase-1 activation after stroke. Because alarmins released from necrotic tissue trigger the sterile inflammation and immunosuppression after ischemic stroke, the focus of future analysis should be inflammasomes that are mainly stimulated by endogenous alarmins.

### **5.2.6 The non-canonical inflammasome pathway**

Although we did not address the role of caspase-11 (caspase-4 and -5 in humans) in T cell death after stroke in this project, a previous study has suggested that caspase-11 can also induce pyroptosis in a caspase-1 independent manner.<sup>167</sup> Caspase-11 can induce a non-canonical pathway that is mainly induced by PAMPs. Both intracellular Gram-negative bacteria released LPS, and circulating LPS from extracellular bacteria can directly and specifically bind to inflammatory caspases, including caspase-4/caspase-5 in humans and caspase-11 in mice. LPS binding stimulates oligomerization and the consequent activation of caspase-4/5/11. The activated caspase-4/5/11 can then not only trigger cell pyroptosis but also activate canonical NLRP3/ASC inflammasome to release IL-1 $\beta$  and IL-18.<sup>244</sup>

Although there is no evidence that caspase-11 can also be triggered by alarmins, the interaction between non-canonical and canonical pathways exists. Active caspase-11 causes NLRP3 inflammasome aggregation, resulting in caspase-1 activation, and pro-IL-1 $\beta$  and pro-IL-18 production. Along with the infections after stroke, PAMPs may also take part in the T cell pyroptosis by activating the non-canonical pathway and aggravating immunosuppression. Thus, in the future, we will further investigate the roles of non-canonical inflammasome pathway and caspase-11/4/5 in T cell death after ischemic stroke.

### 5.3 Concluding remarks

CISB and immunosuppression are two of the main immune-mediated comorbidities after ischemic stroke. Alarmins released from necrotic cells are considered the triggers of these comorbidities in different phases after stroke. As the key pathophysiological element of immune activation after stroke, CISB can be detected immediately after stroke onset and can even last until the chronic phase. In this study, we characterized different behavior aspects after large experimental stroke with a broad battery of behavioral approaches and selected optimal behavior test panels for certain time points. Additionally, we demonstrated the role of peripheral pro-inflammatory cytokines in sickness behavior after stroke through our selected behavior tests. Immunosuppression is another comorbidity after ischemic stroke that increases the risk of severe infections. Our study found that the earliest time point when immune cell reduction occurred was as early as 12 hours after experimental stroke onset. Moreover, we demonstrated that T cell death after stroke was related to alarmin stimulation, while Myd88 and caspase-1 also participated in the T cell death. This cell death pathway is most likely associated with inflammasome assembling and caspase-1 activation. However, our future research should focus on the pro-inflammatory cytokines' influence on behavior domains and more detailed molecular pathways involved in T cell death after stroke (Figure 15).

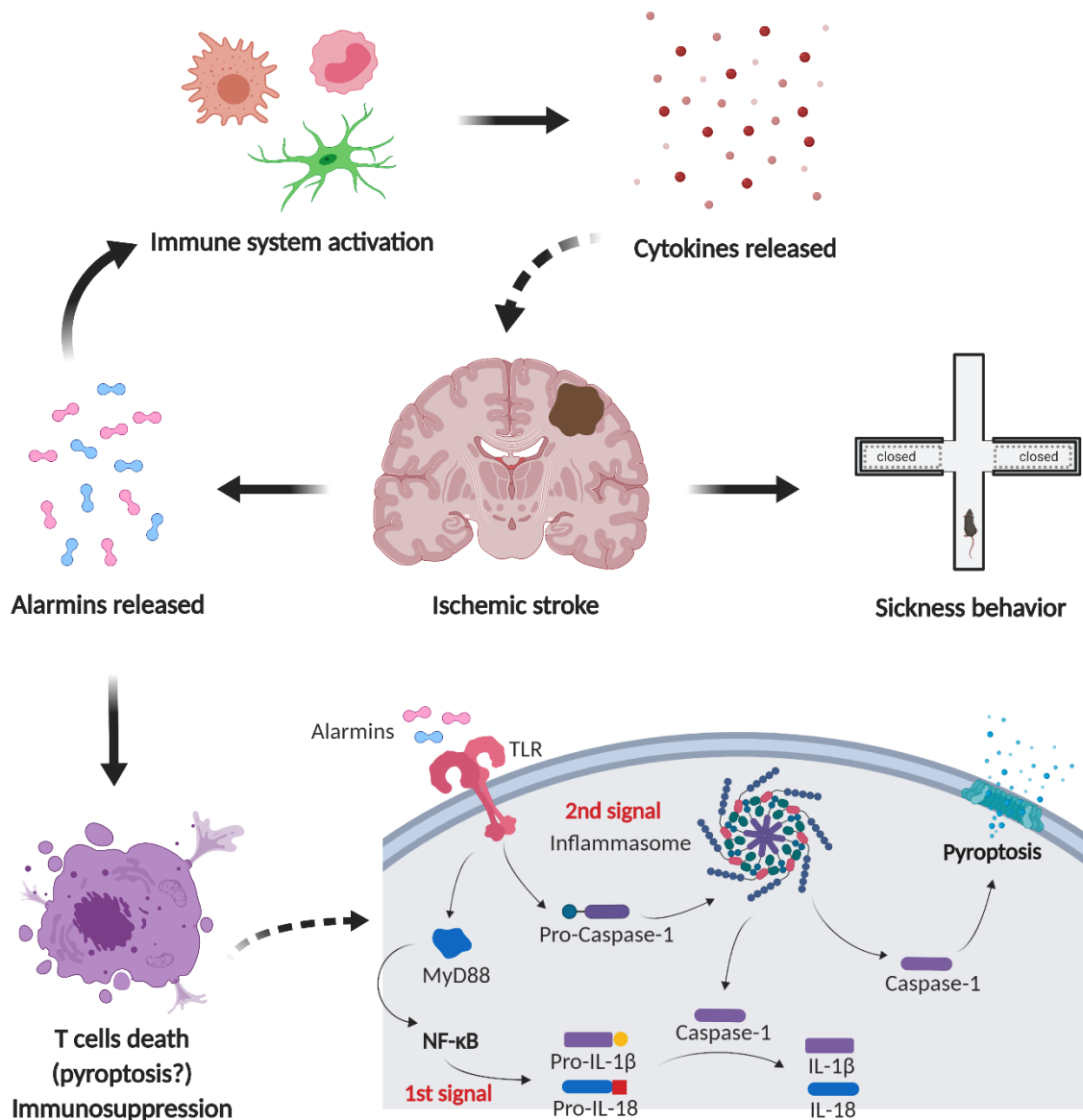


**Figure 15: Brain-released alarmins as mediators of immunological comorbidities after stroke.**

Alarmins released after ischemic stroke work as the main triggers in the mediation of immunological comorbidities. On the one hand, alarmins induce immune system activation and pro-inflammatory cytokine release. Pro-inflammatory cytokines influence behavior domains and induce sickness behavior. On the other hand, alarmins can also induce immunosuppression after stroke (T cell pyroptosis is most likely involved). After alarmins transduce the first and second signals into cell plasma through TLRs, Caspase-1 can be activated after inflammasome assembling; pro-IL-1  $\beta$  and pro-IL-18 that are produced through the NF- $\kappa$ B pathway are cleaved by active caspase-1 and released extracellularly. Additionally, active caspase-1 can also induce cell death (pyroptosis). The imaginary arrows represent the mechanisms that need further investigation.

## References

1. Moskowitz, M.A., Lo, E.H. & Iadecola, C. The science of stroke: mechanisms in search of treatments. *Neuron* **67**, 181-198 (2010).
2. Dirnagl, U., Iadecola, C. & Moskowitz, M.A. Pathobiology of ischaemic stroke: an integrated view. *Trends in neurosciences* **22**, 391-397 (1999).
3. Benjamin, E.J., *et al.* Heart Disease and Stroke Statistics-2017 Update: A Report From the American Heart Association. *Circulation* **135**, e146-e603 (2017).
4. Bejot, Y., Bailly, H., Durier, J. & Giroud, M. Epidemiology of stroke in Europe and trends for the 21st century. *Presse medicale* **45**, e391-e398 (2016).
5. Wong, K.S., Caplan, L.R. & Kim, J.S. Stroke Mechanisms. *Frontiers of neurology and neuroscience* **40**, 58-71 (2016).
6. Rothwell, P.M., Villagra, R., Gibson, R., Donders, R.C. & Warlow, C.P. Evidence of a chronic systemic cause of instability of atherosclerotic plaques. *Lancet* **355**, 19-24 (2000).
7. Ringelstein, E.B., Zeumer, H. & Angelou, D. The pathogenesis of strokes from internal carotid artery occlusion. Diagnostic and therapeutical implications. *Stroke; a journal of cerebral circulation* **14**, 867-875 (1983).
8. Caplan, L.R. & Hennerici, M. Impaired clearance of emboli (washout) is an important link between hypoperfusion, embolism, and ischemic stroke. *Archives of neurology* **55**, 1475-1482 (1998).
9. Kamel, H. & Healey, J.S. Cardioembolic Stroke. *Circulation research* **120**, 514-526 (2017).
10. Caplan, L.R. Intracranial branch atheromatous disease: a neglected, understudied, and underused concept. *Neurology* **39**, 1246-1250 (1989).
11. Lhermitte, F., Gautier, J.C. & Derouesne, C. Nature of occlusions of the middle cerebral artery. *Neurology* **20**, 82-88 (1970).
12. Fisher, C.M. & Caplan, L.R. Basilar artery branch occlusion: a cause of pontine infarction. *Neurology* **21**, 900-905 (1971).
13. Fisher, C.M. Bilateral occlusion of basilar artery branches. *Journal of neurology, neurosurgery, and psychiatry* **40**, 1182-1189 (1977).
14. Fisher, C.M. Capsular infarcts: the underlying vascular lesions. *Archives of neurology* **36**, 65-73 (1979).
15. Adams, H.P., Jr., *et al.* Classification of subtype of acute ischemic stroke. Definitions for use in a multicenter clinical trial. TOAST. Trial of Org 10172 in Acute Stroke Treatment. *Stroke; a journal of cerebral circulation* **24**, 35-41 (1993).
16. Durukan, A. & Tatlisumak, T. Acute ischemic stroke: overview of major experimental rodent models, pathophysiology, and therapy of focal cerebral ischemia. *Pharmacology, biochemistry, and behavior* **87**, 179-197 (2007).
17. Deb, P., Sharma, S. & Hassan, K.M. Pathophysiologic mechanisms of acute ischemic stroke: An overview with emphasis on therapeutic significance beyond thrombolysis. *Pathophysiology : the official journal of the International Society for Pathophysiology* **17**, 197-218 (2010).
18. Xing, C., Arai, K., Lo, E.H. & Hommel, M. Pathophysiologic cascades in ischemic stroke. *International journal of stroke : official journal of the International Stroke Society* **7**, 378-385 (2012).
19. Siesjo, B.K., Katsura, K. & Kristian, T. Acidosis-related damage. *Advances in neurology* **71**, 209-233; discussion 234-206 (1996).
20. Huang, Y. & McNamara, J.O. Ischemic stroke: "acidotoxicity" is a perpetrator. *Cell* **118**, 665-666 (2004).
21. Lo, E.H., Dalkara, T. & Moskowitz, M.A. Mechanisms, challenges and opportunities in stroke. *Nature reviews. Neuroscience* **4**, 399-415 (2003).
22. Kontos, H.A. Oxygen radicals in cerebral ischemia: the 2001 Willis lecture. *Stroke; a journal of cerebral circulation* **32**, 2712-2716 (2001).
23. Qin, A.P., Zhang, H.L. & Qin, Z.H. Mechanisms of lysosomal proteases participating in cerebral ischemia-induced neuronal death. *Neuroscience bulletin* **24**, 117-123 (2008).
24. Fagan, S.C., Hess, D.C., Hohnadel, E.J., Pollock, D.M. & Ergul, A. Targets for vascular protection after acute ischemic stroke. *Stroke; a journal of cerebral circulation* **35**, 2220-2225 (2004).

25. Rothwell, N.J. & Hopkins, S.J. Cytokines and the nervous system II: Actions and mechanisms of action. *Trends in neurosciences* **18**, 130-136 (1995).
26. Nawashiro, H., Tasaki, K., Ruetzler, C.A. & Hallenbeck, J.M. TNF-alpha pretreatment induces protective effects against focal cerebral ischemia in mice. *Journal of cerebral blood flow and metabolism : official journal of the International Society of Cerebral Blood Flow and Metabolism* **17**, 483-490 (1997).
27. Sairanen, T., et al. Evolution of cerebral tumor necrosis factor-alpha production during human ischemic stroke. *Stroke; a journal of cerebral circulation* **32**, 1750-1758 (2001).
28. Vila, N., Castillo, J., Davalos, A. & Chamorro, A. Proinflammatory cytokines and early neurological worsening in ischemic stroke. *Stroke; a journal of cerebral circulation* **31**, 2325-2329 (2000).
29. Barone, F.C. & Feuerstein, G.Z. Inflammatory mediators and stroke: new opportunities for novel therapeutics. *Journal of cerebral blood flow and metabolism : official journal of the International Society of Cerebral Blood Flow and Metabolism* **19**, 819-834 (1999).
30. Smith, W.S. Pathophysiology of focal cerebral ischemia: a therapeutic perspective. *Journal of vascular and interventional radiology : JVIR* **15**, S3-12 (2004).
31. Fisher, M. & Schaebitz, W. An overview of acute stroke therapy: past, present, and future. *Archives of internal medicine* **160**, 3196-3206 (2000).
32. Mergenthaler, P., Dirnagl, U. & Meisel, A. Pathophysiology of stroke: lessons from animal models. *Metabolic brain disease* **19**, 151-167 (2004).
33. Sugawara, T., et al. Neuronal death/survival signaling pathways in cerebral ischemia. *NeuroRx : the journal of the American Society for Experimental NeuroTherapeutics* **1**, 17-25 (2004).
34. Love, S. Apoptosis and brain ischaemia. *Progress in neuro-psychopharmacology & biological psychiatry* **27**, 267-282 (2003).
35. Said-Sadier, N. & Ojcius, D.M. Alarmins, inflammasomes and immunity. *Biomedical journal* **35**, 437-449 (2012).
36. Kerkhoff, C., Radon, Y. & Flaßkamp, H. Alarmins. in *Encyclopedia of Inflammatory Diseases* (ed. Parnham, M.) 1-12 (Springer Basel, Basel, 2015).
37. Mogensen, T.H. Pathogen Recognition and Inflammatory Signaling in Innate Immune Defenses. *Clinical Microbiology Reviews* **22**, 240-273 (2009).
38. Burnstock, G. Purinergic signalling and disorders of the central nervous system. *Nature reviews. Drug discovery* **7**, 575-590 (2008).
39. Marsh, B.J., Williams-Karnesky, R.L. & Stenzel-Poore, M.P. Toll-like receptor signaling in endogenous neuroprotection and stroke. *Neuroscience* **158**, 1007-1020 (2009).
40. Shichita, T., et al. Peroxiredoxin family proteins are key initiators of post-ischemic inflammation in the brain. *Nature medicine* **18**, 911-917 (2012).
41. Gelderblom, M., Sobey, C.G., Kleinschnitz, C. & Magnus, T. Danger signals in stroke. *Ageing research reviews* **24**, 77-82 (2015).
42. Liesz, A., et al. DAMP signaling is a key pathway inducing immune modulation after brain injury. *The Journal of neuroscience : the official journal of the Society for Neuroscience* **35**, 583-598 (2015).
43. Muhammad, S., et al. The HMGB1 receptor RAGE mediates ischemic brain damage. *The Journal of neuroscience : the official journal of the Society for Neuroscience* **28**, 12023-12031 (2008).
44. Yang, H., Wang, H., Chavan, S.S. & Andersson, U. High Mobility Group Box Protein 1 (HMGB1): The Prototypical Endogenous Danger Molecule. *Molecular medicine* **21 Suppl 1**, S6-S12 (2015).
45. Bustin, M. Regulation of DNA-dependent activities by the functional motifs of the high-mobility-group chromosomal proteins. *Molecular and cellular biology* **19**, 5237-5246 (1999).
46. Singh, V., Roth, S., Veltkamp, R. & Liesz, A. HMGB1 as a Key Mediator of Immune Mechanisms in Ischemic Stroke. *Antioxidants & redox signaling* **24**, 635-651 (2016).
47. Kim, J.B., et al. HMGB1, a novel cytokine-like mediator linking acute neuronal death and delayed neuroinflammation in the postischemic brain. *The Journal of neuroscience : the official journal of the Society for Neuroscience* **26**, 6413-6421 (2006).
48. Kim, J.B., Lim, C.M., Yu, Y.M. & Lee, J.K. Induction and subcellular localization of high-mobility group box-1 (HMGB1) in the postischemic rat brain. *Journal of neuroscience research* **86**, 1125-1131 (2008).
49. Schulze, J., et al. Severe stroke induces long-lasting alterations of high-mobility group box 1. *Stroke; a journal of cerebral circulation* **44**, 246-248 (2013).

50. Robson, S.C., *et al.* Loss of ATP diphosphohydrolase activity with endothelial cell activation. *The Journal of experimental medicine* **185**, 153-163 (1997).
51. Marteau, F., Communi, D., Boeynaems, J.M. & Suarez Gonzalez, N. Involvement of multiple P2Y receptors and signaling pathways in the action of adenine nucleotides diphosphates on human monocyte-derived dendritic cells. *Journal of leukocyte biology* **76**, 796-803 (2004).
52. Schnurr, M., *et al.* Extracellular ATP and TNF- $\alpha$  synergize in the activation and maturation of human dendritic cells. *J Immunol* **165**, 4704-4709 (2000).
53. Labasi, J.M., *et al.* Absence of the P2X7 receptor alters leukocyte function and attenuates an inflammatory response. *J Immunol* **168**, 6436-6445 (2002).
54. Solle, M., *et al.* Altered cytokine production in mice lacking P2X(7) receptors. *The Journal of biological chemistry* **276**, 125-132 (2001).
55. Mariathasan, S., *et al.* Cryopyrin activates the inflammasome in response to toxins and ATP. *Nature* **440**, 228-232 (2006).
56. Iadecola, C. & Anrather, J. The immunology of stroke: from mechanisms to translation. *Nature medicine* **17**, 796-808 (2011).
57. Aliprantis, A.O., *et al.* Cell activation and apoptosis by bacterial lipoproteins through toll-like receptor-2. *Science* **285**, 736-739 (1999).
58. Chang, Z.L. Important aspects of Toll-like receptors, ligands and their signaling pathways. *Inflammation research : official journal of the European Histamine Research Society ... [et al.]* **59**, 791-808 (2010).
59. Brasier, A.R. The NF- $\kappa$ B regulatory network. *Cardiovascular toxicology* **6**, 111-130 (2006).
60. Gesuete, R., Kohama, S.G. & Stenzel-Poore, M.P. Toll-like receptors and ischemic brain injury. *Journal of neuropathology and experimental neurology* **73**, 378-386 (2014).
61. Brea, D., *et al.* Toll-like receptors 2 and 4 in ischemic stroke: outcome and therapeutic values. *Journal of cerebral blood flow and metabolism : official journal of the International Society of Cerebral Blood Flow and Metabolism* **31**, 1424-1431 (2011).
62. Caso, J.R., *et al.* Toll-like receptor 4 is involved in brain damage and inflammation after experimental stroke. *Circulation* **115**, 1599-1608 (2007).
63. Tang, S.C., *et al.* Pivotal role for neuronal Toll-like receptors in ischemic brain injury and functional deficits. *Proceedings of the National Academy of Sciences of the United States of America* **104**, 13798-13803 (2007).
64. Downes, C.E., *et al.* MyD88 is a critical regulator of hematopoietic cell-mediated neuroprotection seen after stroke. *PloS one* **8**, e57948 (2013).
65. Lotze, M.T. & Tracey, K.J. High-mobility group box 1 protein (HMGB1): nuclear weapon in the immune arsenal. *Nature reviews. Immunology* **5**, 331-342 (2005).
66. Zhai, D.X., *et al.* RAGE expression is up-regulated in human cerebral ischemia and pMCAO rats. *Neuroscience letters* **445**, 117-121 (2008).
67. Kamide, T., *et al.* RAGE mediates vascular injury and inflammation after global cerebral ischemia. *Neurochemistry international* **60**, 220-228 (2012).
68. Akirav, E.M., *et al.* RAGE expression in human T cells: a link between environmental factors and adaptive immune responses. *PloS one* **7**, e34698 (2012).
69. Manfredi, A.A., *et al.* Maturing dendritic cells depend on RAGE for in vivo homing to lymph nodes. *J Immunol* **180**, 2270-2275 (2008).
70. Xanthis, A., *et al.* Receptor of advanced glycation end products (RAGE) positively regulates CD36 expression and reactive oxygen species production in human monocytes in diabetes. *Angiology* **60**, 772-779 (2009).
71. Burnstock, G. Introduction to purinergic signalling in the brain. *Advances in experimental medicine and biology* **986**, 1-12 (2013).
72. Ulrich, H., Abbracchio, M.P. & Burnstock, G. Extrinsic purinergic regulation of neural stem/progenitor cells: implications for CNS development and repair. *Stem cell reviews* **8**, 755-767 (2012).
73. Volonte, C., Apolloni, S., Skaper, S.D. & Burnstock, G. P2X7 receptors: channels, pores and more. *CNS & neurological disorders drug targets* **11**, 705-721 (2012).
74. Savio, L.E.B., de Andrade Mello, P., da Silva, C.G. & Coutinho-Silva, R. The P2X7 Receptor in Inflammatory Diseases: Angel or Demon? *Frontiers in pharmacology* **9**, 52 (2018).
75. Coutinho-Silva, R., *et al.* P2Z/P2X7 receptor-dependent apoptosis of dendritic cells. *The American journal of physiology* **276**, C1139-1147 (1999).



76. Kawano, A., *et al.* Involvement of P2X4 receptor in P2X7 receptor-dependent cell death of mouse macrophages. *Biochemical and biophysical research communications* **419**, 374-380 (2012).
77. Liu, Y., Xiao, Y. & Li, Z. P2X7 receptor positively regulates MyD88-dependent NF-kappaB activation. *Cytokine* **55**, 229-236 (2011).
78. Melani, A., *et al.* P2X7 receptor modulation on microglial cells and reduction of brain infarct caused by middle cerebral artery occlusion in rat. *Journal of cerebral blood flow and metabolism : official journal of the International Society of Cerebral Blood Flow and Metabolism* **26**, 974-982 (2006).
79. Melani, A., *et al.* Ecto-ATPase inhibition: ATP and adenosine release under physiological and ischemic in vivo conditions in the rat striatum. *Experimental neurology* **233**, 193-204 (2012).
80. Brough, D., Le Feuvre, R.A., Iwakura, Y. & Rothwell, N.J. Purinergic (P2X7) receptor activation of microglia induces cell death via an interleukin-1-independent mechanism. *Molecular and cellular neurosciences* **19**, 272-280 (2002).
81. Arbeloa, J., Perez-Samartin, A., Gottlieb, M. & Matute, C. P2X7 receptor blockade prevents ATP excitotoxicity in neurons and reduces brain damage after ischemia. *Neurobiology of disease* **45**, 954-961 (2012).
82. Domercq, M., *et al.* P2X7 receptors mediate ischemic damage to oligodendrocytes. *Glia* **58**, 730-740 (2010).
83. Meisel, C., Schwab, J.M., Prass, K., Meisel, A. & Dirnagl, U. Central nervous system injury-induced immune deficiency syndrome. *Nature reviews. Neuroscience* **6**, 775-786 (2005).
84. del Zoppo, G.J., Becker, K.J. & Hallenbeck, J.M. Inflammation after stroke: is it harmful? *Archives of neurology* **58**, 669-672 (2001).
85. Ekdahl, C.T., Kokaia, Z. & Lindvall, O. Brain inflammation and adult neurogenesis: the dual role of microglia. *Neuroscience* **158**, 1021-1029 (2009).
86. Liu, T., *et al.* Tumor necrosis factor-alpha expression in ischemic neurons. *Stroke; a journal of cerebral circulation* **25**, 1481-1488 (1994).
87. Liu, T., *et al.* Interleukin-1 beta mRNA expression in ischemic rat cortex. *Stroke; a journal of cerebral circulation* **24**, 1746-1750; discussion 1750-1741 (1993).
88. Wang, X., Yue, T.L., Young, P.R., Barone, F.C. & Feuerstein, G.Z. Expression of interleukin-6, c-fos, and zif268 mRNAs in rat ischemic cortex. *Journal of cerebral blood flow and metabolism : official journal of the International Society of Cerebral Blood Flow and Metabolism* **15**, 166-171 (1995).
89. Wang, X., *et al.* Prolonged expression of interferon-inducible protein-10 in ischemic cortex after permanent occlusion of the middle cerebral artery in rat. *Journal of neurochemistry* **71**, 1194-1204 (1998).
90. Wang, X., Yue, T.L., Barone, F.C. & Feuerstein, G.Z. Monocyte chemoattractant protein-1 messenger RNA expression in rat ischemic cortex. *Stroke; a journal of cerebral circulation* **26**, 661-665; discussion 665-666 (1995).
91. Kim, J.S., *et al.* Expression of monocyte chemoattractant protein-1 and macrophage inflammatory protein-1 after focal cerebral ischemia in the rat. *Journal of neuroimmunology* **56**, 127-134 (1995).
92. Lucas, S.M., Rothwell, N.J. & Gibson, R.M. The role of inflammation in CNS injury and disease. *British journal of pharmacology* **147 Suppl 1**, S232-240 (2006).
93. Swanson, R.A., Ying, W. & Kauppinen, T.M. Astrocyte influences on ischemic neuronal death. *Current molecular medicine* **4**, 193-205 (2004).
94. Abdullahi, W., Tripathi, D. & Ronaldson, P.T. Blood-brain barrier dysfunction in ischemic stroke: targeting tight junctions and transporters for vascular protection. *American journal of physiology. Cell physiology* **315**, C343-C356 (2018).
95. Gelderblom, M., *et al.* Temporal and spatial dynamics of cerebral immune cell accumulation in stroke. *Stroke; a journal of cerebral circulation* **40**, 1849-1857 (2009).
96. Jickling, G.C., *et al.* Targeting neutrophils in ischemic stroke: translational insights from experimental studies. *Journal of cerebral blood flow and metabolism : official journal of the International Society of Cerebral Blood Flow and Metabolism* **35**, 888-901 (2015).
97. Petty, M.A. & Lo, E.H. Junctional complexes of the blood-brain barrier: permeability changes in neuroinflammation. *Progress in neurobiology* **68**, 311-323 (2002).
98. Liesz, A., *et al.* Inhibition of lymphocyte trafficking shields the brain against deleterious neuroinflammation after stroke. *Brain : a journal of neurology* **134**, 704-720 (2011).
99. Neumann, J., *et al.* Very-late-antigen-4 (VLA-4)-mediated brain invasion by neutrophils leads to interactions with microglia, increased ischemic injury and impaired behavior in experimental stroke. *Acta*

- neuropathologica* **129**, 259-277 (2015).
100. Relton, J.K., *et al.* Inhibition of alpha4 integrin protects against transient focal cerebral ischemia in normotensive and hypertensive rats. *Stroke; a journal of cerebral circulation* **32**, 199-205 (2001).
  101. Emsley, H.C., *et al.* An early and sustained peripheral inflammatory response in acute ischaemic stroke: relationships with infection and atherosclerosis. *Journal of neuroimmunology* **139**, 93-101 (2003).
  102. Tuttolomondo, A., *et al.* Plasma levels of inflammatory and thrombotic/fibrinolytic markers in acute ischemic strokes: relationship with TOAST subtype, outcome and infarct site. *Journal of neuroimmunology* **215**, 84-89 (2009).
  103. Lambertsen, K.L., Biber, K. & Finsen, B. Inflammatory cytokines in experimental and human stroke. *Journal of cerebral blood flow and metabolism : official journal of the International Society of Cerebral Blood Flow and Metabolism* **32**, 1677-1698 (2012).
  104. Offner, H., *et al.* Experimental stroke induces massive, rapid activation of the peripheral immune system. *Journal of cerebral blood flow and metabolism : official journal of the International Society of Cerebral Blood Flow and Metabolism* **26**, 654-665 (2006).
  105. del Zoppo, G.J. Acute anti-inflammatory approaches to ischemic stroke. *Annals of the New York Academy of Sciences* **1207**, 143-148 (2010).
  106. Zhu, Y., *et al.* Transforming growth factor-beta 1 increases bad phosphorylation and protects neurons against damage. *The Journal of neuroscience : the official journal of the Society for Neuroscience* **22**, 3898-3909 (2002).
  107. Spera, P.A., Ellison, J.A., Feuerstein, G.Z. & Barone, F.C. IL-10 reduces rat brain injury following focal stroke. *Neuroscience letters* **251**, 189-192 (1998).
  108. Dantzer, R. Cytokine, sickness behavior, and depression. *Neurologic clinics* **24**, 441-460 (2006).
  109. Dantzer, R. & Kelley, K.W. Twenty years of research on cytokine-induced sickness behavior. *Brain, behavior, and immunity* **21**, 153-160 (2007).
  110. Kelley, K.W., *et al.* Cytokine-induced sickness behavior. *Brain, behavior, and immunity* **17 Suppl 1**, S112-118 (2003).
  111. Bluthé, R.M., *et al.* Lipopolysaccharide induces sickness behaviour in rats by a vagal mediated mechanism. *Comptes rendus de l'Academie des sciences. Serie III, Sciences de la vie* **317**, 499-503 (1994).
  112. Bluthé, R.M., Michaud, B., Kelley, K.W. & Dantzer, R. Vagotomy attenuates behavioural effects of interleukin-1 injected peripherally but not centrally. *Neuroreport* **7**, 1485-1488 (1996).
  113. Bluthé, R.M., Michaud, B., Kelley, K.W. & Dantzer, R. Vagotomy blocks behavioural effects of interleukin-1 injected via the intraperitoneal route but not via other systemic routes. *Neuroreport* **7**, 2823-2827 (1996).
  114. Marvel, F.A., Chen, C.C., Badr, N., Gaykema, R.P. & Goehler, L.E. Reversible inactivation of the dorsal vagal complex blocks lipopolysaccharide-induced social withdrawal and c-Fos expression in central autonomic nuclei. *Brain, behavior, and immunity* **18**, 123-134 (2004).
  115. Dantzer, R., O'Connor, J.C., Freund, G.G., Johnson, R.W. & Kelley, K.W. From inflammation to sickness and depression: when the immune system subjugates the brain. *Nature reviews. Neuroscience* **9**, 46-56 (2008).
  116. Laye, S., *et al.* Endogenous brain IL-1 mediates LPS-induced anorexia and hypothalamic cytokine expression. *American journal of physiology. Regulatory, integrative and comparative physiology* **279**, R93-98 (2000).
  117. Kent, S., *et al.* Different receptor mechanisms mediate the pyrogenic and behavioral effects of interleukin 1. *Proceedings of the National Academy of Sciences of the United States of America* **89**, 9117-9120 (1992).
  118. Ericsson, A., Liu, C., Hart, R.P. & Sawchenko, P.E. Type 1 interleukin-1 receptor in the rat brain: distribution, regulation, and relationship to sites of IL-1-induced cellular activation. *The Journal of comparative neurology* **361**, 681-698 (1995).
  119. Vitkovic, L., *et al.* Cytokine signals propagate through the brain. *Molecular psychiatry* **5**, 604-615 (2000).
  120. Grossman, K.J., Goss, C.W. & Stein, D.G. Sickness behaviors following medial frontal cortical contusions in male rats. *Behavioural brain research* **217**, 202-208 (2011).
  121. Dantzer, R. Cytokine, sickness behavior, and depression. *Immunology and allergy clinics of North America* **29**, 247-264 (2009).
  122. Wu, D., Wang, L., Teng, W., Huang, K. & Shang, X. Correlation of fatigue during the acute stage of stroke with serum uric acid and glucose levels, depression, and disability. *European neurology* **72**, 223-227 (2014).
  123. Menlove, L., *et al.* Predictors of anxiety after stroke: a systematic review of observational studies. *Journal of stroke and cerebrovascular diseases : the official journal of National Stroke Association* **24**, 1107-1117 (2015).

124. Balkaya, M., Kröber, J.M., Rex, A. & Endres, M. Assessing Post-Stroke Behavior in Mouse Models of Focal Ischemia. *Journal of Cerebral Blood Flow & Metabolism* **33**, 330-338 (2012).
125. Hunter, A.J., *et al.* Functional assessments in mice and rats after focal stroke. *Neuropharmacology* **39**, 806-816 (2000).
126. Haeusler, K.G., *et al.* Immune responses after acute ischemic stroke or myocardial infarction. *International journal of cardiology* **155**, 372-377 (2012).
127. Gendron, A., *et al.* Temporal effects of left versus right middle cerebral artery occlusion on spleen lymphocyte subsets and mitogenic response in Wistar rats. *Brain research* **955**, 85-97 (2002).
128. Offner, H., Vandenbark, A.A. & Hurn, P.D. Effect of experimental stroke on peripheral immunity: CNS ischemia induces profound immunosuppression. *Neuroscience* **158**, 1098-1111 (2009).
129. Offner, H., *et al.* Splenic atrophy in experimental stroke is accompanied by increased regulatory T cells and circulating macrophages. *J Immunol* **176**, 6523-6531 (2006).
130. Dirnagl, U. Pathobiology of injury after stroke: the neurovascular unit and beyond. *Annals of the New York Academy of Sciences* **1268**, 21-25 (2012).
131. Liesz, A., *et al.* Acquired Immunoglobulin G deficiency in stroke patients and experimental brain ischemia. *Experimental neurology* **271**, 46-52 (2015).
132. Liesz, A., *et al.* Stress mediators and immune dysfunction in patients with acute cerebrovascular diseases. *PloS one* **8**, e74839 (2013).
133. Prass, K., *et al.* Stroke-induced immunodeficiency promotes spontaneous bacterial infections and is mediated by sympathetic activation reversal by poststroke T helper cell type 1-like immunostimulation. *The Journal of experimental medicine* **198**, 725-736 (2003).
134. Urra, X., Cervera, A., Villamor, N., Planas, A.M. & Chamorro, A. Harms and benefits of lymphocyte subpopulations in patients with acute stroke. *Neuroscience* **158**, 1174-1183 (2009).
135. Elenkov, I.J., Wilder, R.L., Chrousos, G.P. & Vizi, E.S. The sympathetic nerve--an integrative interface between two supersystems: the brain and the immune system. *Pharmacological reviews* **52**, 595-638 (2000).
136. Mignini, F., Streccioni, V. & Amenta, F. Autonomic innervation of immune organs and neuroimmune modulation. *Autonomic & autacoid pharmacology* **23**, 1-25 (2003).
137. Elenkov, I.J., Papanicolaou, D.A., Wilder, R.L. & Chrousos, G.P. Modulatory effects of glucocorticoids and catecholamines on human interleukin-12 and interleukin-10 production: clinical implications. *Proceedings of the Association of American Physicians* **108**, 374-381 (1996).
138. Sanders, V.M., *et al.* Differential expression of the beta2-adrenergic receptor by Th1 and Th2 clones: implications for cytokine production and B cell help. *J Immunol* **158**, 4200-4210 (1997).
139. Borovikova, L.V., *et al.* Vagus nerve stimulation attenuates the systemic inflammatory response to endotoxin. *Nature* **405**, 458-462 (2000).
140. Meagher, L.C., Cousin, J.M., Seckl, J.R. & Haslett, C. Opposing effects of glucocorticoids on the rate of apoptosis in neutrophilic and eosinophilic granulocytes. *J Immunol* **156**, 4422-4428 (1996).
141. Woiciechowsky, C., Schoning, B., Lanksch, W.R., Volk, H.D. & Docke, W.D. Mechanisms of brain-mediated systemic anti-inflammatory syndrome causing immunodepression. *Journal of molecular medicine* **77**, 769-780 (1999).
142. Wong, C.H., Jenne, C.N., Lee, W.Y., Leger, C. & Kubes, P. Functional innervation of hepatic iNKT cells is immunosuppressive following stroke. *Science* **334**, 101-105 (2011).
143. Mracsko, E., *et al.* Differential effects of sympathetic nervous system and hypothalamic-pituitary-adrenal axis on systemic immune cells after severe experimental stroke. *Brain, behavior, and immunity* **41**, 200-209 (2014).
144. Faraco, G., *et al.* High mobility group box 1 protein is released by neural cells upon different stresses and worsens ischemic neurodegeneration in vitro and in vivo. *Journal of neurochemistry* **103**, 590-603 (2007).
145. (!!! INVALID CITATION !!!).
146. Zychlinsky, A., Prevost, M.C. & Sansonetti, P.J. Shigella flexneri induces apoptosis in infected macrophages. *Nature* **358**, 167-169 (1992).
147. Tan, M.S., *et al.* Amyloid-beta induces NLRP1-dependent neuronal pyroptosis in models of Alzheimer's disease. *Cell death & disease* **5**, e1382 (2014).
148. Tan, C.C., *et al.* NLRP1 inflammasome is activated in patients with medial temporal lobe epilepsy and contributes to neuronal pyroptosis in amygdala kindling-induced rat model. *Journal of neuroinflammation*

- 12, 18 (2015).
149. Yang, J.R., *et al.* Ischemia-reperfusion induces renal tubule pyroptosis via the CHOP-caspase-11 pathway. *American journal of physiology. Renal physiology* **306**, F75-84 (2014).
150. Adamczak, S.E., *et al.* Pyroptotic neuronal cell death mediated by the AIM2 inflammasome. *Journal of cerebral blood flow and metabolism : official journal of the International Society of Cerebral Blood Flow and Metabolism* **34**, 621-629 (2014).
151. Qiu, Z., *et al.* NLRP3 Inflammasome Activation-Mediated Pyroptosis Aggravates Myocardial Ischemia/Reperfusion Injury in Diabetic Rats. *Oxidative medicine and cellular longevity* **2017**, 9743280 (2017).
152. Han, Y., *et al.* Low-dose Sinapic Acid Abates the Pyroptosis of Macrophages by Downregulation of lncRNA-MALAT1 in Rats With Diabetic Atherosclerosis. *Journal of cardiovascular pharmacology* **71**, 104-112 (2018).
153. Shi, J., *et al.* Cleavage of GSDMD by inflammatory caspases determines pyroptotic cell death. *Nature* **526**, 660-665 (2015).
154. Dong, Z., Pan, K., Pan, J., Peng, Q. & Wang, Y. The Possibility and Molecular Mechanisms of Cell Pyroptosis After Cerebral Ischemia. *Neuroscience bulletin* (2018).
155. Gaidt, M.M. & Hornung, V. Pore formation by GSDMD is the effector mechanism of pyroptosis. *The EMBO journal* **35**, 2167-2169 (2016).
156. Yuan, Y.Y., Xie, K.X., Wang, S.L. & Yuan, L.W. Inflammatory caspase-related pyroptosis: mechanism, regulation and therapeutic potential for inflammatory bowel disease. *Gastroenterology report* **6**, 167-176 (2018).
157. Shi, J., Gao, W. & Shao, F. Pyroptosis: Gasdermin-Mediated Programmed Necrotic Cell Death. *Trends in biochemical sciences* **42**, 245-254 (2017).
158. Poh, L., *et al.* Evidence that NLR4 inflammasome mediates apoptotic and pyroptotic microglial death following ischemic stroke. *Brain, behavior, and immunity* (2018).
159. Fink, S.L., Bergsbaken, T. & Cookson, B.T. Anthrax lethal toxin and Salmonella elicit the common cell death pathway of caspase-1-dependent pyroptosis via distinct mechanisms. *Proceedings of the National Academy of Sciences of the United States of America* **105**, 4312-4317 (2008).
160. Ghiringhelli, F., *et al.* Activation of the NLRP3 inflammasome in dendritic cells induces IL-1 $\beta$ -dependent adaptive immunity against tumors. *Nature medicine* **15**, 1170-1178 (2009).
161. Deora, V., *et al.* The microglial NLRP3 inflammasome is activated by amyotrophic lateral sclerosis proteins. *Glia* (2019).
162. Sellin, M.E., *et al.* Epithelium-intrinsic NAIP/NLRC4 inflammasome drives infected enterocyte expulsion to restrict Salmonella replication in the intestinal mucosa. *Cell host & microbe* **16**, 237-248 (2014).
163. Chen, K.W., *et al.* The neutrophil NLRC4 inflammasome selectively promotes IL-1 $\beta$  maturation without pyroptosis during acute Salmonella challenge. *Cell reports* **8**, 570-582 (2014).
164. Vigano, E., *et al.* Human caspase-4 and caspase-5 regulate the one-step non-canonical inflammasome activation in monocytes. *Nature communications* **6**, 8761 (2015).
165. Arbore, G., *et al.* T helper 1 immunity requires complement-driven NLRP3 inflammasome activity in CD4(+) T cells. *Science* **352**, aad1210 (2016).
166. Malik, A. & Kanneganti, T.D. Inflammasome activation and assembly at a glance. *Journal of cell science* **130**, 3955-3963 (2017).
167. Kayagaki, N., *et al.* Non-canonical inflammasome activation targets caspase-11. *Nature* **479**, 117-121 (2011).
168. Adachi, O., *et al.* Targeted disruption of the MyD88 gene results in loss of IL-1- and IL-18-mediated function. *Immunity* **9**, 143-150 (1998).
169. Liliensiek, B., *et al.* Receptor for advanced glycation end products (RAGE) regulates sepsis but not the adaptive immune response. *The Journal of clinical investigation* **113**, 1641-1650 (2004).
170. Roth, S., *et al.* Brain-released alarmins and stress response synergize in accelerating atherosclerosis progression after stroke. *Science translational medicine* **10**(2018).
171. Singh, V., *et al.* Microbiota Dysbiosis Controls the Neuroinflammatory Response after Stroke. *The Journal of neuroscience : the official journal of the Society for Neuroscience* **36**, 7428-7440 (2016).
172. Bederson, J.B., *et al.* Rat middle cerebral artery occlusion: evaluation of the model and development of a neurologic examination. *Stroke; a journal of cerebral circulation* **17**, 472-476 (1986).
173. Orsini, F., *et al.* Targeting mannose-binding lectin confers long-lasting protection with a surprisingly wide therapeutic window in cerebral ischemia. *Circulation* **126**, 1484-1494 (2012).

174. Komada, M., Takao, K. & Miyakawa, T. Elevated plus maze for mice. *Journal of visualized experiments : JoVE* (2008).
175. Seibenhener, M.L. & Wooten, M.C. Use of the Open Field Maze to measure locomotor and anxiety-like behavior in mice. *Journal of visualized experiments : JoVE*, e52434 (2015).
176. Klein, S., Bankstahl, J.P., Loscher, W. & Bankstahl, M. Sucrose consumption test reveals pharmacoresistant depression-associated behavior in two mouse models of temporal lobe epilepsy. *Experimental neurology* **263**, 263-271 (2015).
177. Can, A., *et al.* The mouse forced swim test. *Journal of visualized experiments : JoVE*, e3638 (2012).
178. Schallert, T., Fleming, S.M., Leasure, J.L., Tillerson, J.L. & Bland, S.T. CNS plasticity and assessment of forelimb sensorimotor outcome in unilateral rat models of stroke, cortical ablation, parkinsonism and spinal cord injury. *Neuropharmacology* **39**, 777-787 (2000).
179. Dunham, N.W. & Miya, T.S. A note on a simple apparatus for detecting neurological deficit in rats and mice. *Journal of the American Pharmaceutical Association. American Pharmaceutical Association* **46**, 208-209 (1957).
180. Jones, B.J. & Roberts, D.J. A rotarod suitable for quantitative measurements of motor incoordination in naive mice. *Naunyn-Schmiedebergs Archiv fur experimentelle Pathologie und Pharmacologie* **259**, 211 (1968).
181. Schallert, T., *et al.* Tactile extinction: distinguishing between sensorimotor and motor asymmetries in rats with unilateral nigrostriatal damage. *Pharmacology, biochemistry, and behavior* **16**, 455-462 (1982).
182. Bradman, M.J., Ferrini, F., Salio, C. & Merighi, A. Practical mechanical threshold estimation in rodents using von Frey hairs/Semmes-Weinstein monofilaments: Towards a rational method. *Journal of neuroscience methods* **255**, 92-103 (2015).
183. Handley, S.L. & Mithani, S. Effects of alpha-adrenoceptor agonists and antagonists in a maze-exploration model of 'fear'-motivated behaviour. *Naunyn-Schmiedeberg's archives of pharmacology* **327**, 1-5 (1984).
184. CS., H. Emotional behavior in the rat: defecation and urination as measures of individual differences in emotionality. *Journal of Comparative Psychology* **18**, 385-403 (1934).
185. Willner, P., Towell, A., Sampson, D., Sophokleous, S. & Muscat, R. Reduction of sucrose preference by chronic unpredictable mild stress, and its restoration by a tricyclic antidepressant. *Psychopharmacology* **93**, 358-364 (1987).
186. Wu, C., Zhang, J. & Chen, Y. Study on the behavioral changes of a post-stroke depression rat model. *Experimental and therapeutic medicine* **10**, 159-163 (2015).
187. Vahid-Ansari, F., Lagace, D.C. & Albert, P.R. Persistent post-stroke depression in mice following unilateral medial prefrontal cortical stroke. *Translational psychiatry* **6**, e863 (2016).
188. Lister, R.G. The use of a plus-maze to measure anxiety in the mouse. *Psychopharmacology* **92**, 180-185 (1987).
189. Lemon, C.H. Perceptual and neural responses to sweet taste in humans and rodents. *Chemosensory perception* **8**, 46-52 (2015).
190. Gorwood, P. Neurobiological mechanisms of anhedonia. *Dialogues in clinical neuroscience* **10**, 291-299 (2008).
191. Porsolt, R.D., Le Pichon, M. & Jalfre, M. Depression: a new animal model sensitive to antidepressant treatments. *Nature* **266**, 730-732 (1977).
192. Porsolt, R.D., Bertin, A. & Jalfre, M. Behavioral despair in mice: a primary screening test for antidepressants. *Archives internationales de pharmacodynamie et de therapie* **229**, 327-336 (1977).
193. Shim, R. & Wong, C.H. Ischemia, Immunosuppression and Infection--Tackling the Predicaments of Post-Stroke Complications. *International journal of molecular sciences* **17**(2016).
194. Prass, K., *et al.* Desferrioxamine induces delayed tolerance against cerebral ischemia in vivo and in vitro. *Journal of cerebral blood flow and metabolism : official journal of the International Society of Cerebral Blood Flow and Metabolism* **22**, 520-525 (2002).
195. Yonchuk, J.G., *et al.* Circulating soluble receptor for advanced glycation end products (sRAGE) as a biomarker of emphysema and the RAGE axis in the lung. *American journal of respiratory and critical care medicine* **192**, 785-792 (2015).
196. Chiang, T., Messing, R.O. & Chou, W.H. Mouse model of middle cerebral artery occlusion. *Journal of visualized experiments : JoVE* (2011).
197. Schottke, H. & Giabbiconi, C.M. Post-stroke depression and post-stroke anxiety: prevalence and predictors.

- International psychogeriatrics* **27**, 1805-1812 (2015).
198. Crawley, J.N. Exploratory behavior models of anxiety in mice. *Neuroscience and biobehavioral reviews* **9**, 37-44 (1985).
  199. Belzung, C. & Griebel, G. Measuring normal and pathological anxiety-like behaviour in mice: a review. *Behavioural brain research* **125**, 141-149 (2001).
  200. Winter, B., *et al.* Anxious and hyperactive phenotype following brief ischemic episodes in mice. *Biological psychiatry* **57**, 1166-1175 (2005).
  201. Kilic, E., *et al.* Delayed melatonin administration promotes neuronal survival, neurogenesis and motor recovery, and attenuates hyperactivity and anxiety after mild focal cerebral ischemia in mice. *Journal of pineal research* **45**, 142-148 (2008).
  202. Jiang, Y., Deacon, R., Anthony, D.C. & Campbell, S.J. Inhibition of peripheral TNF can block the malaise associated with CNS inflammatory diseases. *Neurobiology of disease* **32**, 125-132 (2008).
  203. Eskilsson, A., *et al.* Immune-induced fever is mediated by IL-6 receptors on brain endothelial cells coupled to STAT3-dependent induction of brain endothelial prostaglandin synthesis. *The Journal of neuroscience : the official journal of the Society for Neuroscience* **34**, 15957-15961 (2014).
  204. Egencioglu, E., Anesten, F., Schele, E. & Palsdottir, V. Interleukin-6 is important for regulation of core body temperature during long-term cold exposure in mice. *Biomedical reports* **9**, 206-212 (2018).
  205. Kozak, W., Conn, C.A. & Kluger, M.J. Lipopolysaccharide induces fever and depresses locomotor activity in unrestrained mice. *The American journal of physiology* **266**, R125-135 (1994).
  206. Tanaka, T., Narazaki, M. & Kishimoto, T. IL-6 in inflammation, immunity, and disease. *Cold Spring Harbor perspectives in biology* **6**, a016295 (2014).
  207. Kim, D. Postoperative Hypothermia. *Acute Crit Care* **34**, 79-80 (2019).
  208. Comstedt, P., Storgaard, M. & Lassen, A.T. The Systemic Inflammatory Response Syndrome (SIRS) in acutely hospitalised medical patients: a cohort study. *Scandinavian journal of trauma, resuscitation and emergency medicine* **17**, 67 (2009).
  209. Crawley, J.N. Behavioral phenotyping of transgenic and knockout mice: experimental design and evaluation of general health, sensory functions, motor abilities, and specific behavioral tests. *Brain research* **835**, 18-26 (1999).
  210. Boleij, H., Salomons, A.R., van Sprundel, M., Arndt, S.S. & Ohi, F. Not All Mice Are Equal: Welfare Implications of Behavioural Habituation Profiles in Four 129 Mouse Substrains. *PloS one* **7**, e42544 (2012).
  211. Nelson, R.J. & Chiavegatto, S. Aggression in knockout mice. *ILAR journal* **41**, 153-162 (2000).
  212. Patel, A., Siegel, A. & Zalcman, S.S. Lack of aggression and anxiolytic-like behavior in TNF receptor (TNF-R1 and TNF-R2) deficient mice. *Brain, behavior, and immunity* **24**, 1276-1280 (2010).
  213. Lubjuhn, J., *et al.* Functional testing in a mouse stroke model induced by occlusion of the distal middle cerebral artery. *Journal of neuroscience methods* **184**, 95-103 (2009).
  214. Moon, S.K., Alaverdashvili, M., Cross, A.R. & Whishaw, I.Q. Both compensation and recovery of skilled reaching following small photothrombotic stroke to motor cortex in the rat. *Experimental neurology* **218**, 145-153 (2009).
  215. Bains, R.S., *et al.* Analysis of Individual Mouse Activity in Group Housed Animals of Different Inbred Strains using a Novel Automated Home Cage Analysis System. *Frontiers in behavioral neuroscience* **10**, 106 (2016).
  216. Wang, Z., Mirbozorgi, S.A. & Ghovanloo, M. An automated behavior analysis system for freely moving rodents using depth image. *Medical & biological engineering & computing* **56**, 1807-1821 (2018).
  217. Seifert, H.A., *et al.* A transient decrease in spleen size following stroke corresponds to splenocyte release into systemic circulation. *Journal of neuroimmune pharmacology : the official journal of the Society on NeuroImmune Pharmacology* **7**, 1017-1024 (2012).
  218. Kim, E., Yang, J., Beltran, C.D. & Cho, S. Role of spleen-derived monocytes/macrophages in acute ischemic brain injury. *Journal of cerebral blood flow and metabolism : official journal of the International Society of Cerebral Blood Flow and Metabolism* **34**, 1411-1419 (2014).
  219. Hurn, P.D. 2014 Thomas Willis Award Lecture: sex, stroke, and innovation. *Stroke; a journal of cerebral circulation* **45**, 3725-3729 (2014).
  220. Sahota, P., *et al.* Changes in spleen size in patients with acute ischemic stroke: a pilot observational study. *International journal of stroke : official journal of the International Stroke Society* **8**, 60-67 (2013).
  221. Chiu, N.L., *et al.* The Volume of the Spleen and Its Correlates after Acute Stroke. *Journal of stroke and*

- cerebrovascular diseases : the official journal of National Stroke Association* **25**, 2958-2961 (2016).
222. Zhou, W., *et al.* Postischemic brain infiltration of leukocyte subpopulations differs among murine permanent and transient focal cerebral ischemia models. *Brain pathology* **23**, 34-44 (2013).
  223. Frank, D. & Vince, J.E. Pyroptosis versus necroptosis: similarities, differences, and crosstalk. *Cell death and differentiation* (2018).
  224. Kerr, J.F., Wyllie, A.H. & Currie, A.R. Apoptosis: a basic biological phenomenon with wide-ranging implications in tissue kinetics. *British journal of cancer* **26**, 239-257 (1972).
  225. Vermes, I., Haanen, C., Steffens-Nakken, H. & Reutelingsperger, C. A novel assay for apoptosis. Flow cytometric detection of phosphatidylserine expression on early apoptotic cells using fluorescein labelled Annexin V. *Journal of immunological methods* **184**, 39-51 (1995).
  226. Gorczyca, W., Traganos, F., Jesionowska, H. & Darzynkiewicz, Z. Presence of DNA strand breaks and increased sensitivity of DNA in situ to denaturation in abnormal human sperm cells: analogy to apoptosis of somatic cells. *Experimental cell research* **207**, 202-205 (1993).
  227. Bronte, V., Serafini, P., Mazzoni, A., Segal, D.M. & Zanovello, P. L-arginine metabolism in myeloid cells controls T-lymphocyte functions. *Trends in immunology* **24**, 302-306 (2003).
  228. Rodriguez, P.C. & Ochoa, A.C. Arginine regulation by myeloid derived suppressor cells and tolerance in cancer: mechanisms and therapeutic perspectives. *Immunological reviews* **222**, 180-191 (2008).
  229. Cookson, B.T. & Brennan, M.A. Pro-inflammatory programmed cell death. *Trends in microbiology* **9**, 113-114 (2001).
  230. Shi, J., *et al.* Inflammatory caspases are innate immune receptors for intracellular LPS. *Nature* **514**, 187-192 (2014).
  231. Wang, Y., *et al.* Chemotherapy drugs induce pyroptosis through caspase-3 cleavage of a gasdermin. *Nature* **547**, 99-103 (2017).
  232. Rogers, C., *et al.* Cleavage of DFNA5 by caspase-3 during apoptosis mediates progression to secondary necrotic/pyroptotic cell death. *Nature communications* **8**, 14128 (2017).
  233. Land, W.G. The Role of Damage-Associated Molecular Patterns in Human Diseases: Part I - Promoting inflammation and immunity. *Sultan Qaboos University medical journal* **15**, e9-e21 (2015).
  234. Gelderblom, M., Arunachalam, P. & Magnus, T. gammadelta T cells as early sensors of tissue damage and mediators of secondary neurodegeneration. *Frontiers in cellular neuroscience* **8**, 368 (2014).
  235. Steele, A.K., *et al.* Microbial exposure alters HIV-1-induced mucosal CD4+ T cell death pathways Ex vivo. *Retrovirology* **11**, 14 (2014).
  236. Bergsbaken, T., Fink, S.L. & Cookson, B.T. Pyroptosis: host cell death and inflammation. *Nature reviews. Microbiology* **7**, 99-109 (2009).
  237. Nystrom, S., *et al.* TLR activation regulates damage-associated molecular pattern isoforms released during pyroptosis. *The EMBO journal* **32**, 86-99 (2013).
  238. Yang, H., *et al.* MD-2 is required for disulfide HMGB1-dependent TLR4 signaling. *The Journal of experimental medicine* **212**, 5-14 (2015).
  239. Balosso, S., Liu, J., Bianchi, M.E. & Vezzani, A. Disulfide-containing high mobility group box-1 promotes N-methyl-D-aspartate receptor function and excitotoxicity by activating Toll-like receptor 4-dependent signaling in hippocampal neurons. *Antioxidants & redox signaling* **21**, 1726-1740 (2014).
  240. Wang, H., Yang, H., Czura, C.J., Sama, A.E. & Tracey, K.J. HMGB1 as a late mediator of lethal systemic inflammation. *American journal of respiratory and critical care medicine* **164**, 1768-1773 (2001).
  241. Yang, H., Wang, H., Czura, C.J. & Tracey, K.J. The cytokine activity of HMGB1. *Journal of leukocyte biology* **78**, 1-8 (2005).
  242. Xu, J., *et al.* Macrophage endocytosis of high-mobility group box 1 triggers pyroptosis. *Cell death and differentiation* **21**, 1229-1239 (2014).
  243. Martinon, F., Burns, K. & Tschopp, J. The inflammasome: a molecular platform triggering activation of inflammatory caspases and processing of proIL-beta. *Molecular cell* **10**, 417-426 (2002).
  244. Yang, J., Zhao, Y. & Shao, F. Non-canonical activation of inflammatory caspases by cytosolic LPS in innate immunity. *Current opinion in immunology* **32**, 78-83 (2015).

## Appendix

### Scoring sheets for the 56 points Neuroscore

General deficits	Timepoint of scoring
Hair	0. Hair neat and clean
	1. Fur dirty & local piloerection
	2. Piloerection and dirty hair > 2 body parts
Ears (mouse in open area)	0. normal (ears are stretched laterally and behind; react by straightening to follow noises)
	1. Stretched laterally but not behind (one or both); react to noise
	2. Same as 1. But no reaction to noise
Eyes	0. Open & clean, following movements
	1. open & aqueous mucus, slowly following movements
	2. Open & dark mucus
	3. Ellipsoidal shaped & dark mucus
	4. Closed
Posture (placed on palm and swing gently)	0. Mouse stands in an upright position with back parallel to palm; swinging does not effect
	1. Mouse stands humpbacked, Flattens body during swing
	2. Head or part of trunk lies on palm
	3. Mouse lies on side and is not able to gather stability
	4. Mouse lies in prone position and does not recover upright after swing
Spontaneous activity (mouse in open area)	0. Mouse stays alert and explores actively
	1. Mouse seems alert, only explores sluggishly environment
	2. Mouse hardly explores surrounding area
	3. Mouse is somnolent and numb, few on-spot movements
	4. No spontaneous movements
Epileptic behavior (mouse in open area)	0. None
	3. Mouse is reluctant to handling, show hyperactivity
	6. Mouse is aggressive, stressed and stares
	9. Mouse shows hyperexcitability, chaotic movements and convulsion after handling
	Generalized seizures associated with wheezing and unconsciousness
Total Score for general deficits (0-28)	



<b>Focal deficits</b>	Timepoint of scoring
Body symmetry (nose-tail observation)	0. Normal posture, trunk elevated, tail: straight
	1. Slight asymmetry, body leans to one side, tail: slightly bent
	2. Moderate asymmetry, body leans to one side, hindlimbs stretched, tail: bent
	3. Prominent asymmetry, body bent, one side lies on floor, tail: bent
	4. Strong asymmetry, body highly bent, constant lying on one side, tail: highly bent
Gait (mouse in open area)	0. normal gait, symmetric and quick
	1. stiff & inflexible, humpbacked walk and slower
	2. Limping with asymmetric movements
	3. Trembling, drifting and falling
	4. No spontaneous movement (trembling after gentle push)
Climbing (mouse on 45° ramp, placed in center)	0. normal, mouse climbs quickly
	1. Climbs with strain, limb weakness visible
	2. Holds on a slope, neither slip nor climb
	3. Slides down the ramp, unsuccessful fall prevention
	4. Immediately slips with no prevention effort
Circling behavior (mouse in open area)	0. Absent
	1. Predominantly one-side turns
	2. Circles to one side, not constantly
	3. Constant circling to one side
	4. Pivoting and swaying
Forelimb asymmetry (mouse suspended by tail)	0. Normal
	1. Light asymmetry, mild flexion of the contralateral forelimb
	2. Marked asymmetry, clear flexion of contralateral limb, body bends ipsilateral
	3. Prominent asymmetry, contralateral forelimb adheres to trunk
	4. Strong asymmetry, little body/limb movement
Compulsory circling (mouse on forelimbs on bench)	0. Absent, a normal extension of forelimbs
	1. The tendency to turn to one side, extension of both forelimbs
	2. Circling movement to one side, slower movements
	3. Pivots to one side sluggishly, turns to one side
	4. Not advancing (front part of trunk on floor)
Whisker response (mouse in open area)	0. normal
	1. light asymmetry, responds slowly to stimulation on the contralateral side
	2. Prominent asymmetry, no response to contralateral side stimulation
	3. Absent contralateral response, slow ipsilateral response

## Appendix

---

	4. Absent bilateral response
Total Score for general deficits (0-28)	

---

## Acknowledgments

First of all, I would like to thank all the people who helped me with my research and the completion of my dissertation.

I would sincerely like to thank my supervisor, PD Dr. Arthur Liesz, for his guidance through each stage of my project. He always inspired my interest in the field of neuroscience and immunology. Whenever I have questions and difficulties about my project, he always approached me with fruitful discussion and helpful advice. I am grateful that I have been given the opportunity to pursue an ambitious research topic under good supervision and work in such a great scientific environment.

Exceptional gratitude to Prof. Dr. Martin Dichgans for letting me work in the Institute for Stroke and Dementia Research (ISD). It gave me the chance to know many great researchers and colleagues who work on different topics of neuroscience and always bring me new thoughts.

I would also like to acknowledge my colleagues of Stroke-Immunology Lab: Kerstin, Stefan, Vikram, Gemma, Rebecca, Julia, Corinne, and Steffanie. Thank you all for helping me, encouraging me, and discussing with me during the last years.

Special thanks to Melanie, Uta, Barbara, and Natalie, who gave me a lot of technical support and a great help in daily laboratory routine.

---

Many thanks to the animal facility of the ISD/CSD for their help with the experimental animal work and management of my mice lines.

And last but not least, thanks to my beloved parents and my husband, Kevin. Thank you all so much for your unlimited patience, support, motivation, and love. Without you all, I would not have been able to finish this dissertation.